

## PMFermiCOLPEm Resource

---

**From:** Tonacci, Mark  
**Sent:** Wednesday, September 02, 2009 6:58 AM  
**To:** McBride, Mark; Caverly, Jill; Tiruneh, Nebiyu  
**Cc:** Hale, Jerry; FermiCOL Resource  
**Subject:** Fermi's RAI Response for Hydro RAI  
**Attachments:** NRC3-09-0026[2].pdf

This includes revised responses for several of the RAIs they already submitted and we had a call about.

Mark Tonacci  
Senior Project Manager  
Division of New Reactor Licensing  
ESBWR/ABWR Licensing Branch  
301-415-4045

**Hearing Identifier:** Fermi\_COL\_Public  
**Email Number:** 511

**Mail Envelope Properties** (C56E360E9D804F4B95BC673F886381E71FBE0EF7F1)

**Subject:** Fermi's RAI Response for Hydro RAI  
**Sent Date:** 9/2/2009 6:57:43 AM  
**Received Date:** 9/2/2009 6:58:07 AM  
**From:** Tonacci, Mark

**Created By:** Mark.Tonacci@nrc.gov

**Recipients:**

"Hale, Jerry" <Jerry.Hale@nrc.gov>  
Tracking Status: None  
"FermiCOL Resource" <FermiCOL.Resource@nrc.gov>  
Tracking Status: None  
"McBride, Mark" <Mark.McBride@nrc.gov>  
Tracking Status: None  
"Caverly, Jill" <Jill.Caverly@nrc.gov>  
Tracking Status: None  
"Tiruneh, Nebiyu" <Nebiyu.Tiruneh@nrc.gov>  
Tracking Status: None

**Post Office:** HQCLSTR02.nrc.gov

<b>Files</b>	<b>Size</b>	<b>Date &amp; Time</b>
MESSAGE	256	9/2/2009 6:58:07 AM
NRC3-09-0026[2].pdf	14808064	

**Options**

**Priority:** Standard  
**Return Notification:** No  
**Reply Requested:** No  
**Sensitivity:** Normal  
**Expiration Date:**  
**Recipients Received:**



10 CFR 52.79

September 1, 2009  
NRC3-09-0026

U. S. Nuclear Regulatory Commission  
Attention: Document Control Desk  
Washington DC 20555-0001

- References:
- 1) Fermi 3  
Docket No. 52-033
  - 2) Letter from Jerry Hale (USNRC) to Peter W. Smith (Detroit Edison), "Request for Additional Information Letter No. 2 Related to the SRP Sections 02.04.13 for the Fermi 3 Combined License Application," dated January 14, 2009
  - 3) Letter from Jack M. Davis (Detroit Edison) to USNRC, "Detroit Edison Company Response to NRC Request for Additional Information Letters No. 1 and No. 2," NRC3-09-0001, dated February 16, 2009

Subject: Detroit Edison Company Revised Response to NRC Request for Additional Information Letter No. 2

---

In Reference 2, the NRC requested additional information to support the review of certain portions of the Fermi 3 Combined License Application (COLA). Detroit Edison provided responses to the NRC questions contained in this letter in Reference 3.

In response to Request for Additional Information (RAI) Question 2.4.13-1 and RAI Question 2.4.13-6, Detroit Edison committed to performing laboratory testing to determine site specific hydrologic characteristics of the bedrock aquifer and the glacial overburden near the Fermi 3 site. Detroit Edison further committed to updating the radionuclide transport analysis with laboratory results and providing these results to the NRC in a subsequent submittal.

Detroit Edison has completed the laboratory testing and updated the radionuclide transport analysis as described above. Revised responses to RAI 2.4.13-1 and RAI 2.4.13-6 are provided in this letter as Attachments 1 and 3, respectively. A complete revision of the Final Safety Analysis Report (FSAR) Section 2.4.13 was necessitated due to the laboratory testing results and updating of the radionuclide transport analysis. The proposed FSAR revision is provided as Attachment 4.

On August 18, 2009, Detroit Edison conducted a teleconference with the NRC Staff. In this call, the NRC requested Detroit Edison to supply additional information to RAI Question 2.4.13-4. The requested additional information is contained in Attachment 2.

Information contained in these responses will be incorporated into a future COLA submission as described in the RAI response.

If you have any questions, or need additional information, please contact me at (313)235-3341.

I state under penalty of perjury that the foregoing is true and correct. Executed on the 1<sup>st</sup> day of September 2009.

Sincerely,



Peter W. Smith, Director  
Nuclear Development – Licensing & Engineering  
Detroit Edison Company

USNRC  
NRC3-09-0026  
Page 3

Attachments: 1) Revised Response to RAI Letter No. 2 (Question No. 2.4.13-1)  
2) Revised Response to RAI Letter No. 2 (Question No. 2.4.13-4)  
3) Revised Response to RAI Letter No. 2 (Question No. 2.4.13-6)  
4) Proposed FSAR Section 2.4.13 revision  
5) Reference No. 1 from RAI 02.04.13-6 (Full Report)  
6) Reference No. 2 from RAI 02.04.13-6 (Full Report)

cc: Jack M. Davis, Senior Vice President and Chief Nuclear Officer  
Mark Tonacci, NRC Fermi 3 Project Manager  
Stephen Lemont, NRC Fermi 3 Environmental Project Manager  
Fermi 2 Resident Inspector  
NRC Region III Regional Administrator  
NRC Region II Regional Administrator  
Supervisor, Electric Operators, Michigan Public Service Commission  
Michigan Department of Environmental Quality  
Radiological Protection and Medical Waste Section

**Attachment 1  
NRC3-09-0026**

**Revised Response to RAI Letter No. 2  
(eRAI Tracking No. 1944)**

**RAI Question No. 2.4.13-1**

### **NRC RAI 2.4.13-1**

*Provide site-specific measured hydrologic parameters necessary to perform radionuclide transport analysis under the assumed release scenario as required in 10 CFR 100.20(c). More specifically, provide data and discussions about the hydrologic characteristics of the bedrock aquifer (Bass Islands Group) and the glacial overburden near Fermi Unit 3, including their thickness, depths to water tables, hydraulic conductivities, distribution coefficients, porosities; bulk mass densities, and retardation factors; the vertical and horizontal groundwater velocities of the overburden; suction heads; and the groundwater velocity of the bedrock aquifer.*

### **Revised Response**

Detroit Edison initially responded to RAI 02.04.13-1 by letter NRC3-09-0001, dated February 16, 2009. As part of the initial response to RAI 02.04.13-01, the majority of the requested parameters were provided, primarily through reference to information provided in other sections in the FSAR.

FSAR Section 2.5.4 provides a discussion of the properties of the subsurface materials. Approximate elevation ranges and average thickness for each subsurface material type encountered at the Fermi 3 site is provided in Table 2.5.4-201. Static and dynamic engineering properties are summarized in Table 2.5.4-202, including the total unit weight for the Overburden and Bass Islands Group. A more detailed discussion of the Overburden and Bass Islands Group subsurface materials is provided in Sections 2.5.4.2.1.1.3 and 2.5.4.2.1.2.1, respectively.

FSAR Section 2.4.12.2.3.2 describes the site groundwater levels and movement. The data presented was developed based on piezometers and monitoring wells installed and developed in support of the Fermi 3 project. In addition, water levels in some existing Fermi site wells installed as part of other projects were also measured and recorded. Table 2.4-229 presents construction details of wells considered in the analysis in Section 2.4.12. Water elevation recorded in each well is presented in Table 2.4-231. Water level contour maps were developed based on the recorded water elevations in each well for both the Overburden and the Bass Island's aquifer. Figures 2.4-242 through 2.4-245 provide the water table maps for the Overburden and Figures 2.4-246 through 2.4-249 provide the potentiometric maps for the Bass Islands aquifer. These are the quarterly water level maps. Monthly water level maps are provided in FSAR Appendix 2.4.BB. Groundwater flow patterns for both the Overburden and the Bass Islands aquifer are depicted on the associated figures.

Section 2.4.12.2.4 provides a discussion of the, hydrogeologic properties of the subsurface materials. Hydraulic conductivity of the Overburden was determined as described in Section 2.4.12.2.4.1. Data for the hydraulic conductivity for the Overburden, at the various monitoring locations, is provided in Table 2.4-232 for the monitored strata. Hydraulic

conductivity of the Bass Islands aquifer was determined as described in Section 2.4.12.2.4.2. Data for the hydraulic conductivity for the Bass Island aquifer is provided in Table 2.4-233 for the monitored depth of the well or piezometer. The hydraulic conductivities are also displayed by location on Figures 2.4-252 and 2.4-253 for the Overburden and Bass Islands aquifer, respectively.

As described in Section 2.4.12.3.2, no porosity field data was collected. In lieu of using field data, literature values for porosity were used to determine groundwater velocity. Velocity calculations were performed using high and low range estimates (10 — 25 percent for glacial till, 25 percent for rock fill, 1 to 20 percent for limestone/dolomite) to bracket the range of possible results. Subsequently, as described in the response to RAI 2.4.13-6, additional information has been provided to substantiate the porosity values used in the radionuclide transport analysis.

In addition, as part of the initial response to RAI 02.04.13-1, Detroit Edison committed to perform laboratory testing to determine distribution coefficients and retardation factors. Based on the results from the laboratory testing, an updated analysis would be provided in a subsequent submittal. This laboratory testing and updated analyses has subsequently been completed.

Distribution (adsorption) coefficients ( $K_d$  values) were determined based on laboratory testing of rock samples from the Bass Islands formation. Samples for the laboratory testing were taken from nine different locations on site. The locations for the laboratory testing samples were selected based on the postulated groundwater flow path either to the west to the closest off-site water well or to the east to Lake Erie. Water samples from on-site monitoring wells screened in the Bass Islands aquifer approximately along the flow paths were used during the laboratory testing. In order to simulate the fractured nature of the Bass Islands formation, the samples were broken into pieces for the laboratory testing. The material was not crushed or pulverized as this may not conservatively represent the sub-surface conditions.

Distribution coefficient measurements were obtained for cerium, cesium, cobalt, iron, manganese, ruthenium, silver, strontium, yttrium, and zinc. Selection of radionuclides for determination of distribution coefficients was based on the activity of the equipment drain collection tank source term (including progenies) from ESBWR DCD, Rev. 5, Table 12.2-13a, and screening evaluations. The screening evaluations conservatively determined the concentrations of the various radionuclides at the receptor (i.e., nearest off-site well or Lake Erie) considering only the decay of the radionuclides during the transport to the receptor. The results from the screening evaluation were then compared to the 10 CFR Part 20, Appendix B, Table 2, limits. Radionuclides were selected for the laboratory analysis where the concentration predicted in the conservative screening evaluation exceeded the limit.

Subsequently, more detailed modeling techniques were employed. The models were set-up to analyze two different receptors (a well located off-site to the west and Lake Erie to the east). Radionuclide concentrations in groundwater along the transport pathway towards each receptor

as a result of an accidental release of an equipment drain collection tank contents directly to the groundwater were modeled using RESRAD-OFFSITE.

Parameters such as distribution coefficients, hydraulic conductivity, porosity, and hydraulic gradient used in the analysis are provided in Table 2.4-234 of the proposed mark-up for FSAR Section 2.4.13. Dilution of the radionuclide source term during the instantaneous release outside the radwaste building is not modeled in the analysis. All radioisotope constituents of the source term in the ESBWR DCD, Revision 5, Table 12.2-13a are included in the analysis. Parameters were selected to conservatively represent the hydrogeologic properties from the surface to the bottom of the Bass Islands Aquifer. As an example of the conservatism employed in the analysis, Section 2.4.12.2.4.2 reports the maximum average hydraulic conductivity of the Bass Islands as 2.1 meters/day (767 meters/year). The groundwater transport analyses were performed with a value of 197,719 meters/year based on the rock fill. This input alone represents a factor of conservatism of approximately 250.

As discussed above, distribution coefficients were determined by laboratory analysis for samples from several onsite locations. In the transport analysis, the minimum distribution coefficient values were used for each element analyzed regardless of their sample location. Distribution coefficients for other elements in the analysis were assigned a value of zero, which is conservative since it assumes no retardation during transport. Using the minimum distribution coefficient values ensures that the transport analysis results are conservative.

The results of the updated analysis show that the radionuclides predicted at the closest off site well and Lake Erie are less than the 10 CFR 20, Appendix B, Table 2, Column 2 limits. Meeting 10 CFR 20 limits at the closest off site well and Lake Erie demonstrates that the radiological consequences of a postulated failure of one of the equipment drain collection tanks are also acceptable for larger distances from the radwaste building.

10 CFR 20, Appendix B, Table 2 imposes additional requirements when the identity and concentration of each radionuclide in a mixture are known. In this case, the ratio present in the mixture and the concentration otherwise established in 10 CFR 20 for the specified radionuclides not in a mixture must be determined. The sum of such ratios for all of the radionuclides in the mixture may not exceed "1" (i.e., "unity"). The sum of fractions approach has been applied to the radionuclide concentrations for both pathways. The sum of fractions for the mixtures at the closest off site well and at Lake Erie are less than unity.

### **Proposed COLA Revision**

A proposed mark-up for FSAR Section 2.4.13 to reflect the updated analysis is provided in Attachment 4 of this letter.

**Attachment 2  
NRC3-09-0026**

**Revised Response to RAI Letter No. 2  
(eRAI Tracking No. 1944)**

**RAI Question No. 2.4.13-4**

**NRC RAI 2.4.13-4**

*Provide a discussion on post-construction groundwater levels and their influence on the radionuclide pathways*

**Revised Response**

FSAR, Section 2.4.12, discusses groundwater conditions at the Fermi 3 site. Section 2.4.12.2.5 describes that current groundwater flow conditions are influenced by the quarry operations in the vicinity. As described, due to the quarry operations, the present flow pattern is reversed from the pre-quarry development flow pattern. If the quarries were to stop operating, water levels in the county could potentially recover to the point that the flow direction beneath the site might revert to the natural pre-development patterns.

As further discussed in Section 2.4.12.2.5, construction of Fermi 3 includes excavation into the Bass Islands Group to build foundations. This activity will require temporary dewatering of the excavation site to levels approximately 45 to 50 feet below the present groundwater elevation. This will alter groundwater flow locally near the excavation site. As described in Section 2.4.12.2.5.1, this temporary condition was evaluated, including construction techniques to minimize the impacts. This will alter groundwater flow locally near the excavation site, however, the altered local effects are not expected to have significant effect on the overall groundwater flow for the area.

Excavation during construction for Fermi 3 will be performed in the overburden and bedrock, which both contain groundwater. During excavation, the native glacial till overlying the bedrock will be removed. The glacial till acts as a confining unit over the bedrock and limits groundwater movement between the bedrock and the overburden.

As discussed in FSAR Section 2.5.4.5, excavation will be facilitated using methods to exclude groundwater from the excavation. Methods discussed for the perimeter of the excavation include a reinforced concrete diaphragm wall, grout curtain/sheet pile combination, and/or freeze wall, combined with grouting at the bottom of the excavation.

FSAR Figures 2.5.4-202, 2.5.4-203, and 2.5.4-204 depict the approach to backfill the Fermi 3 power block excavation, which is summarized below:

- Concrete backfill will be placed at the bottom of the excavation between the bedrock and the foundation.
- Above the concrete backfill, structural fill will be placed between the bedrock and the foundations. The structural fill will consist of gravel meeting the requirements specified in the ESBWR DCD.
- Above the bedrock surface to the ground surface the remainder of the excavation will be backfilled with gravel fill meeting requirements of the ESBWR DCD.

The following discussion addresses the potential influence of these construction related activities on post-construction groundwater levels and their effect on the radionuclide pathways. The discussion addresses groundwater in the bedrock and overburden, and groundwater flow between the bedrock and overburden.

In both the overburden and bedrock, the foundations constructed for the Fermi 3 structures would cause horizontal groundwater flow to be diverted around the area enclosed by the foundations.

Within the bedrock, specific post-construction impacts to the vertical groundwater flows associated with the diaphragm wall, grout curtain/sheet piles, and freeze wall are estimated to be as described below.

- Diaphragm wall: For the case where a diaphragm wall is used with grouting to seal the bottom of the excavation, the enclosure would cause horizontal flow to be diverted around the enclosed area. Grouting below the bottom of the excavation would impede vertical groundwater flow in the bedrock below the foundations. A release of radionuclides within the diaphragm wall would tend to be contained in the enclosed area.
- Grout curtain/sheet piles: For the case where a grout curtain and sheet piles are used with grouting to seal the bottom of the excavation, the enclosure would cause horizontal flow to be diverted around the enclosed area. Grouting below the bottom of the excavation would impede vertical groundwater flow in the bedrock below the foundations. A release of radionuclides within the diaphragm wall would tend to be contained in the enclosed area.
- Freeze Wall: For the case where a freeze wall is used with grouting to seal the bottom of the excavation, the freeze wall would be eliminated following construction, so there would be no post-construction impacts to the groundwater flow. Grouting of the bottom of the excavation would impede vertical groundwater flow in bedrock below the foundations.

Within the overburden, specific post-construction impacts to horizontal groundwater flow associated with the diaphragm wall, grout curtain/sheet piles, and freeze wall are estimated to be as described below.

- Diaphragm wall: Following construction, the upper portion of the diaphragm wall within the overburden would be breached at a number of locations to allow flow of groundwater within the overburden in and out of the area enclosed by the diaphragm wall. Therefore, following construction, the area enclosed by the diaphragm wall would have minimal impact to horizontal groundwater flow.
- Grout curtain/sheet piles: Following construction, the grout curtain/sheet piles will be removed within the overburden. Therefore, there will be no post-construction impacts to horizontal groundwater flow.
- Freeze wall: The freeze wall would be eliminated following construction. Therefore, there will be no post-construction impacts to horizontal groundwater flow.

Removal of the glacial till during excavation will allow the potential for groundwater flow between the bedrock and the overburden. As discussed in FSAR Section 2.4.12, the head in the overburden is higher than the head in the bedrock. Therefore, post-construction groundwater flow will be vertically downward from the overburden to the bedrock. Flow from the overburden could possibly result in a depression in the overburden groundwater surface level and a corresponding rise in the groundwater level in the bedrock in the immediate area of the Fermi 3 excavation. The resulting combined water level would likely equalize at a level between the two pre-construction groundwater levels.

Since the Radwaste Building foundation rests on bedrock, the downward flow of groundwater from the overburden to the bedrock will result in the postulated radionuclide release to the bedrock to remain within the bedrock. The potential rise in the groundwater level within the bedrock would result in an increased flow gradient from the location of source to the receptors. In the area of the Fermi 3 power block, during the pre-application groundwater monitoring period, the groundwater level in the overburden was observed to be approximately 5 feet higher than the groundwater level in the bedrock. If it is conservatively assumed that the groundwater level in the bedrock rises 5 feet to match the observed overburden groundwater level, then the gradient to the off-site well would increase from 0.002 to 0.0034. The 5 foot rise in the bedrock groundwater level is considered conservative since the new water level adjacent to the Fermi 3 excavation would likely reach equilibrium between the groundwater level of the overburden and bedrock groundwater levels.

As discussed in the response to RAI 2.4.13-1, the radionuclide transport analysis for flow through bedrock was performed using the hydraulic conductivity of the rock fill, which is approximately 250 times higher than the hydraulic conductivity of the bedrock. The conservative conductivity was used to provide a bounding analysis. As shown in the Darcy's Law equation (equation is shown in response to RAI 2.4.13-6), the velocity, and associated travel times, of the groundwater movement from the radwaste building to the receptor is directly related to the gradient and the hydraulic conductivity. Based on this relationship, the possible increase in the hydraulic gradient is a small factor compared to the large conservatism added by the assumed hydraulic conductivity. That is, the conservative nature of the bounding hydraulic conductivity more than offsets the potential increase in the gradient due to post construction affect.

Section 2.4.12.4 discusses post-construction groundwater monitoring. One of the purposes of the post-construction groundwater monitoring is to ensure that any construction impacts are identified and evaluated. If necessary, the analysis would be updated to reflect any post-construction changes to the local groundwater flow.

### **Proposed COLA Revision**

None

**Attachment 3  
NRC3-09-0026**

**Revised Response to RAI Letter No. 2  
(eRAI Tracking No. 1944)**

**RAI Question No. 2.4.13-6**

### **NRC RAI 2.4.13-6**

*Provide a description of the process followed to determine the conceptual models for surface and subsurface pathways and for site characteristics that affect transport of radioactive liquid effluents in ground and surface waters to ensure that the most conservative of plausible conceptual models has been identified pursuant to the guidance provided in SRP 2.4.13. Also provide analysis based on the most conservative of all the plausible models to demonstrate compliance with 10 CFR part 20 Appendix B Table 2 ECL limits. In the supplemental information that contained the analysis of radionuclide transport for an assumed failure, the results show exceedance of the ECL limits for 12 radionuclide isotopes for both assumed receptors (Lake Erie to the east and a receptor well to the west). The applicant also stated that even if the conservatism assumed in the analysis, more specifically the maximum groundwater velocity, dilution, assumption of continuous ingestion were to be relaxed, the resulting concentrations will still be above the ECL limits. Please include in the analysis the basis for the preceding conclusion of the applicant.*

### **Revised Response**

Detroit Edison initially responded to RAI 02.04.13-6 by letter NRC3-09-0001, dated February 16, 2009. As part of this response, Detroit Edison committed to perform laboratory testing to determine distribution coefficients and retardation factors. Based on the results from the laboratory testing, an updated analysis would be provided in a subsequent submittal. This laboratory testing and updated analyses has subsequently been completed.

An initial step prior to the developing the models for the radionuclide transport analyses is an understanding of the groundwater flow patterns at the site. FSAR Section 2.4.12.2.3.2 describes the site groundwater levels and movement. The data presented in Section 2.4.12.2.3.2 was developed based on piezometers and monitoring wells installed and developed in support of the Fermi 3 project. In addition, water levels in some existing Fermi site wells installed as part of other projects were also measured and recorded. Monitoring well and piezometer locations were selected in order to understand the groundwater flow patterns at the site. Water elevation recorded in each well is presented in Table 2.4-231. Water level contour maps were developed based on the recorded water elevations in each well for both the Overburden and the Bass Island's aquifer. Figures 2.4-242 through 2.4-245 provide the water table maps for the Overburden and Figures 2.4-246 through 2.4-249 provide the potentiometric maps for the Bass Islands aquifer. These are the quarterly water level maps. Monthly water level maps are provided in FSAR Appendix 2.4.BB. Groundwater flow patterns for both the Overburden and the Bass Islands aquifer are depicted on the associated figures. The projected flow path(s) for the radionuclide transport analysis are determined based on these groundwater flow patterns.

Subsequent to understanding the groundwater flow patterns, the radionuclide transport models are developed. The process to developing these models includes:

- Identification of the source of the postulated radionuclide release. The first step is to identify the potential source of the release. This is performed to maximize the potential consequences from the release by selecting a tank based on volume and concentration of radionuclides.
- Identification of the release path for the postulated source of radionuclides. The potential release path to the aquifer is identified based on the tank selected in the first step. The release path from the tank/building is then considered in order to identify the aquifer that the radionuclides could be released to.
- Identification of the potential path(s) for the groundwater flow in the aquifer that the radionuclides are released to. The groundwater flow path is determined based on analysis of the data collected during field investigation and characterization activities. The analysis of the field data considers current impacts to the identified groundwater flow to evaluate key influences that may be impacting the groundwater flow, and how changes to these key influences could change the groundwater flow.
- Identification of potential receptor(s) in the identified groundwater flow path(s). Potential receptor(s) are then identified for the current groundwater flow and possible groundwater flow should potential changes be identified in preceding step.

Each of these is described in more detail below.

The source of the radionuclide release is assumed to be one of the equipment drain collection tanks. Each tank has a capacity of 140 m<sup>3</sup> (37,000 gal) and radionuclide concentrations as given in DCD Table 12.2-13a. These tanks are located on the lowest level of the radwaste building (level B2F), which has a floor elevation of approximately 540 feet NAVD88 (FSAR Figure 2.5.4-204). One of the tanks is postulated to rupture, and 80 percent of the liquid volume (112 m<sup>3</sup> or 29,600 gal) is assumed to be released following the guidance provided in BTP 11-6. Following tank rupture, it is conservatively assumed that a pathway is created that allows the entire 112 m<sup>3</sup> to enter the groundwater instantaneously.

The release from the basement elevation of the radwaste building would enter the Bass Islands aquifer. The assumption of instantaneous release to the groundwater following tank rupture is conservative because it requires failure of the floor drain system, plus it ignores the barriers presented by the basemat concrete and the steel liners incorporated into the tank cubicles of the radwaste building, which is seismically designed. It should also be recognized that level B2F of the radwaste building is well below the water table. Piezometric head contour maps presented in FSAR Figure 2.4-246 through Figure 2.4-249 indicate that the ambient water table in the vicinity of the radwaste building is about 567 feet NAVD88, or 27 ft above the radwaste building floor elevation. If the basemat or exterior walls of the radwaste building and associated steel liners were to fail simultaneously, groundwater would flow into the radwaste building, precluding the release of liquid effluents out of the building. Only if the interior of the radwaste building was flooded to a level higher than the surrounding groundwater would there be a pathway for liquid effluents to be released out of the building and to the groundwater. Hence, the assumption of an

accidental release of liquid effluents from the radwaste building to groundwater is extremely conservative, given the design features of the radwaste building intended to prevent an accidental release and the hydrogeologic conditions at the site.

After release from the radwaste building to the Bass Islands aquifer, the transport is analyzed. Groundwater will flow in the direction of decreasing hydraulic head. As described above, the determination of potential flow paths is based on analysis of data collected during the site investigation and characterization. The data and analyses are described in more detail in FSAR Section 2.4.12.

FSAR Section 2.4.12.3.1 describes potential pathways in the bedrock (Bass Islands aquifer). As described in Section 2.4.12.3.1 there are two potential pathways for groundwater:

- The documented present day condition, in which the groundwater flow direction in the Bass Islands aquifer is westward off-site.
- A possible future condition in which the flow direction has returned to the east toward Lake Erie.

As discussed in Section 2.4.12.3.1, the present day condition is attributed to dewatering associated with quarrying operations westward of the site. The possible future condition is intended to account for the case where the quarrying operations were to cease. For the purposes of the analyses, both potential flow paths are considered.

To the west off-site, the assumed receptor is a well located at the west corner of Enrico Fermi Drive and Toll Road as shown on FSAR Figure 2.4-236. To the east, the receptor is Lake Erie. The distances from the source to each receptor are conservatively selected. For the path from the radwaste building to the well off-site to the west, the source location is assumed to be the closest western side of the radwaste building. For the path from the radwaste building to Lake Erie, the source is assumed to be the closest eastern side of the radwaste building.

The conceptual transport model is used to evaluate the accidental release of radioactive liquid effluent to groundwater. The conceptual model used for the transport analysis was developed based on data collected during the site investigation, as described in FSAR Sections 2.4.12. The inputs and assumptions used in the conceptual model for the radionuclide transport analysis are described below.

Radionuclide concentrations in groundwater along the transport pathway toward the closest off site well or Lake Erie as a result of an accidental release of an equipment drain collection tank contents directly to the groundwater were modeled using RESRAD-OFFSITE.

As described in the response to RAI 02.04.13-1, in the transport analysis, the minimum distribution coefficient values were used for each element analyzed irrespective of their sample location. Distribution coefficients for other elements in the analysis were assigned a value of

zero, which is conservative since it assumes no retardation during transport. Using the minimum distribution coefficient values ensures that the transport analysis results are conservative.

Aquifer parameters were established for the Bass Island aquifer (see Section 2.4.12). For this accidental release groundwater transport model, the hydraulic conductivity and hydraulic gradient measured at the site were selected to ensure very conservative results.

The total porosity value was used to be conservative with respect to available information for other areas of the Bass Islands formation in the State of Michigan [Reference 1, see Attachment 5 for Report]. The effective porosity value was initially selected from a report of similar material (i.e., dolomite) [Reference 2, see Attachment 6 for Report], and confirmed to be conservative through sensitivity cases with RESRAD-OFFSITE.

The travel times of the groundwater movement from the radwaste building to the receptor were computed from a variation of Darcy's Law:

$$t = \frac{x}{V} = \frac{x}{KI / \theta}$$

Where:

- t = time to move distance x (yr)
- x = distance of contaminant movement (m)
- V = average interstitial groundwater velocity (m/yr)
- K = hydraulic conductivity (m/yr)
- I = hydraulic gradient
- $\theta$  = effective porosity

The values of parameters used are shown in Table 2.4-234 in the proposed mark-up for FSAR Section 2.4.13.

The results of the updated analysis show that the radionuclides predicted at the closest off site well and Lake Erie are less than the 10 CFR 20, Appendix B, Table 2, Column 2 limits. Meeting 10 CFR 20 limits at the closest off site well and Lake Erie demonstrates that the radiological consequences of a postulated failure of one of the equipment drain collection tanks are also acceptable for larger distances from the radwaste building.

10 CFR 20, Appendix B, Table 2 imposes additional requirements when the identity and concentration of each radionuclide in a mixture are known. In this case, the ratio present in the mixture and the concentration otherwise established in 10 CFR 20 for the specified radionuclides not in a mixture must be determined. The sum of such ratios for all of the radionuclides in the mixture may not exceed "1" (i.e., "unity"). The sum of fractions approach has been applied to the radionuclide concentrations for both pathways. The sum of fractions for the mixtures at the closest off site well and at Lake Erie are less than unity.

#### References

1. Midwest Regional Carbon Sequestration Partnership (MRCSP), Fact Sheet for Partnership Field Validation Test, Submitted by Battelle, dated November 2007.  
[http://www.netl.doe.gov/publications/proceedings/07/rcsp/factsheets/17-MRCSP\\_Michigan%20Basin%20Geologic%20Test.pdf](http://www.netl.doe.gov/publications/proceedings/07/rcsp/factsheets/17-MRCSP_Michigan%20Basin%20Geologic%20Test.pdf)
2. USGS Scientific Investigations Report 2004-5031, "Simulation of Ground-Water Flow, Surface Water Flow, and a Deep Sewer Tunnel System in the Menomonee Valley, Milwaukee, Wisconsin"

#### **Proposed COLA Revision**

A proposed mark-up for FSAR Section 2.4.13 to reflect the updated analysis is provided in Attachment 4 of this letter.

**Attachment 4  
NRC3-09-0026**

**FSAR Section 2.4.13 Revision**

**Markup of Detroit Edison COLA**  
(following 41 pages)

The following markup represents how Detroit Edison intends to reflect this RAI response in the next submittal of the Fermi 3 COLA Revision 2. However, the same COLA content may be impacted by revisions to the ESBWR DCD, responses to other COLA RAIs, other COLA changes, plant design changes, editorial or typographical corrections, etc. As a result, the final COLA content that appears in a future submittal may be different than presented here.

EF3 COL 2.0-24-A

2.4.13 **Accidental Releases of Liquid Effluents to Ground and Surface Waters**

Mitigating design features specified in NUREG 0800 Branch Technical Position (BTP) 11-6 are incorporated into the design of Fermi 3 to preclude an accidental release of liquid effluents. Descriptions of these features are provided below.

Below-grade tanks containing radioactivity are located on levels B1F and B2F of the Radwaste Building. The Radwaste Building is designed to seismic requirements as specified in DCD Table 3.2-1. In addition, as described in DCD Section 11.2.2.3, compartments containing high level liquid radwaste are steel lined up to a height capable of containing the release of all liquid radwaste in the compartment. Leaks as a result of major cracks in tanks result in confinement of the liquid radwaste in the compartment and the building sump system for containment in other tanks or emergency tanks. Because of these design capabilities, it is not considered feasible that any major event involving the release of liquid radwaste into these volumes results in the release of these liquids to the groundwater environment via the liquid pathway.

The Condensate Storage Tank (CST), part of the Condensate Storage and Transfer System (CS&TS), is the only above-grade tank that potentially could contain radioactivity outside of containment, the reactor building, or the radwaste building. The CS&TS, described in DCD Section 9.2.6, meets GDC 60 by compliance with RG 1.143, Position C.1.2 for design features provided to control the release of liquid effluents containing radioactive material. The basin surrounding the tank is designed to prevent uncontrolled runoff in the event of a tank failure. The basin volume is sized to contain the total tank capacity. Tank overflow is also collected in this basin. A sump located inside the retention basin has provisions for sampling collected liquids prior to routing them to the Liquid Waste Management System (LWMS) or the storm sewer as per sampling and release requirements. These design features are intended to preclude the release of liquids from the CST to either the ground or surface water environment via the liquid pathway.

The mitigating design features described above demonstrate that the radioactive waste management systems, structures, and components for

Fermi 3, as defined in RG 1.143, include features to preclude accidental releases of radionuclides into potential liquid pathways. Nevertheless, an analysis of accidental releases of radioactive liquid effluents in groundwater is performed. Descriptions and results of these analyses are provided herein.

The source term provided in DCD Table 12.2-13a, Liquid Waste Management System Equipment Drain Collection Tank Activity, is used in the analysis of an accidental release of liquid effluents from an equipment drain collection tank and the radwaste building structure to the groundwater system. This source term is appropriate because these tanks collect radioactive liquids from various pieces of plant equipment and are upstream of liquid processing by the LWMS.

#### 2.4.13.1 **Groundwater Analysis**

The purpose of this section is to provide a conservative analysis of a postulated accidental release of radioactive liquid effluents to the groundwater at the Fermi 3 site. The accident scenario is described. The model used to evaluate radionuclide transport is presented, along with potential pathways of contamination to water users. The radionuclide transport analysis is described, and the results are summarized. The radionuclide concentrations to which a water user might be exposed are compared against the regulatory limits.

##### 2.4.13.1.1 **Accident Scenario**

A liquid radwaste tank outside of containment is postulated to rupture with its contents released to the groundwater. The volume of the liquid assumed to be released and the associated radionuclide concentrations were selected to produce an accident scenario that leads to the most adverse contamination of groundwater, or surface water via the groundwater pathway.

Radwaste tanks outside of containment are located on the levels B1F and B2F of the radwaste building as shown on DCD Figure 1.2-25. The radwaste tanks having the largest volumes include the three equipment

drain collection tanks and the equipment drain sample tank, all in the lowest level, B2F. Each of these tanks has a volume of 140 m<sup>3</sup> (37,000 gal) according to DCD Tables 12.2-13a and 12.2-13b.

Estimates of activity concentrations in various liquid radwaste tanks are provided in DCD Tables 12.2-13a through 12.2-13g. Of these tanks, the limiting tank in terms of radionuclide activity is the Equipment Drain Collection Tank, and its activity is provided in DCD Table 12.2-13a.

The accident scenario assumes that one of the equipment drain collection tanks ruptures and its contents are released to the groundwater. Note that this accident scenario is conservative because the radwaste building is seismically designed in accordance with RG 1.143, Class RW-IIa, as described in DCD Section 12.2.1.4. Also, the concrete in each tank cubicle is provided with a steel liner, as described in DCD Section 11.2.2.3, to prevent any potential liquid releases to the environment.

#### 2.4.13.1.2 Model

Subsection 2.4.12.3 describes the conceptual model used to evaluate groundwater pathways and transport of contamination in groundwater. This conceptual model is used to evaluate the accidental release of radioactive liquid effluent to groundwater. Key elements and assumptions embodied in this evaluation are described and discussed below.

As indicated above, one of the equipment drain collection tanks is assumed to be the source of the release, with each tank having a capacity of 140 m<sup>3</sup> (37,000 gal) and radionuclide concentrations as given in DCD Table 12.2-13a. These tanks are located on the lowest level of the radwaste building (level B2F), which has a floor elevation of approximately 540 feet NAVD88 (Figure 2.5.4-204). One of the tanks is postulated to rupture, and 80 percent of the liquid volume (112 m<sup>3</sup> or 29,600 gal) is assumed to be released following the guidance provided in BTP 11-6. Following tank rupture, it is conservatively assumed that a

pathway is created that allows the entire 112 m<sup>3</sup> to enter the groundwater in the Bass Islands aquifer instantaneously.

The assumption of instantaneous release to the groundwater following tank rupture is conservative because it requires failure of the floor drain system, plus it ignores the barriers presented by the basement concrete and the steel liners incorporated into the tank cubicles of the radwaste building, which is seismically designed. It should also be recognized that level B2F of the radwaste building is well below the water table. Potentiometric surface contour maps presented in Figure 2.4-247 through Figure 2.4-249 indicate that the ambient water table in the vicinity of the radwaste building is about 567 feet NAVD88, or 27 ft above the radwaste building floor elevation. If the basement or exterior walls of the radwaste building and associated steel liners were to fail simultaneously, groundwater would flow into the radwaste building, precluding the release of liquid effluents out of the building. Only if the interior of the radwaste building was flooded to a level higher than the surrounding groundwater would there be a pathway for liquid effluents to be released out of the building and to the groundwater. Hence, the assumption of an accidental release of liquid effluents from the radwaste building to groundwater is extremely conservative, given the design features of the radwaste building intended to prevent an accidental release and the hydrogeologic conditions at the site.

With the postulated instantaneous release of the contents of an equipment drain collection tank to groundwater, radionuclides enter the Bass Islands aquifer and migrate with the groundwater in the direction of decreasing hydraulic head. Subsection 2.4.12.3.1 describes potential pathways in the bedrock (Bass Islands aquifer). As described in Subsection 2.4.12.3.1 there are two potential pathways for groundwater:

- The documented present day condition, in which the groundwater flow direction in the Bass Islands aquifer is westward off-site.
- A possible future condition in which the flow direction reverses and is toward Lake Erie.

The present day condition is attributed to dewatering associated with quarrying operations westward of the site. The possible future reversal is intended to account for the case where the quarrying operations ceased. For the purposes of this evaluation, both potential flow paths are considered. For each potential flow path, the flow path is assumed to be a straight line between the radwaste building and the receptor. To the westward off-site, the assumed receptor is a well. To the east, the receptor is Lake Erie. Additional analysis conservatism exists in that no credit is taken for dilution either in route to or at the receptor.

#### 2.4.13.1.3 Radionuclide Transport Analysis

The radionuclide transport analysis is conducted using conservative assumptions and coefficients, to estimate the radionuclide concentrations that might expose existing and future water users based on an instantaneous release of the radioactive liquid from an equipment drain collection tank.

Radionuclide concentrations resulting from the analysis are compared against the effluent concentration limits (ECLs) identified in 10 CFR 20, Appendix B, Table 2, Column 2, to determine acceptability. It is noted that using the ECLs identified in 10 CFR 20, Appendix B, Table 2, is conservative as (per 10 CFR 20, Appendix B) "the concentration values given in Columns 1 and 2 of Table 2 are equivalent to the radionuclide concentrations which, if inhaled or ingested continuously over the course of a year, would produce a total effective dose equivalent of 0.05 rem (50 millirem or 0.5 millisieverts)." In the case of this postulated release of the radioactive liquid to the groundwater at the Fermi site, it is not expected that the radioactivity will be present at the receptor continuously over the course of the year. As the radioactivity reaches the receptor, it is flowing either in the lake water (for the postulated release eastward to Lake Erie) or in the groundwater (postulated release westward off-site). This flow mechanism does not simply cease at the receptor, but would continue to flow past the receptor.

This analysis accounts for the parent radionuclides assumed present in the radwaste tank plus progeny radionuclides that are generated

subsequently during transport. The analysis considered all progeny in the decay chain sequences that are important for dosimetric purposes. Reference 2.4-291 and Reference 2.4-292 were used to identify the member for which the decay chain sequence can be truncated. For some of the radionuclides assumed present in an equipment drain collection, consideration of up to three members of the decay chain sequence was required. The derivation of the equations governing the transport of the parent and progeny radionuclides follows.

Transport of the parent radionuclide along a groundwater pathline is governed by the advection-dispersion-reaction equation, which is given as:

$$R \frac{\partial C}{\partial t} = D \frac{\partial^2 C}{\partial x^2} - v \frac{\partial C}{\partial x} - \lambda RC \quad (1)$$

where: C = radionuclide concentration; R = retardation factor; D = coefficient of longitudinal hydrodynamic dispersion; v = average linear velocity; and  $\lambda$  = radioactive decay constant. The retardation factor is defined from the relationship:

$$R = 1 + \frac{\rho_b K_d}{n_e} \quad (2)$$

where:  $\rho_b$  = bulk density;  $K_d$  = distribution coefficient; and  $n_e$  = effective porosity. The average linear velocity is determined using Darcy's law, which is:

$$v = \frac{K}{n_e} \frac{dh}{dx} \quad (3)$$

where: K = hydraulic conductivity; and dh/dx = hydraulic gradient. The radioactive decay constant can be written as:

$$\lambda = \frac{\ln 2}{t_{1/2}} \quad (4)$$

where:  $t_{1/2}$  = radionuclide half-life. Using the method of characteristics approach in Reference 2.4-293, the material derivative of concentration can be written as:

$$\frac{dC}{dt} = \frac{\partial C}{\partial t} + \frac{dx}{dt} \frac{\partial C}{\partial x} \quad (5)$$

Conservatively neglecting hydrodynamic dispersion, the characteristic equations for Equation (1) can be expressed as follows:

$$\frac{dC}{dt} = -\lambda C \quad (6)$$

$$\frac{dx}{dt} = \frac{v}{R} \quad (7)$$

The solutions of the system of equations comprising Equation (6) and Equation (7) can be obtained by integration to yield the characteristic curves of Equation (1). For the parent radionuclide, the equations representing the characteristic curves can be obtained as:

$$C_1 = C_{10} \exp(-\lambda_1 t) \quad (8)$$

$$t = R_1 L / v \quad (9)$$

where:  $C_1$  = concentration of the parent radionuclide;  $C_{10}$  = initial concentration of the parent radionuclide;  $\lambda_1$  = radioactive decay constant for the parent radionuclide;  $R_1$  = retardation factor for the parent radionuclide; and  $L$  = groundwater pathline length.

Similar relationships exist for progeny radionuclides. For the first progeny in the decay chain, the advection-dispersion-reaction equation is:

$$R_2 \frac{\partial C_2}{\partial t} = D \frac{\partial^2 C_2}{\partial x^2} - v \frac{\partial C_2}{\partial x} + d_{12} \lambda_1 R_1 C_1 - \lambda_2 R_2 C_2 \quad (10)$$

where: subscript 2 denotes the first progeny radionuclide; and  $d_{12}$  = fraction of parent radionuclide transitions that result in production of first progeny radionuclide. The characteristic equations for Equation (10), again conservatively neglecting hydrodynamic dispersion, can be derived as:

$$\frac{dC_2}{dt} = d_{12} \lambda_1' C_1 - \lambda_2 C_2 \quad (11)$$

$$\frac{dx}{dt} = \frac{v}{R_2} \quad (12)$$

Where:  $\lambda_1' = \lambda_1 R_1 / R_2$ . Recognizing that Equation (11) is formally similar to Equation B.43 of Reference 2.4-292, these equations can be integrated to yield:

$$C_2 = K_1 \exp(-\lambda_1' t) + K_2 \exp(-\lambda_2 t) \quad (13)$$

$$t = R_2 L / v \quad (14)$$

For which:

$$K_1 = \frac{d_{12} \lambda_2 C_{10}}{\lambda_2 - \lambda_1'}$$

$$K_2 = C_{20} - \frac{d_{12} \lambda_2 C_{10}}{\lambda_2 - \lambda_1'}$$

The advection-dispersion-reaction equation for the second progeny in the decay chain is:

$$R_3 \frac{\partial C_3}{\partial t} = D \frac{\partial^2 C_3}{\partial x^2} - v \frac{\partial C_3}{\partial x} + d_{13} \lambda_1 R_1 C_1 + d_{23} \lambda_2 R_2 C_2 - \lambda_3 R_3 C_3 \quad (15)$$

where: subscript 3 denotes the second progeny radionuclide;  $d_{13}$  = fraction of parent radionuclide transitions that result in production of second progeny radionuclide; and  $d_{23}$  = fraction of first progeny radionuclide transitions that result in production of second progeny radionuclide. The characteristic equations for Equation (15), again conservatively neglecting hydrodynamic dispersion, can be derived as

$$\frac{dC_3}{dt} = d_{13} \lambda'_1 C_1 + d_{23} \lambda'_2 C_2 - \lambda_3 C_3 \quad (16)$$

$$\frac{dx}{dt} = \frac{v}{R_3} \quad (17)$$

where:  $\lambda'_1 = \lambda_1 R_1 / R_3$ ; and  $\lambda'_2 = \lambda_2 R_2 / R_3$ . Considering the formal similarity of Equation (16) to Equation B.54 of Reference 2.4-292, Equation (16) and Equation (17) can be integrated to yield:

$$C_3 = K_1 \exp(-\lambda'_1 t) + K_2 \exp(-\lambda'_2 t) + K_3 \exp(-\lambda_3 t) \quad (18)$$

$$t = R_3 L / v \quad (19)$$

For which:

$$K_1 = \frac{d_{13} \lambda_3 C_{10}}{\lambda_3 - \lambda'_1} + \frac{d_{23} \lambda'_2 d_{12} \lambda_3 C_{10}}{(\lambda_3 - \lambda'_1)(\lambda'_2 - \lambda'_1)}$$

$$K_2 = \frac{d_{23} \lambda_3 C_{20}}{\lambda_3 - \lambda'_2} + \frac{d_{23} \lambda'_2 d_{12} \lambda_3 C_{10}}{(\lambda_3 - \lambda'_2)(\lambda'_2 - \lambda'_1)}$$

$$K_3 = C_{30} - \frac{d_{13} \lambda_3 C_{10}}{\lambda_3 - \lambda'_1} - \frac{d_{23} \lambda_3 C_{20}}{\lambda_3 - \lambda'_2} + \frac{d_{23} \lambda'_2 d_{12} \lambda_3 C_{10}}{(\lambda_3 - \lambda'_1)(\lambda_3 - \lambda'_2)}$$

To estimate the radionuclide concentrations in groundwater discharging to the receptor, Equation (8), Equation (13), and Equation (18) were applied as appropriate along the groundwater pathline that would originate at the radwaste building and terminate at the receptor.

#### **a. Transport Considering Radioactive Decay Only**

This analysis is conservatively performed considering radioactive decay only. This analysis also conservatively assumes that all radionuclides migrate at the same rate as groundwater and considers no adsorption and retardation, which would otherwise result in lower radionuclide concentrations at the receptors. The concentrations of the radionuclides assumed to be released from an equipment drain collection tank are decayed for a period equal to the groundwater travel time from the point of release to the receptor, using Equation (8), Equation (13), or Equation (18) as appropriate with  $R_1 = R_2 = R_3 = 1$ .

As discussed above, per Equation (2), the Retardation Factor (R) is a function of the material properties. As discussed in Subsection 2.5.1.2.4.3, the Bass Islands formation is highly fractured with a variable frequency of fracturing. During the on-site investigation, some of the fractures were observed to be filled, while others had no filling. Groundwater travel through the Bass Islands aquifer would follow the open fractures as this provides the path of least resistance. Flow through the open fractures would also provide the lower values for distribution coefficients and retardation factors. Literature values for distribution coefficients that would conservatively represent the conditions at the site were not identified. Due to the presence of the fractures, testing methods are considered to be limited in their capability to represent the subsurface conditions. Thus, overall, determination of values for distribution coefficients accounting for the fractures in the Bass Islands aquifer may introduce a level of uncertainty to the results. In order to bound potential uncertainties, a value of  $K_d$  is used that results in a value of one (1) for the Retardation Factors (Equation (2)).

Evaluating transport considering radioactive decay only, requires an estimate of the groundwater travel time. In Subsection 2.4.12.3.2 the groundwater travel time between the radwaste building and the two possible receptors is estimated based on site-specific hydrogeologic characteristics. Table 2.4-234 summarizes the pertinent results from Subsection 2.4.12.3.2. Maximum flow velocities from Subsection 2.4.12.3.2, as reflected in Table 2.4-234, are used to provide bounding results.

Using Equation (8), Equation (13), or Equation (18) as appropriate with  $R = 1$ , the initial concentrations were decayed over the travel times reflected in Table 2.4-234 for both potential flow paths. Radioactive decay data and decay chain specifications were taken from NUREG/CR-5512, Vol. 1, Table E.1 (Reference 2.4-292). Radioactive decay data for some of the shorter-lived radionuclides were obtained from Reference 2.4-291. Table 2.4-235 and Table 2.4-236 summarize the results and identify those radionuclides for which the ratio of groundwater concentration to ECL would exceed 1 (i.e., unity). These radionuclides are H-3, Mn-54, Fe-55, Co-60, Zn-65, Sr-90, Y-90, Ru-106, Ag-110m, Cs-134, Cs-137 and Ce-144.

#### 2.4.13.1.4 Comparison with 10 CFR 20 ECL

The radionuclide transport analysis presented in Subsection 2.4.13.1.3 indicates that several of the radionuclides included in the evaluation could exceed their corresponding ECL for the conservative conditions modeled.

It is recognized that 10 CFR 20, Appendix B, Table 2, imposes additional requirements when the identity and concentration of each radionuclide in a mixture are known. In this case, the ratio present in the mixture and the concentration otherwise established in 10 CFR 20, Appendix B for the specific radionuclide not in a mixture must be determined. The sum of such ratios for all of the radionuclides in the mixture may not exceed "1" (i.e., "unity"). Given that several of the radionuclides exceed their

corresponding ECL, the sum of all of the ratios would also be greater than unity.

As described above, this analysis is based on multiple conservatisms that are used to provide a bounding result. To summarize, these conservatisms are as follows.

- The assumption that the tank ruptures is considered to be very conservative. Minor tank leakage would be expected to occur prior to a significant leak occurring. Plant operators would be alerted to leakage during walkdowns and would take actions to mitigate the impacts from such leakage. As described in DCD Section 15.3.16.1, a liquid radwaste release caused by operator error is also considered a remote possibility. Operating techniques and administrative procedures emphasize detailed system and equipment operating instructions. A positive action interlock system is also provided to prevent inadvertent opening of a drain valve.
- The radwaste building is designed to seismic requirements as specified in DCD Table 3.2-1. The compartments that contain these tanks are steel lined up to a height capable of containing the release of all liquid radwaste in the tank. This design and additional barrier are not credited in the analysis.
- The potentiometric head is approximately 27 ft above the radwaste building floor elevation. Thus, if leakage should occur due to a crack in the building floor or wall, it would be expected that the leakage would be into the building and not out of the building. These hydrogeologic conditions are not credited in the analysis.
- The analysis is based on the maximum groundwater flow velocity based on Subsection 2.4.12. Using the maximum groundwater flow velocity results in the minimum decay time and thus the maximum radionuclide concentrations.
- For the postulated release to Lake Erie, no credit is taken for dilution in the lake water as the release traverses to a drinking water intake. The closest drinking water intake from Lake Erie is more than 1500 meters (4920 feet) to the South. Thus, significant dilution would be expected for the postulated release to Lake Erie. It is noted that this

same dilution factor would not be present for the postulated release westward off-site (i.e., where the receptor is a well).

- The limits (ECLs) to which the groundwater concentrations are compared are conservative as the 10 CFR 20, Appendix B, ECLs are based on continuous ingestion over a year. In this case of this postulated release of the radioactive liquid to the groundwater, it is not expected that the radioactivity will be present continuously over the course of the year.

It is noted that reducing the extent of the analytical conservatisms discussed above (specifically the last three bullets) would not be expected to produce results that are less than the 10 CFR 20, Appendix B, ECLs. Thus, additional measures (as discussed below) are implemented as part of the Fermi 3 design to ensure that the ECLs are not exceeded.

#### 2.4.13.5 Mitigation Measures

BTP 11-6, Section D, discusses two alternatives for supporting a conclusion that the postulated failure of a tank and its associated components has been evaluated and the design is acceptable and meets the requirements of General Design Criteria 60 and 61 for the control of releases of radioactive materials to the environment and provides an adequate level of safety during normal reactor operation. One alternative for supporting this conclusion is an analysis determining radionuclide concentrations in the applicable failed components and the effect of site hydrology for those systems that have not been provided with special design features to mitigate the effects of failures. As discussed above, such an analysis using conservative inputs and assumptions indicates that the results for some radionuclides are greater than the respective limits.

Per BTP 11-6, a second alternative for supporting a conclusion that the postulated failure of a tank is acceptable and meets the requirements of General Design Criteria 60 and 61 is to provide design features to mitigate the consequences of the postulated tank failure. The Fermi 3

~~design supports the conclusion that the design features provided are acceptable in mitigating the effects of tank failure involving radioactive liquids. Therefore, based on these design features, a postulated liquid release to the environment at Fermi 3 is mitigated in a manner consistent with regulatory guidance to preclude the possible release.~~

---

**EF3 COL 2.0-25-A**

**2.4.14 Technical Specifications and Emergency Operation Requirements**

The design plant grade elevation for safety-related SSCs is located above the design basis flood level, as stated in Subsection 2.4.2, and above the maximum groundwater elevation, as stated in Subsection 2.4.12. Safety-related SSCs for the plant are protected from external floods as discussed in Section 3.4. The elevation of exterior access openings, which are above the PMF and local PMP flood levels, and the design of exterior penetrations below design flood and groundwater levels, which are appropriately sealed, result in a design and site combination that do not necessitate emergency procedures or meet the criteria for Technical Specification LCOs to ensure safety-related functions at the plant.

The plant elevation is also above flood and groundwater elevations for Regulatory Treatment of Non-Safety Systems (RTNSS) SSCs used to provide the makeup water to the UHS (IC/PCCS pools) from 72 hours to 7 days after an accident. The Seismic Category I FWSC SSCs are also protected from external floods. Therefore, no technical specifications or emergency procedures are required to prevent hydrological phenomena from degrading the UHS.

---

**2.4.15 References**

- 2.4-201 The Great Lakes: An Environmental Atlas and Resource Book. "State of the Great Lakes 2005." November 2005, <http://binational.net/solec/English/SOLEC%202004/Tagged%20PDFs/SOGL%202005%20Report/English%20Version/Lake%20Sections/Lake%20Erie%20-%20tagged.pdf>, accessed 7 February 2007.
- 2.4-202 Great Lakes Information Network. 1 November 2006, <http://www.great-lakes.net/envt/flora-fauna/people.html>, accessed 8 October 2007.

- 2.4-282 Royle, M., "Standard Operating Procedures for Borehole Packer Testing."
- 2.4-283 McDonald, M., and A. Harbaugh, "A Modular Three-Dimensional Finite-Difference Ground-Water Flow Model," Techniques of Water-Resources Investigations of the United States Geological Survey, Book 6, Chapter A1, 1988.
- 2.4-284 Harbaugh, A.W., E.R. Banta, M.C. Hill, and M.G. McDonald, "MODFLOW-2000, The U.S. Geological Survey Modular Ground-Water Model – User Guide to Modularization Concepts and the Ground-Water Flow Processes," U.S. Geological Survey Open-File Report 00-92, Reston, Virginia, 2000.
- 2.4-285 Brigham Young University Environmental Modeling Research Laboratory, "Groundwater Modeling System Tutorials," Version 6.0, Vols. I, II, and III, October 20, 2005.
- 2.4-286 Dames & Moore, "Rock Foundation Treatment Residual Heat Removal Complex Fermi II Nuclear Power Plant for the Detroit Edison Company," July 3, 1974.
- 2.4-287 Fetter, C.W., "Applied Hydrogeology," Bell & Howell Co., Columbus, OH, 1980.
- 2.4-288 Driscoll F.G., "Groundwater and Wells," 2nd Edition, Johnson (Well Screen) Division, St. Paul Minnesota, 1986.
- 2.4-289 Detroit Edison, "Fermi 2, Offsite Dose Calculation Manual," Revision 14, 1999.
- 2.4-290 U.S. Nuclear Regulatory Commission, "Integrated Ground-Water Monitoring Strategy for NRC-Licensed Facilities and Sites: Logic, Strategic Approach and Discussion," Advanced Environmental Solutions LLC for Division of Fuel, Engineering, and Radiological Research, Office of Nuclear Regulatory Research, NUREG/CR-6948, November 2007.
- 2.4-291 ~~National Nuclear Data Center, <http://www.nndc.bnl.gov/mird/>, accessed November 6, 2008.~~
- 2.4-292 ~~NUREG/CR-5512, Volume 1, Residual Radioactive Contamination from Decommissioning.~~

2.4-293 ~~Kenikow, L. F., and J. D. Bredehoeft, Computer Model of  
Two-Dimensional Solute Transport and Dispersion in Ground  
Water, Chapter C2, Book 7, Techniques of Water-Resources  
Investigations of the United States Geological Survey, 1978.~~

**Table 2.4-234**

**Groundwater Flow Estimates**

[EF3 COL 2.0-24-A]

<b>Conceptual Flow Path</b>	<b>Distance (feet)</b>	<b>Velocity (feet/day)</b>	<b>Travel Time (Days)</b>
Eastward to Lake Erie	1476	1.76	839
Westward Off-Site	4756	3.5	1359

Table 2.4-235

**Radionuclide Concentrations at Receptor Based on Eastward Flow Path to Lake Erie (Sheet 1 of 4)**

[EF3 COL 2.0-24-A]

Radio-nuclide	Progeny	Branching Fraction				Decay Rate (days <sup>-1</sup> )	Initial Concentration (µCi/cm <sup>3</sup> )	Groundwater Concentration (µCi/cm <sup>3</sup> )	ECL (µCi/cm <sup>3</sup> )	GW/ ECL
		Half-Life (days)	d12	d13	d23					
H-3		4.51E+03			1.54E-04	2.63E-03	2.31E-03	2.00E-03	2.31E+00	
Na-24		6.25E-01			1.11E+00	1.28E-03	0.00E+00	5.00E-05	0.00E+00	
P-32		1.43E+01			4.85E-02	5.35E-04	1.20E-21	9.00E-06	1.33E-16	
Cr-51		2.77E+01			2.50E-02	7.05E-02	5.46E-11	5.00E-04	1.09E-07	
Mn-54		3.13E+02			2.21E-03	2.66E-03	4.15E-04	3.00E-05	1.38E+01	
Mn-56		1.07E-01			6.48E+00	2.05E-03	0.00E+00	7.00E-05	0.00E+00	
Fe-55		9.86E+02			7.03E-04	8.32E-02	4.62E-02	1.00E-04	4.62E+02	
Fe-59		4.45E+01			1.56E-02	1.03E-03	2.20E-09	1.00E-05	2.20E-04	
Co-58		7.08E+01			9.79E-03	4.76E-03	1.30E-06	2.00E-05	6.48E-02	
Co-60		1.93E+03			3.59E-04	1.69E-02	1.25E-02	3.00E-06	4.17E+03	
Ni-63		3.51E+04			1.97E-05	8.76E-05	8.61E-05	1.00E-04	8.61E-01	
Cu-64		5.29E-01			1.31E+00	1.60E-03	0.00E+00	2.00E-04	0.00E+00	
Zn-65		2.44E+02			2.84E-03	7.16E-02	6.82E-03	5.00E-06	1.32E+03	
Rb-89		1.06E-02			6.54E+01	3.38E-05	0.00E+00	9.00E-04	0.00E+00	
Sr-89		5.05E+01	1.0000		1.37E-02	3.86E-03	3.88E-08	8.00E-06	4.86E-03	
Sr-90		1.06E+04			6.54E-05	6.03E-04	5.71E-04	5.00E-07	1.14E+03	
Y-90		2.67E+00	1.0000		2.60E-01	1.88E-05	5.71E-04	7.00E-06	8.15E+01	
Sr-91		3.96E-01			1.75E+00	1.54E-03	0.00E+00	2.00E-05	0.00E+00	
Y-91m		3.45E-02	0.5780		2.01E+01	0.00E+00	0.00E+00	2.00E-03	0.00E+00	
Y-91		5.85E+01		0.4220	1.18E-02	1.70E-03	8.28E-08	8.00E-06	1.04E-02	

Table 2.4-235

**Radionuclide Concentrations at Receptor Based on Eastward Flow Path to Lake Erie (Sheet 2 of 4)**

[EF3 COL 2.0-24-A]

Radio-nuclide	Progeny	Branching Fraction				Decay Rate (days <sup>-1</sup> )	Initial Concentration (µCi/cm <sup>3</sup> )	Groundwater Concentration (µCi/cm <sup>3</sup> )	ECL (µCi/cm <sup>3</sup> )	GW/ECL
		Half-Life (days)	d12	d13	d23					
Sr-92		1.15E-01				6.13E+00	8.78E-04	0.00E+00	4.00E-05	0.00E+00
Y-92	Y-92	1.48E-01	1.0000			4.68E+00	7.22E-04	0.00E+00	4.00E-05	0.00E+00
Y-93		4.21E-01				1.65E+00	1.62E-03	0.00E+00	2.00E-05	0.00E+00
Zr-95		6.40E+01				1.08E-02	3.62E-04	4.12E-08	2.00E-05	2.06E-03
Nb-95m		3.61E+00	0.0070			1.92E-01	0.00E+00	3.06E-10	3.00E-05	1.02E-05
Nb-95		3.52E+01		0.9930	1.0000	1.97E-02	2.37E-04	9.16E-08	3.00E-05	3.05E-03
Mo-99		2.75E+00				2.52E-01	5.59E-03	9.31E-95	2.00E-05	4.66E-90
Tc-99m		2.51E-01	0.8760			2.76E+00	4.65E-04	8.98E-95	1.00E-03	8.98E-92
Ru-103		3.93E+01				1.76E-02	6.46E-04	2.44E-10	3.00E-05	8.15E-06
Rh-103m		3.90E-02	0.9970			1.78E+01	6.30E-07	2.44E-10	6.00E-03	4.06E-08
Ru-106		3.68E+02				1.88E-03	2.21E-04	4.55E-05	3.00E-06	1.52E+01
Rh-106		3.45E-04	1.0000			2.01E+03	7.97E-10	4.55E-05		
Ag-110m		2.50E+02				2.77E-03	7.22E-05	7.06E-06	6.00E-06	1.18E+00
Ag-110		2.85E-04	0.0132			2.43E+03	0.00E+00	9.39E-08		
Te-129m		3.36E+01				2.06E-02	1.16E-03	3.57E-11	7.00E-06	5.10E-06
Te-129		4.83E-02	0.6500			1.44E+01	0.00E+00	2.32E-11	4.00E-04	5.81E-08
Te-131m		1.25E+00				5.55E-01	1.31E-04	1.60E-206	8.00E-06	2.00E-201
Te-131		1.74E-02	0.2220			3.98E+01	0.00E+00	3.61E-207	8.00E-05	4.51E-203
I-131		8.04E+00		0.7780	1.0000	8.62E-02	1.86E-02	7.57E-34	1.00E-06	7.57E-28
Te-132		3.26E+00				2.13E-01	3.27E-05	1.24E-82	9.00E-06	1.38E-77

**Table 2.4-235 Radionuclide Concentrations at Receptor Based on Eastward Flow Path to Lake Erie (Sheet 3 of 4)**

[EF3 COL 2.0-24-A]

Radio-nuclide	Progeny	Branching Fraction				Decay Rate (days <sup>-1</sup> )	Initial Concentration (µCi/cm <sup>3</sup> )	Groundwater Concentration (µCi/cm <sup>3</sup> )	ECL (µCi/cm <sup>3</sup> )	GW/ ECL
		Half-Life (days)	d12	d13	d23					
I-132	I-132	9.58E+02	1.0000			7.24E+00	1.28E-82	1.00E-04	1.28E-78	
I-133	Xe-133m	8.67E-01	0.0290			7.99E-01	1.16E-293	7.00E-06	1.66E-288	
	Xe-133	5.25E+00	0.9710	1.0000		3.17E-01	1.60E-149			
I-134		3.65E-02				1.90E+01	0.00E+00	4.00E-04	0.00E+00	
I-135		2.75E-01				2.52E+00	0.00E+00	3.00E-05	0.00E+00	
	Xe-135m	1.06E-02	0.1540			6.54E+01	0.00E+00			
	Xe-135	3.79E-01	0.8460	1.0000		1.83E+00	0.00E+00			
Cs-134		7.53E+02				9.21E-04	1.99E-03	9.19E-04	9.00E-07	
Cs-136		1.31E+01				5.29E-02	1.96E-04	1.06E-23	6.00E-06	
Cs-137		1.10E+04				6.30E-05	5.65E-03	5.36E-03	1.00E-06	
	Ba-137m	1.77E-03	0.9460			3.92E+02	1.00E-07	5.07E-03		
Cs-138		2.24E-02				3.09E+01	1.52E-04	0.00E+00	4.00E-04	
Ba-140		1.27E+01				5.46E-02	4.73E-03	6.33E-23	8.00E-06	
	La-140	1.68E+00	1.0000			4.13E-01	7.08E-04	7.30E-23	9.00E-06	
Ce-141		3.25E+01				2.13E-02	8.03E-04	1.38E-11	3.00E-05	
Ce-144		2.84E+02				2.44E-03	2.12E-04	2.74E-05	3.00E-06	
	Pr-144m	5.07E-03	0.0178			1.37E+02	0.00E+00	4.89E-07	9.15E+00	
	Pr-144	1.20E-02	0.9822	1.0000		5.78E+01	2.78E-08	2.74E-05	6.00E-04	
W-187		9.96E-01				6.96E-01	3.11E-04	1.22E-257	3.00E-05	

~~Table 2.4-235 Radionuclide Concentrations at Receptor Based on Eastward Flow Path to Lake Erie (Sheet 4 of 4)~~

~~[EFS COL 2.0-24-A]~~

~~Branching Fraction~~

Radio-nuclide	Progeny	Half-Life (days)	Branching Fraction		Decay Rate (days <sup>-1</sup> )	Initial Concentration (µCi/cm <sup>3</sup> )		ECL (µCi/cm <sup>3</sup> )	GW/ ECL
			d12	d13		d123	d123		
Np-239		2.36E+00			2.94E-01	1.94E-02	2.20E-109	2.00E-05	1.10E-104
	Pu-239	8.79E+06	1.0000		7.89E-08	0.00E+00	5.20E-09	2.00E-08	2.60E-01

Table 2.4-236

**Radionuclide Concentrations at Receptor Based on Westward Flow Path (Sheet 1 of 4)**

[EF3 COL 2.0-24-A]

Radio-nuclide	Progeny	Branching Fraction				Decay Rate (days <sup>-1</sup> )	Initial Concentration (µCi/cm <sup>3</sup> )	Groundwater Concentration (µCi/cm <sup>3</sup> )	ECL	
		Half-Life (days)	d12	d13	d23				(µCi/cm <sup>3</sup> )	GW/ ECL
H-3		4.51E+03			1.54E-04	2.63E-03	2.13E-03	1.00E-03	2.13E+00	
Na-24		6.25E-01			1.11E+00	1.28E-03	0.00E+00	5.00E-05	0.00E+00	
P-32		1.43E+01			4.85E-02	5.35E-04	1.58E-32	9.00E-06	1.53E-27	
Cr-51		2.77E+01			2.50E-02	7.05E-02	1.23E-16	5.00E-04	2.46E-13	
Mn-54		3.13E+02			2.21E-03	2.66E-03	1.31E-04	3.00E-05	4.38E+00	
Mn-56		1.07E-01			6.48E+00	2.05E-03	0.00E+00	7.00E-05	0.00E+00	
Fe-55		9.86E+02			7.03E-04	8.32E-02	3.20E-02	1.00E-04	3.20E+02	
Fe-59		4.45E+01			1.56E-02	1.03E-03	6.71E-13	1.00E-05	6.71E-08	
Co-58		7.08E+01			5.79E-03	4.76E-03	8.00E-09	2.00E-05	4.00E-04	
Co-60		1.93E+03			3.59E-04	1.69E-02	1.04E-02	3.00E-06	3.46E+03	
Ni-63		3.51E+04			1.97E-05	8.76E-05	8.53E-05	1.00E-04	8.53E-01	
Cu-64		5.29E-01			1.31E+00	1.60E-03	0.00E+00	2.00E-04	0.00E+00	
Zn-65		2.44E+02			2.84E-03	7.16E-02	1.51E-03	5.00E-06	3.02E+02	
Rb-89		1.06E-02			6.54E+01	3.38E-05	0.00E+00	9.00E-04	0.00E+00	
Sr-89		5.05E+01	1.0000		1.37E-02	3.86E-03	3.10E-11	8.00E-06	3.88E-06	
Sr-90		1.06E+04	1.0000		6.54E-05	6.03E-04	5.51E-04	5.00E-07	1.10E+03	
Sr-91		3.96E-01			2.60E-01	1.88E-05	5.52E-04	7.00E-06	7.88E+01	
Y-90		3.45E-02	0.5780		1.75E+00	1.54E-03	0.00E+00	2.00E-05	0.00E+00	
Y-91m		5.85E+01		0.4220	2.01E+01	0.00E+00	0.00E+00	2.00E-03	0.00E+00	
Y-91				1.0000	1.18E-02	1.70E-03	1.75E-10	8.00E-06	2.19E-05	

**Table 2.4-236**

**Radionuclide Concentrations at Receptor Based on Westward Flow Path (Sheet 2 of 4)**

[EF3 COL 2.0-24-A]

**Branching Fraction**

Radio-nuclide	Progeny	Half-Life (days)	d12	d13	d23	Decay Rate (days <sup>-1</sup> )	Initial Concentration (µCi/cm <sup>3</sup> )	Groundwater Concentration (µCi/cm <sup>3</sup> )	ECL (µCi/cm <sup>3</sup> )	GW/ ECL
Sr-92		1.13E+01				6.13E+00	8.78E-04	0.00E+00	4.00E-05	0.00E+00
Y-92		1.48E+01	1.0000			4.68E+00	7.22E-04	0.00E+00	4.00E-05	0.00E+00
Y-93		4.21E+01				1.65E+00	1.62E-03	0.00E+00	2.00E-05	0.00E+00
Zr-95		6.40E+01				1.08E-02	3.62E-04	1.48E-10	2.00E-05	7.41E-06
Nb-95m		3.61E+00	0.0070			1.92E-01	0.00E+00	1.10E-12	3.00E-05	3.67E-08
Nb-95		3.52E+01		0.9930	1.0000	1.97E-02	2.37E-04	3.30E-10	3.00E-05	1.10E-05
Mo-99		2.75E+00				2.52E-01	5.59E-03	1.22E-151	2.00E-05	6.10E-147
Te-99m		2.51E-01	0.8760			2.76E+00	4.65E-04	1.18E-151	1.00E-03	1.18E-148
Ru-103		3.93E+01				1.76E-02	6.46E-04	2.56E-14	3.00E-05	8.52E-10
Rh-103m		3.90E-02	0.9970			1.78E+01	6.30E-07	2.55E-14	6.00E-03	4.25E-12
Ru-106		3.68E+02				1.88E-03	2.21E-04	1.71E-05	3.00E-06	5.70E+00
Rh-106		3.45E-04	1.0000			2.01E+03	7.97E-10	1.71E-05		
Ag-110m		2.50E+02				2.77E-03	7.22E-05	1.67E-06	6.00E-06	2.79E-01
Ag-110		2.85E-04	0.0133			2.43E+03	0.00E+00	2.22E-08		
Te-129m		3.36E+01				2.06E-02	1.16E-03	7.89E-16	7.00E-06	1.13E-10
Te-129		4.89E-02	0.6500			1.44E+01	0.00E+00	5.13E-16	4.00E-04	1.28E-12
Te-131m		1.25E+00				5.55E-01	1.31E-04	0.00E+00	8.00E-06	0.00E+00
Te-131		1.74E-02	0.2220			3.98E+01	0.00E+00	0.00E+00	8.00E-05	8.00E+00
I-131		8.04E+00		0.7780	1.0000	8.62E-02	1.86E-02	2.65E-53	1.00E-06	2.65E-47
Te-132		3.26E+00				2.13E-01	3.27E-05	1.29E-130	9.00E-06	1.43E-125

**Radionuclide Concentrations at Receptor Based on Westward Flow Path (Sheet 3 of 4)**

[EF3 COL 2.0-24-A]

Radio-nuclide	Progeny	Branching Fraction				Decay Rate (days <sup>-1</sup> )	Initial Concentration (µCi/cm <sup>3</sup> )	Groundwater Concentration (µCi/cm <sup>3</sup> )	ECL (µCi/cm <sup>2</sup> )	GW/ ECL
		Half-Life (days)	d12	d13	d23					
I-132	I-132	9.58E+02	1.0000			7.24E+00	1.33E-130	1.00E-04	1.33E-126	
I-133		8.67E-01				7.99E-01	0.00E+00	7.00E-06	0.00E+00	
	Xe-133m	2.19E+00	0.0290			3.17E-01	0.00E+00	5.97E-191		
	Xe-133	5.25E+00		0.9710	1.0000	1.32E-01	0.00E+00	4.05E-81		
I-134		3.65E-02				1.90E+01	1.18E-03	0.00E+00	4.00E-04	
I-135		2.75E-01				2.52E+00	5.92E-03	0.00E+00	3.00E-05	
	Xe-135m	1.06E-02	0.1540			6.54E+01	0.00E+00	0.00E+00		
	Xe-135	3.79E-01		0.8460	1.0000	1.83E+00	0.00E+00	0.00E+00		
Cs-134		7.53E+02				9.27E-04	1.99E-03	5.70E-04	9.00E-07	
Cs-136		1.31E+01				5.29E-02	1.96E-04	1.21E-35	6.00E-06	
Cs-137		1.10E+04				6.30E-05	5.65E-08	5.19E-03	1.00E-06	
	Ba-137m	1.77E-03	0.9460			3.92E+02	1.00E-07	4.91E-03		
Cs-138		2.24E-02				3.09E+01	1.52E-04	0.00E+00	4.00E-04	
Ba-140		1.27E+01				5.46E-02	4.73E-03	3.05E-35	8.00E-06	
	La-140	1.68E+00	1.0000			4.13E-01	7.08E-04	3.52E-35	9.00E-06	
Ce-141		3.25E+01				2.13E-02	8.03E-04	2.12E-16	3.00E-05	
Ce-144		2.84E+02				2.44E-03	2.12E-04	7.72E-06	3.00E-06	
	Pr-144m	5.07E-03	0.0178			1.37E+02	0.00E+00	1.37E-07		
	Pr-144	1.20E-02		0.9822	1.0000	5.78E+01	2.78E-08	7.72E-06	6.00E-04	
	W-167	9.96E-01				6.96E-01	3.11E-04	0.00E+00	3.00E-05	

Table 2.4-236

Radionuclide Concentrations at Receptor Based on Westward Flow Path (Sheet 4 of 4)

[EF3 COL 2.0-24-A]

Radio-nuclide	Progeny	Branching Fraction			Decay Rate (days <sup>-1</sup> )	Initial Concentration (µCi/cm <sup>3</sup> )	Groundwater Concentration (µCi/cm <sup>3</sup> )	ECL (µCi/cm <sup>3</sup> )	GW/ ECL
		Half-Life (days)	d12	d13					
Np-239		2.36E+00			2.94E-01	1.94E-02	1.14E-175	2.00E-05	5.72E-171
	Pu-239	8.79E+06	1.0000		7.89E-08	0.00E+00	5.20E-09	2.00E-08	2.60E-01

**Table 2.0-2R**

**Limits Imposed on Acceptance Criteria in Section II of SRP by ESBWR Design (Sheet 3 of 5)**

[EF3 COL 2.0-2-A through 2.0-30-A] |

		<b>ESBWR DCD Parameters,</b>				
<b>Section</b>	<b>Subject</b>	<b>Considerations and/or Limits</b>	<b>COL Information</b>			
<b>EF3 COL 2.0-16-A</b>	Probable Maximum Surge and Seiche Flooding	Probable maximum surge and seiche flooding level does not exceed the maximum flood level defined in DCD Table 2.0-1.	Probable maximum tsunami flooding level does not exceed the maximum flood level defined in DCD Table 2.0-1.	COL Item 2.0-16-A is addressed in Subsection 2.4.5.		
<b>EF3 COL 2.0-17-A</b>	Probable Maximum Tsunami Flooding	Probable maximum tsunami flooding level does not exceed the maximum flood level defined in DCD Table 2.0-1.	Probable maximum tsunami flooding level does not exceed the maximum flood level defined in DCD Table 2.0-1.	COL Item 2.0-17-A is addressed in Subsection 2.4.6.		
<b>EF3 COL 2.0-18-A</b>	Ice Effects	None	None	COL Item 2.0-18-A is addressed in Subsection 2.4.7.		
<b>EF3 COL 2.0-19-A</b>	Cooling Water Canals and Reservoirs	None	None	COL Item 2.0-19-A is addressed in Subsection 2.4.8.		
<b>EF3 COL 2.0-20-A</b>	Channel Diversions	None	None	COL Item 2.0-20-A is addressed in Subsection 2.4.9.		
<b>EF3 COL 2.0-21-A</b>	Flooding Protection Requirements	None	None	COL Item 2.0-21-A is addressed in Subsection 2.4.10.		
<b>EF3 COL 2.0-22-A</b>	Cooling Water Supply	None	None	COL Item 2.0-22-A is addressed in Subsection 2.4.11.		
<b>EF3 COL 2.0-23-A</b>	Groundwater	Per DCD Table 2.0-1	Per DCD Table 2.0-1	COL Item 2.0-23-A is addressed in Subsection 2.4.12.		
<b>EF3 COL 2.0-24-A</b>	Accidental Releases of Liquid Effluents in Ground and Surface Waters	None	Addressed consistent with, and as per <del>DCD Section 46.3.16</del>	COL Item 2.0-24-A is addressed in Subsection 2.4.13.		
<b>EF3 COL 2.0-25-A</b>	Technical Specifications and Emergency Operation Requirements	None	None	COL Item 2.0-25-A is addressed in Subsection 2.4.14.		
<b>Fermi 3 Combined License Application</b>	2-4	The source term provided in DCD Table 12.2-13a, "Liquid Waste Management System Equipment Drain Collection Tank Activity," is used in the effects analysis.				Revision 1 March 2009

---

**EF3 COL 2.0-24-A 2.4.13 Accidental Releases of Liquid Effluents to Ground and Surface Waters**

**2.4.13.1 Mitigating Design Features**

Mitigating design features specified in NUREG 0800 Branch Technical Position (BTP) 11-6 are incorporated into the design of Fermi 3 to preclude an accidental release of liquid effluents. Descriptions of these features are provided below.

Below-grade tanks containing radioactivity are located on levels B1F and B2F of the Radwaste Building. The Radwaste Building is designed to seismic requirements as specified in DCD Table 3.2-1. In addition, as described in DCD Section 11.2.2.3, compartments containing high level liquid radwaste are steel lined up to a height capable of containing the release of all liquid radwaste in the compartment. Leaks as a result of major cracks in tanks result in confinement of the liquid radwaste in the compartment and the building sump system for containment in other tanks or emergency tanks. Because of these design capabilities, it is not considered feasible that any major event involving the release of liquid radwaste into these volumes results in the release of these liquids to the groundwater environment via the liquid pathway.

The Condensate Storage Tank (CST), part of the Condensate Storage and Transfer System (CS&TS), is the only above-grade tank that potentially could contain radioactivity outside of containment, the reactor building, or the radwaste building. The CS&TS, described in DCD Section 9.2.6, meets GDC 60 by compliance with RG 1.143, Position C.1.2 for design features provided to control the release of liquid effluents containing radioactive material. The basin surrounding the tank is designed to prevent uncontrolled runoff in the event of a tank failure. The basin volume is sized to contain the total tank capacity. Tank overflow is also collected in this basin. A sump located inside the retention basin has provisions for sampling collected liquids prior to routing them to the Liquid Waste Management System (LWMS) or the storm sewer as per sampling and release requirements. These design features are intended to preclude the release of liquids from the CST to either the ground or surface water environment via the liquid pathway.

The mitigating design features described above demonstrate that the radioactive waste management systems, structures, and components

for Fermi 3, as defined in RG 1.143, include features to preclude accidental releases of radionuclides into potential liquid pathways. Nevertheless, an analysis of accidental releases of radioactive liquid effluents in groundwater is performed. Descriptions and results of these analyses are provided herein.

#### 2.4.13.2 **Groundwater Analysis**

The discussion in Section 2.4.13.1 demonstrates that the Fermi 3 LWMS design will preclude accidental release of radioactive liquid effluents to the environment. Nevertheless, in accordance with SRP 11.2, analyses of the bounding release of radioactive liquid effluents to the groundwater and consequently to the nearest sources of potable water in an unrestricted area are performed.

This section provides a conservative and bounding analysis of a postulated, accidental release of radioactive liquid effluents to the groundwater. The accident scenario is described, and the model used to evaluate radionuclide transport is presented, along with potential pathways of contamination to water users. The radionuclide transport analysis is described, and the results are summarized. The radionuclide concentrations are compared against the regulatory limits.

##### 2.4.13.2.1 **Accident Scenario**

A liquid radwaste tank outside of containment is postulated to fail, coincident with the non-mechanistic failure of the above described mitigation design features, thus allowing the tank contents to be released to groundwater. The volume of the liquid assumed released and the associated radionuclide concentrations were selected to produce an accident scenario that leads to the most adverse contamination of groundwater.

Radwaste tanks outside of containment are located on levels B1F and B2F of the radwaste building as shown on DCD Figure 1.2-25. The radwaste tanks having the largest volumes include the three equipment drain collection tanks and the two equipment drain sample tanks, all in the lowest level, B2F. Each of these tanks has a volume of approximately 37,000 gallons (140 m<sup>3</sup>) per DCD Table 11.2-2a.

Activity concentrations in various liquid radwaste tanks are provided in DCD Tables 12.2-13a through 12.2-13g. Of these tanks, the limiting tank in terms of radionuclide activity is the equipment drain collection tank; whose activity is provided in DCD Table 12.2-13a (see DCD Table 2.0-2, for Section 2.4.13).

The scenario assumes that one of the equipment drain collection tanks fails and its contents are released directly to the groundwater. Note that this accident scenario is extremely conservative because the radwaste building is seismically designed in accordance with RG 1.143, Class RW-IIa, as described in DCD Section 12.2.1.4. Also, each tank cubicle is provided with a steel liner, as described in DCD Section 11.2.2.3, to preclude any potential liquid releases to the environment.

#### **2.4.13.2.2 Transport Model**

Based on the COL stage investigations of the Fermi 3 power block and surrounding area documented in Section 2.4.12, specific site characteristics related to groundwater and transport pathway through the underlying material were developed.

The conceptual transport model is used to evaluate the accidental release of radioactive liquid effluent to groundwater. Key elements and assumptions embodied in this evaluation are described and discussed below.

As indicated earlier, one of the equipment drain collection tanks is assumed to be the source of the release, with each tank having a capacity of 140 m<sup>3</sup> (37,000 gal) and radionuclide concentrations as given in DCD Table 12.2-13a. These tanks are located on the lowest level of the radwaste building (level B2F), which has a floor elevation of approximately 540 feet NAVD88 (Figure 2.5.4-204). One of the tanks is postulated to rupture, and 80 percent of the liquid volume (112 m<sup>3</sup> or 29,600 gal) is assumed to be released following the guidance provided in BTP 11-6. Following tank rupture, it is conservatively assumed that a pathway is created that allows the entire 112 m<sup>3</sup> to enter the groundwater (unconfined aquifer) instantaneously.

The assumption of instantaneous release to the groundwater following tank rupture is conservative because it requires failure of the floor drain system, plus it ignores the barriers presented by the basemat concrete and the steel liners incorporated into the tank cubicles of the radwaste building, which is seismically designed. It should also be recognized that level B2F of the radwaste building is well below the water table. Piezometric head contour maps presented in Figure 2.4-246 through Figure 2.4-249 indicate that the ambient water table in the vicinity of the radwaste building is about 567 feet NAVD88, or 27 ft above the radwaste building floor elevation. If the basemat or exterior walls of the radwaste building and associated steel liners were to fail simultaneously, groundwater would flow into the radwaste building,

precluding the release of liquid effluents out of the building. Only if the interior of the radwaste building was flooded to a level higher than the surrounding groundwater would there be a pathway for liquid effluents to be released out of the building and to the groundwater. Hence, the assumption of an accidental release of liquid effluents from the radwaste building to groundwater is extremely conservative, given the design features of the radwaste building intended to prevent an accidental release and the hydrogeologic conditions at the site.

In the worst-case postulated accidental release scenario, radionuclides are released directly to the Bass Islands aquifer and migrate with the groundwater in the direction of decreasing hydraulic head. Section 2.4.12.3.1 describes potential pathways in the bedrock (Bass Islands aquifer). As described in Section 2.4.12.3.1 there are two potential pathways for groundwater:

- The documented present day condition, in which the groundwater flow direction in the Bass Islands aquifer is westward off-site.
  
- A possible future condition in which the flow direction has returned to the east toward Lake Erie.

The present day condition is attributed to dewatering associated with quarrying operations westward of the site. The possible future condition is intended to account for the case where the quarrying operations were to cease. For the purposes of this evaluation, both potential flow paths are considered. To the west off-site, the assumed receptor is a well located at the west corner of Enrico Fermi Drive and Toll Road as shown on Figure 2.4-236. To the east, the receptor is Lake Erie. The distances from the source to each receptor are conservatively selected. For the path from the radwaste building to the well off-site to the west, the source location is assumed to be the closest western side of the radwaste building. For the path from the radwaste building to Lake Erie, the source is assumed to be the closest eastern side of the radwaste building.

The analysis allows for radionuclide decay during transport by groundwater, and considers this decay in the analysis. Radionuclide transport by groundwater is affected by adsorption by the surrounding soils.

The Fermi site is assumed to continually receive the average annual precipitation; precipitation that does not run off or is not lost to

evapotranspiration infiltrates through the unsaturated zone and into the groundwater.

Parameters such as distribution coefficients, hydraulic conductivity, porosity, and hydraulic gradient used in the analysis are provided in Table 2.4-234. Dilution of the radionuclide source term during the instantaneous release outside the radwaste building is not modeled in the analysis. Additionally, all radioisotope constituents of the source term in DCD Table 12.2-13a are included in the analysis. Values were selected to conservatively bound the hydrogeologic properties from the surface to the bottom of the Bass Islands Aquifer. As an example of the conservatism, Section 2.4.12.2.4.2 reports the maximum average hydraulic conductivity of the Bass Islands as 2.1 meters/day (767 meters/year). The groundwater analyses were performed with a value of 197,719 meters/year based on the rock fill. This input alone represents a factor of conservatism of approximately 250. This conservatism was selected to provide a bounding analysis.

Distribution (adsorption) coefficients ( $K_d$  values) were determined based on laboratory testing of rock samples from the Bass Islands formation. Samples for the laboratory testing were taken from nine different locations on site. The locations for the laboratory testing samples were selected based on the postulated groundwater flow path either to the west to the off site water well or to the east to Lake Erie. Water samples from on-site monitoring wells screened in the Bass Islands aquifer approximately along the flow paths were used during the laboratory testing. Based on the use of site water samples for the laboratory testing, impacts due to potential contaminants in the groundwater at the site that could affect the transport and adsorption are accounted for. In order to simulate the fractured nature of the Bass Islands formation, the samples were broken into pieces for the laboratory testing. The material was not crushed or pulverized as this may not conservatively represent the sub-surface conditions.

Distribution coefficient measurements were obtained for cerium, cesium, cobalt, iron, manganese, ruthenium, silver, strontium, yttrium, and zinc. Selection of radionuclides for determination of distribution coefficients was based on the activity of the equipment drain collection tank source term and screening evaluations. The screening evaluations determined concentrations for the various radionuclides present in the equipment drain collection tank, including the associated progeny(s) considering only the decay of the radionuclides during the transport to the nearest off site water well and surface water body. The results from the screening evaluation were then compared to the 10 CFR Part 20, Appendix B, Table 2, limits. Radionuclides were selected for the

laboratory analysis where the concentration predicted, crediting decay only, exceeded the limit.

In the transport analysis, the minimum distribution coefficient values were used for each element analyzed irrespective of their sample location. Distribution coefficients for other elements in the analysis were assigned a value of zero, which is conservative since it assumes no retardation during transport. Using the minimum distribution coefficient values ensures that the transport analysis results are conservative.

Aquifer parameters were established for the Bass Island aquifer (see Section 2.4.12). For this accidental release groundwater transport model, the hydraulic conductivity and hydraulic gradient measured at the site were selected to ensure very conservative results.

The total porosity value was used to be conservative with respect to available information for other areas of the Bass Islands formation in the State of Michigan (References 2.4-295). The effective porosity value was initially selected from a report of similar material (i.e., dolomite), Reference 2.4-291, and confirmed to be conservative through sensitivity cases with RESRAD-OFFSITE.

The travel times of the groundwater movement from the radwaste building to the receptor were computed from a variation of Darcy's Law:

$$t = \frac{x}{V} = \frac{x}{KI/\theta}$$

Where: t = time to move distance x (yr)

x = distance of contaminant movement (m)

V = average interstitial groundwater velocity (m/yr)

K = hydraulic conductivity (m/yr)

I = hydraulic gradient

$\theta$  = effective porosity

The values of parameters used are shown in Table 2.4-234.

#### 2.4.13.2.3 Radionuclide Transport Analysis

Radionuclide concentrations in groundwater along the transport pathway toward the closest off site well or Lake Erie as a result of an accidental release of an equipment drain collection tank contents directly to the groundwater were modeled using RESRAD-OFFSITE (Reference 2.4-292). Except for the distance from the radwaste building to the receptors and the dispersivities, the inputs for both postulated flow paths are the same.

The RESRAD-OFFSITE computer code evaluates the radiological dose to an individual who is exposed while located outside the area of initial (primary) release. The primary release, which is the source of all the radionuclides modeled by the code, is a layer of soil below the radwaste building. The code models the movement of the radionuclides from the primary release to user-defined points along the transport pathway.

The groundwater pathway mechanism is a first-order transport model that considers the effects of different transport rates for radionuclides and progeny nuclides, while allowing decay during the transport process. Concentrations of each radionuclide transmitted to the assumed drinking water source (closest off site well or Lake Erie) are determined by the transport through the groundwater system, dilution by groundwater and infiltrating surface water from the overburden soils, adsorption, and decay.

Any radionuclides at the point of analysis are assumed to remain at the analysis receptor point for a period of one year.

For the RESRAD-OFFSITE analysis, the longitudinal and transverse horizontal dispersivity values to the closest off site well and Lake Erie were estimated using References 2.4-292 through 2.4-294. The values used in the analysis are shown in Table 2.4-234.

#### 2.4.13.2.4 **Comparison with 10 CFR 20 ECL**

Table 2.4-235 lists the radionuclides predicted at the closest off site well and compares their concentrations to 10 CFR 20, Appendix B, Table 2, Column 2 limits. All radionuclide concentrations are under the limits. The predicted activity with respect to the 10 CFR 20 limits for Strontium-90 is a factor of 8.7 under the limits. Meeting 10 CFR 20 limits at the closest off site well demonstrates that the radiological consequences of a postulated failure of one of the equipment drain collection tanks are also acceptable for larger distances from the radwaste building.

Table 2.4-236 lists the radionuclides predicted at Lake Erie and compares their concentrations to 10 CFR 20, Appendix B, Table 2, Column 2 limits. All radionuclide concentrations are under the limits. The predicted activity with respect to the 10 CFR 20 limits for Strontium-90 is a factor of 4.5 under the limits. Meeting 10 CFR 20 limits at Lake Erie demonstrates that the radiological consequences of a postulated failure of one of the equipment drain collection tanks are also acceptable for larger distances from the radwaste building.

10 CFR 20, Appendix B, Table 2 imposes additional requirements when the identity and concentration of each radionuclide in a mixture are known. In this case, the ratio present in the mixture and the concentration otherwise established in 10 CFR 20 for the specified radionuclides not in a mixture must be determined. The sum of such ratios for all of the radionuclides in the mixture may not exceed "1" (i.e., "unity"). The sum of fractions approach has been applied to the radionuclide concentrations for both pathways. Results are summarized in Tables 2.4-235 and 2.4-236. As shown in Tables 2.4-235 and 2.4-236, the sum of fractions for the mixtures at the closest off site well and at Lake Erie are less than unity.

10 CFR 20, Appendix B states, "The columns in Table 2 of this appendix captioned "Effluents," "Air," and "Water," are applicable to the assessment and control of dose to the public, particularly in the implementation of the provisions of §20.1302. The concentration values given in Columns 1 and 2 of Table 2 are equivalent to the radionuclide concentrations which, if inhaled or ingested continuously over the course of a year, would produce a total effective dose equivalent of 0.05 rem (50 millirem or 0.5 millisieverts). Thus, meeting the concentration limits of 10 CFR 20, Appendix B, Table 2, Column 2 results in a dose of less than 0.05 rem and therefore demonstrates that the requirements of 10 CFR 20.1301 and 10 CFR 20.1302 are met.

## References

- 2.4-291 USGS Scientific Investigations Report 2004-5031, "Simulation of Ground-Water Flow, Surface Water Flow, and a Deep Sewer Tunnel System in the Menomonee Valley, Milwaukee, Wisconsin"
- 2.4-292 Yu, C. et. al., NUREG/CR-6937, "User's Manual for RESRAD-OFFSITE Version 2," Argonne National Laboratory, June 2007.
- 2.4-293 Boulding, J.R. and Ginn, J.S., "Practical Handbook of Soil, Vadose Zone, and Ground-Water Contamination, Assessment and Prevention," CRC Press, Boca Raton, Florida, 2004.
- 2.4-294 Electric Power Research Institute (EPRI), Estimation of Hydrodynamic Dispersivity in Selected Subsurface Materials, EPRI RP2485-05, EPRI, Palo Alto, California, 1994.
- 2.4-295 Midwest Regional Carbon Sequestration Partnership (MRCSP), Fact Sheet for Partnership Field Validation Test, Submitted by Battelle, dated November 2007. [http://www.netl.doe.gov/publications/proceedings/07/rcsp/factsheets/17-MRCSP\\_Michigan%20Basin%20Geologic%20Test.pdf](http://www.netl.doe.gov/publications/proceedings/07/rcsp/factsheets/17-MRCSP_Michigan%20Basin%20Geologic%20Test.pdf)

**Table 2.4-234 (Sheet 1 of 2)**  
**Site Specific RESRAD-OFFSITE Inputs**

Parameter	Description	Value
Cerium Kd (cm <sup>3</sup> /g)	Radionuclide-specific distribution coefficient	4575
Cesium Kd (cm <sup>3</sup> /g)	Radionuclide-specific distribution coefficient	1078
Cobalt Kd (cm <sup>3</sup> /g)	Radionuclide-specific distribution coefficient	640
Iron Kd (cm <sup>3</sup> /g)	Radionuclide-specific distribution coefficient	2.88
Manganese Kd (cm <sup>3</sup> /g)	Radionuclide-specific distribution coefficient	394
Ruthenium Kd (cm <sup>3</sup> /g)	Radionuclide-specific distribution coefficient	42.9
Silver Kd (cm <sup>3</sup> /g)	Radionuclide-specific distribution coefficient	0.41
Strontium Kd (cm <sup>3</sup> /g)	Radionuclide-specific distribution coefficient	0.44
Yttrium Kd (cm <sup>3</sup> /g)	Radionuclide-specific distribution coefficient	3183
Zinc Kd (cm <sup>3</sup> /g)	Radionuclide-specific distribution coefficient	16.7
Total porosity (unitless)	Total soil porosity, which is the ratio of the soil pore volume to the total volume	0.25
Effective porosity (unitless)	The amount of interconnected pore space through which fluids can pass, expressed as a percent of bulk volume	0.01
Hydraulic conductivity (m/yr)	A coefficient of proportionality describing the rate at which water can move through a permeable medium	197,719
Hydraulic gradient to surface water body and off site well (unitless)	Change in groundwater elevation per unit of distance in the direction of groundwater flow to a surface water body or off site well.	0.002

**Table 2.4-234 (Sheet 2 of 2)**  
**Site Specific RESRAD-OFFSITE Inputs**

Parameter	Description	Value
Distance to the nearest off site water well not in a restricted area (ft. (m))	Distance to the nearest off-site water well	4373 (1333)
Distance to the nearest surface water body (Lake Erie) (ft. (m))	Distance to the nearest off-site surface water body that contributes to a potable drinking water source	1554 (474)
Precipitation (m/yr)	Site annual average precipitation	0.892
Dry bulk density (gm/cm <sup>3</sup> )	Mass of (dry) solids in a unit volume of soil. A range of average dry bulk densities was determined based on tests.	1.68 – 2.4
Longitudinal Dispersivity to Lake Erie (m)	Ratio between the longitudinal dispersion coefficient and pore water velocity with a dimension of length. This value is based on the aquifer materials and the distance downgradient from the contaminant source.	8.21
Transverse Horizontal Dispersivity to Lake Erie (m)	Ratio between the horizontal lateral dispersion coefficient and pore water velocity with a dimension of length. This value is based on the aquifer materials and the distance downgradient from the contaminant source.	1.03
Longitudinal Dispersivity to off site well (m)	Ratio between the longitudinal dispersion coefficient and pore water velocity with a dimension of length. This value is based on the aquifer materials and the distance downgradient from the contaminant source.	11.77
Transverse Horizontal Dispersivity to off site well (m)	Ratio between the horizontal lateral dispersion coefficient and pore water velocity with a dimension of length. This value is based on the aquifer materials and the distance downgradient from the contaminant source.	3.30

**Table 2.4-235 (Page 1 of 2) – Comparison of Liquid Release Concentrations With 10 CFR 20 Concentrations – Off Site Water Well**

<b>Nuclide</b>	<b>Maximum Concentration (μCi/ml)</b>	<b>10 CFR 20 Concentration (μCi/ml)</b>	<b>Max Concentration / 10 CFR Limit</b>
Ac-227	1.01E-31	5.00E-09	2.02E-23
Ag-110m	5.25E-09	6.00E-06	8.75E-04
Ba-140	6.33E-07	8.00E-06	7.91E-02
Co-60	2.31E-20	3.00E-06	7.71E-15
Cr-51	2.00E-05	5.00E-04	4.00E-02
Cs-134	4.81E-46	9.00E-07	5.35E-40
Cs-137	3.98E-14	1.00E-06	3.98E-08
Cu-64	1.60E-13	2.00E-04	7.98E-10
Fe-55	9.38E-07	1.00E-04	9.38E-03
Fe-59	3.55E-11	1.00E-05	3.55E-06
Fr-223	1.39E-33	8.00E-06	1.74E-28
H-3	2.44E-06	1.00E-03	2.44E-03
I-129	4.17E-15	2.00E-07	2.09E-08
I-132	5.84E-10	1.00E-04	5.84E-06
La-140	7.22E-07	9.00E-06	8.02E-02
Mn-54	7.80E-42	3.00E-05	2.60E-37
Mo-99	6.03E-08	2.00E-05	3.02E-03
Na-24	9.93E-13	5.00E-05	1.99E-08
Nb-93m	1.75E-16	2.00E-04	8.77E-13
Nb-95	2.21E-07	3.00E-05	7.38E-03
Nb-95m	1.33E-09	3.00E-05	4.45E-05
Ni-63	8.21E-08	1.00E-04	8.21E-04
Np-239	1.26E-07	2.00E-05	6.31E-03
P-32	8.01E-08	9.00E-06	8.91E-03
Pa-231	8.67E-28	6.00E-09	1.45E-19
Pb-211	4.16E-33	2.00E-04	2.08E-29
Pr-144	4.91E-12	2.00E-05	2.46E-07
Pu-239	4.99E-12	2.00E-08	2.49E-04
Ra-223	4.20E-33	1.00E-07	4.20E-26
Re-187	1.70E-20	8.00E-03	2.12E-18
Rh-103m	3.78E-10	6.00E-03	6.30E-08
Ru-103	6.74E-38	3.00E-05	2.25E-33
Ru-106	9.40E-15	3.00E-06	3.13E-09
Sr-89	7.02E-08	8.00E-06	8.78E-03
Sr-90	5.76E-08	5.00E-07	1.15E-01
Sr-91	3.09E-41	2.00E-05	1.55E-36
Tc-99	1.89E-13	6.00E-05	3.16E-09
Tc-99m	5.82E-08	1.00E-03	5.82E-05
Te-129	2.53E-07	4.00E-04	6.33E-04
Te-129m	3.89E-07	7.00E-06	5.55E-02
Te-132	5.67E-10	9.00E-06	6.30E-05
Th-227	1.84E-32	2.00E-06	9.20E-27
Th-231	1.27E-21	5.00E-05	2.54E-17
U-235	1.28E-21	3.00E-07	4.28E-15
W-187	2.01E-11	3.00E-05	6.70E-07

**Table 2.4-235 (Page 2 of 2) – Comparison of Liquid Release Concentrations With 10 CFR 20 Concentrations – Off Site Water Well**

<b>Nuclide</b>	<b>Maximum Concentration (μCi/ml)</b>	<b>10 CFR 20 Concentration (μCi/ml)</b>	<b>Max Concentration / 10 CFR Limit</b>
Zn-65	3.50E-10	5.00E-06	7.00E-05
Zr-93	9.83E-15	4.00E-05	2.46E-10
Zr-95	1.88E-07	2.00E-05	9.42E-03
<b>SUM of FRACTIONS</b>			<b>4.29E-01</b>

**Table 2.4-236 (Page 1 of 2) – Comparison of Liquid Release Concentrations With 10 CFR 20 Concentrations – Lake Erie**

<b>Nuclide</b>	<b>Maximum Concentration (μCi/ml)</b>	<b>10 CFR 20 Concentration (μCi/ml)</b>	<b>Max Concentration / 10 CFR Limit</b>
Ac-227	8.56E-23	5.00E-09	1.71E-14
Ag-110m	4.54E-09	6.00E-06	7.57E-04
Ba-140	4.10E-08	8.00E-06	5.12E-03
Co-60	1.48E-13	3.00E-06	4.94E-08
Cr-51	2.34E-06	5.00E-04	4.69E-03
Cs-134	8.95E-24	9.00E-07	9.95E-18
Cs-137	1.99E-11	1.00E-06	1.99E-05
Cu-64	3.13E-12	2.00E-04	1.56E-08
Fe-55	1.79E-06	1.00E-04	1.79E-02
Fe-59	3.69E-10	1.00E-05	3.69E-05
Fr-223	1.18E-24	8.00E-06	1.48E-19
H-3	1.90E-06	1.00E-03	1.90E-03
I-129	5.15E-15	2.00E-07	2.57E-08
I-132	3.64E-11	1.00E-04	3.64E-07
I-134	2.51E-33	4.00E-04	6.27E-30
La-140	4.61E-08	9.00E-06	5.12E-03
Mn-54	3.63E-22	3.00E-05	1.21E-17
Mo-99	4.34E-09	2.00E-05	2.17E-04
Na-24	6.50E-12	5.00E-05	1.30E-07
Nb-93m	5.08E-17	2.00E-04	2.54E-13
Nb-95	8.02E-08	3.00E-05	2.67E-03
Nb-95m	3.63E-10	3.00E-05	1.21E-05
Ni-63	6.61E-08	1.00E-04	6.61E-04
Np-239	1.08E-08	2.00E-05	5.40E-04
P-32	5.66E-09	9.00E-06	6.28E-04
Pa-231	8.55E-23	6.00E-09	1.43E-14
Pb-211	8.56E-23	2.00E-04	4.28E-19
Pr-144	2.51E-16	2.00E-05	1.26E-11
Pu-239	3.94E-12	2.00E-08	1.97E-04
Ra-223	8.56E-23	1.00E-07	8.56E-16
Re-187	1.29E-20	8.00E-03	1.61E-18
Rh-103m	1.08E-13	6.00E-03	1.80E-11
Ru-103	3.20E-21	3.00E-05	1.07E-16
Ru-106	6.00E-12	3.00E-06	2.00E-06
Sr-89	4.55E-08	8.00E-06	5.68E-03
Sr-90	1.12E-07	5.00E-07	2.25E-01
Sr-91	8.87E-23	2.00E-05	4.44E-18
Sr-92	9.76E-46	4.00E-05	2.44E-41
Tc-99	1.51E-13	6.00E-05	2.52E-09
Tc-99m	4.18E-09	1.00E-03	4.18E-06
Te-129	3.49E-08	4.00E-04	8.73E-05
Te-129m	5.37E-08	7.00E-06	7.67E-03
Te-132	3.54E-11	9.00E-06	3.93E-06
Th-227	8.44E-23	2.00E-06	4.22E-17
Th-231	4.37E-21	5.00E-05	8.74E-17

**Table 2.4-236 (Page 2 of 2) – Comparison of Liquid Release Concentrations With 10 CFR 20 Concentrations – Lake Erie**

<b>Nuclide</b>	<b>Maximum Concentration (μCi/ml)</b>	<b>10 CFR 20 Concentration (μCi/ml)</b>	<b>Max Concentration / 10 CFR Limit</b>
U-235	4.38E-21	3.00E-07	1.46E-14
W-187	1.35E-11	3.00E-05	4.49E-07
Y-90	1.11E-07	7.00E-06	1.59E-02
Y-91	2.88E-23	8.00E-06	3.60E-18
Y-91m	5.12E-23	2.00E-03	2.56E-20
Y-92	9.73E-46	4.00E-05	2.43E-41
Zn-65	1.67E-08	5.00E-06	3.33E-03
Zr-93	9.03E-16	4.00E-05	2.26E-11
Zr-95	4.91E-08	2.00E-05	2.46E-03
<b>SUM of FRACTIONS</b>			<b>3.00E-01</b>

**Attachment 5  
NRC3-09-0026**

**Reference No. 1 from RAI 02.04.13-6**

**Midwest Regional Carbon Sequestration Partnership (MRCSP), Fact Sheet  
for Partnership Field Validation Test, Submitted by Battelle, dated November  
2007  
(following 8 pages)**

# FACT SHEET FOR PARTNERSHIP FIELD VALIDATION TEST

## Midwest Regional Carbon Sequestration Partnership (MRCSP)

NETL Cooperative Agreement DE-FC26-05NT42589

DOE/NETL Project Manager: Lynn Brickett,  
[Lynn.Brickett@NETL.DOE.GOV](mailto:Lynn.Brickett@NETL.DOE.GOV)

Submitted by Battelle

November 2007



<b>Michigan Basin Geologic Test, Otsego County Michigan</b>	
Principal Investigator	Dave Ball, Battelle (614-424-4901; balld@battelle.org)
Test Location	Charlton 30/31 Field, Otsego County, Michigan
Amount and Source of CO <sub>2</sub>	~10,000 metric tons                      Source = DTE Turtle Lake Gas Processing Plant, Otsego Co., Michigan
Field Test Partners (Primary Sponsors)	DTE Energy (Detroit Edison)
	Core Energy LLC
	Western Michigan University/Michigan Basin Core Research Laboratory
<b>Summary of Field Test Site and Operations:</b>	
<p>The site is located at State-Charlton 30/31 field, Southern Dover Township/Northern Chester Township, Otsego County, Michigan (Figure 1). This location is an enhanced oil recovery (EOR) field operated by Core Energy and is in the vicinity of a DTE gas processing plant outside of Gaylord, Michigan. The area is composed of state forest in rolling to hilly topography with little development beyond some farms and scattered homes.</p> <p>The objective at this site is to test CO<sub>2</sub> sequestration in deep saline rock formations (Figure 2). This portion of the basin is in an area of active enhanced oil recovery (EOR) projects, which provide a secondary research objective. High purity CO<sub>2</sub> is available from a DTE or other natural gas processing plants in the area. Oil and gas production in the area of the Michigan Basin site is active. Currently, gas is produced from Antrim shales in the area. CO<sub>2</sub> is a byproduct of the gas produced, and it is removed at gas processing plants before the gas is ready for use. Periodically, this CO<sub>2</sub> is used for enhanced oil recovery in the Niagaran Reefs. The CO<sub>2</sub> is captured, compressed, and injected in the reefs to flush out residual oil in the rocks. This makes a significant amount of infrastructure available for testing CO<sub>2</sub> sequestration in saline formations located adjacent to Niagaran Reefs.</p> <p>The site is situated in the Michigan Basin, a regional geologic structure in which sedimentary rocks form a basin in the lower peninsula of Michigan. Like most of the MRCSP region, thick sequences of sedimentary rock overlie Precambrian age basement rock at the site (Figure 3). The objective at this site is injection in a deep regional saline formation(s).</p> <p>The target sequestration interval is the Bass Islands Dolomite. The Bass Islands Group in the Michigan</p>	

Basin consists mostly of light brown to buff dolostone with argillaceous dolostone and anhydrite present lower in the section. The entire Bass Islands interval reaches a thickness of 300-600 ft in the central basin but thins substantially due to erosional unconformity in the southwest corner of the basin. Near the well site, the Bass Islands formation can be correlated in well logs. In addition, higher quality logs in Otsego County show that very good lithologic correlation for the unit across the county. In core from the test well, the Bass Islands Group was present at a depth interval of 3,442-3,700 ft. A high-density anhydrite interval was present in the lower section at 3,515-3,700 ft. Transitional upsection in core and logs is a porous and permeable dolostone unit at 3,442-3,515 ft, informally referred to here as the Bass Islands dolomite. This interval in core is the main injection target and is characterized by interbedded, laminated algal dolomudstone, minor cross-bedded and sandy dolograins, intraclast beds, and disrupted karstic breccia zones. The Bass Islands Dolomite is overlain by the Lower Devonian Bois Blanc Formation, a wide spread lithostratigraphic unit in the Michigan basin subsurface characterized by cherty carbonates ranging from calcareous chert, to cherty limestone and dolostone, to limestone and dolomitic limestone. This unit is considered an intermediate containment zone. The Bois Blanc Formation was present at a depth of 3,190-3,442 ft in State-Charlton #4-30. Core from the test well consists of a distinctive and complex mixture of sparsely fossiliferous, moderately burrowed, chert-rich limestone, cherty dolomitic limestone and dolostone. Complex alteration of these lithofacies has resulted in highly variable textures including differential compaction structures. Nodular gray chert in core shows irregular alteration to a lighter colored, probably more micro-porous texture at nodule selvages. This alteration style is volumetrically minor and constitutes less than 10% of cherty lithofacies. Rock layers dip toward the south at about 50 ft/mile in the study area, and no faulting or fracturing exists in the area beyond subtle changes in thickness.

Shale and dense limestone units in the Bois-Blanc-Amherstberg group provide containment immediately above the Bass Islands Dolomite. In most parts of the basin, the Amherstburg is dense, tight limestone and will likely be a good sealing unit. The Amherstburg ranges in thickness from a zero edge in the southwest to more than 300 ft thick in the central basin. The Amherstburg is the middle formation of the Detroit River Group and consists mostly of limestone. An informal, subsurface sandstone member, called the Filer sandstone, occurs in areas to the west. In the test well, the Amherstburg was 248 ft thick at a depth interval of 2,942-3,190 ft. The Amherstburg Formation in core consists of fossiliferous, dense, skeletal wackestone to mud-rich packstone. The rock is generally very dense with little visible porosity in most intervals. Additional salt and anhydrite layers, which are considered excellent sealing units, are present in the overlying Lucas Formation. Possibly due to these salt layers, the rocks are saturated with brine in excess of 100,000 mg/L. The deepest underground source of drinking water in the area is from shallow glacial drift less than 50 ft deep. Total thickness of glacial drift is over 500 ft thick.

Many oil and gas wells penetrate the target storage reservoir in the area. In fact, over 135 wells in the area were identified. However, most of the wells are cased through the target injection interval or completed in the shallower Antrim shale. Therefore, borehole leakage is not considered a significant pathway. No other leakage routes were identified.

Geology at the site is very well-characterized due to oil and gas exploration in the area. Many wells have been drilled in the area. As such, many well logs are available. In addition, a 3D seismic survey was completed through the area as part of another DOE program and was made available to MRCSP. However, most wells did not log the target zone (Bass Islands Dolomite). Consequently, there are only basic logs through the interval. Some additional logging and sidewall cores through the zone are necessary to confirm what looks like good porosity and permeability.

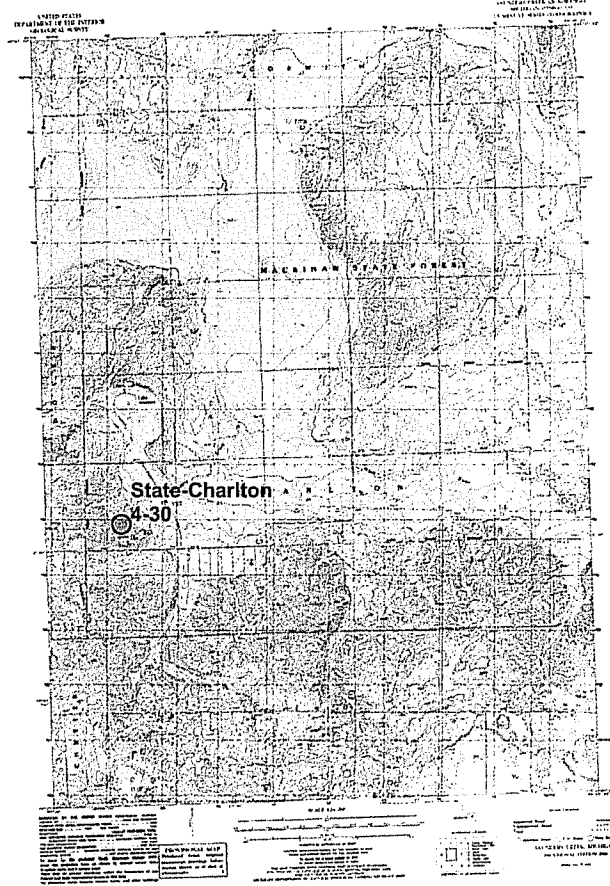


Figure 1. Site location map

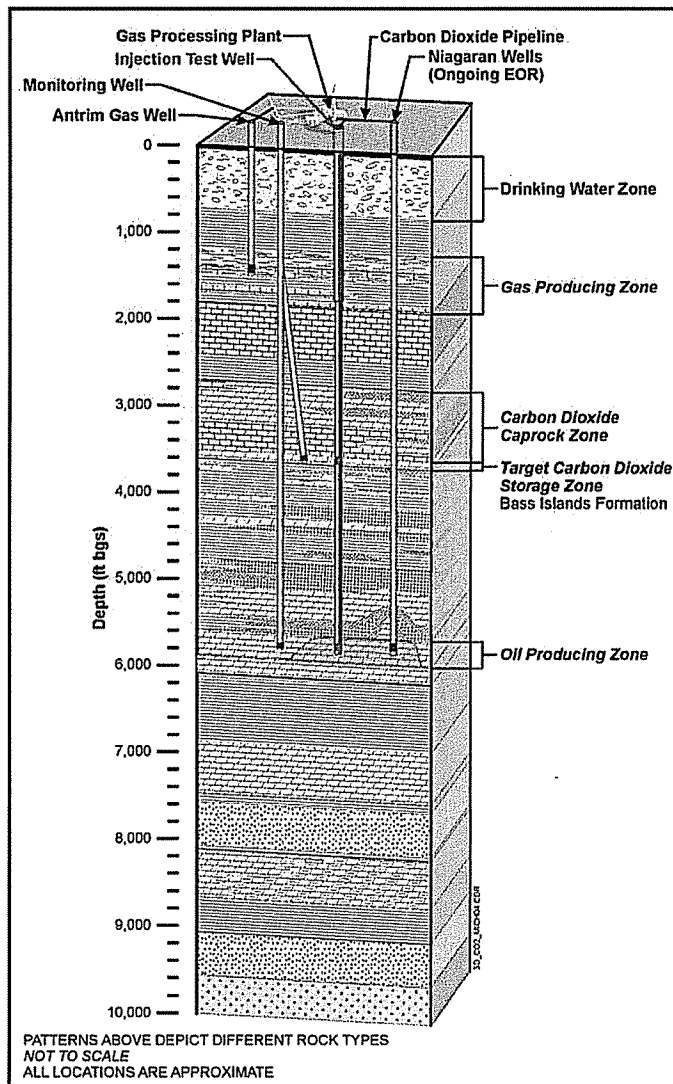
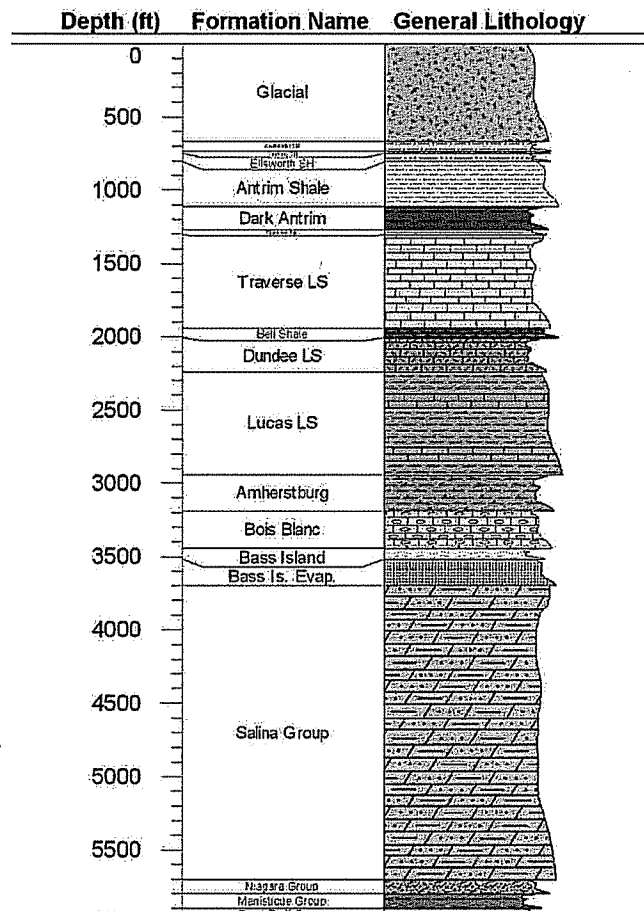


Figure 2. Conceptual diagram of CO<sub>2</sub> sequestration tests for Otsego County Michigan site



**Figure 3. Geologic stratigraphic column showing estimated lithology (the Bass Islands Dolomite is shown at 3400-3500 ft).**

The overall site plan for the Michigan Basin Site is to utilize existing infrastructure to facilitate a CO<sub>2</sub> injection test and monitoring. General steps of the site plan are listed as follows:

- 1) Preliminary Geologic Assessment of Potential Storage Reservoirs and Caprocks – This work involved compiling available well logs, developing geologic cross-sections, delineating target storage reservoirs, and identifying any issues related to geologic storage that may affect the project. Michigan Core Research Laboratory has completed this task.
- 2) Site Characterization Field Work – Drilling of an injection test well at State-Charlton #4-30 was completed at the Michigan Basin Otsego County Site in late November 2006. Drilling started the first week of November and proceeded into the target interval at 3500 ft. Some problems were encountered drilling through the salt and shale layers of the Detroit River Group. Approximately 180 ft of full rock core were collected from the Bois Blanc-Bass Islands interval in four core runs (this represents the first full rock core obtained from this formation in the Michigan Basin). A nearby plugged Niagaran Oil well (#C3-30) was recompleted for monitoring. It was drilled directionally at a kickoff depth of approximately 1700 ft and drilled toward the State-Charlton #4-30 test well about 500 ft laterally away from the injection well.
- 3) Injection System Design and Construction – An injection system was designed and constructed at the Michigan Basin Site in early 2007. This system is integrated with the existing EOR infrastructure at the area and does not involve any extensive new or innovative design elements. A short branch of pipe was run to the injection well from the existing 6 inch diameter supercritical EOR line nearby the injection site.
- 4) CO<sub>2</sub> Injection Testing and Monitoring – The goal is to inject up to several hundred metric tons of CO<sub>2</sub>

per day into the Bois Blanc-Bass Islands interval. Injection rates and duration of the test are dependent on formation capacity and budget. It is anticipated that the injection will occur over a period of several months and that some injectivity testing will be included in early stage injection to determine maximum injection rates. At this point, injection will take place into the new State-Charlton #4-30 injection well with monitoring occurring in the recompleted #C3-30 EOR well. This site is amenable to 3D seismic and has been subject to extensive 3D surveying; therefore, this option is being considered in addition to other monitoring methods.

5) Post Injection Monitoring and Site Closure – Once injection has been completed, some closure monitoring will be performed to assess the fate of the injected CO<sub>2</sub>. There is currently periodic CO<sub>2</sub> flooding for EOR in Niagaran Reefs at the proposed Michigan Basin Site and there has not been any sign of leakage or other problems. Consequently, closure monitoring will focus on ensuring the CO<sub>2</sub> has been safely sequestered and monitoring any geochemical changes over time in the reservoirs.

**Research Objectives:**

The primary research objective is to test CO<sub>2</sub> sequestration in the Bass Islands Dolomite, a significant CO<sub>2</sub> sequestration target for the area. While the sequestration target is fairly shallow at the test site, it is more significant toward the south where it is considered to have very high sequestration potential. Therefore, test results should be applicable to other parts of the Michigan Basin, which is a very attractive sequestration target in the MRCSP region. In addition, these tests support sequestration of CO<sub>2</sub> from gas processing operations along the northern reef trend in Michigan.

At this site, a fairly significant volume of CO<sub>2</sub> (10,000 tons) is planned for injected because the source is available from the nearby DTE Energy gas processing plant. This may allow for more extensive monitoring of the injected CO<sub>2</sub> such as 4D seismic and/or cross-well seismic. In addition, an abandoned EOR well will be retrofitted at the site for monitoring.

**Summary of Modeling and MMV Efforts (Use the table provided for MMV):**

Numerical simulations of CO<sub>2</sub> injection were completed with the STOMP CO<sub>2</sub> simulator, which was designed model complex, coupled hydrologic, chemical, and thermal processes, including multifluid flow and transport partitioning of CO<sub>2</sub> into the aqueous phase, and chemical interactions with aqueous fluids and rock minerals with the accurate representation of fluid properties. Initial reservoir simulations with the reservoir model STOMP CO<sub>2</sub> of the proposed injection tests indicate that the injected CO<sub>2</sub> would extend less than 500 ft from well and the pressure increase would extend less than 1,000 ft from the well (Figure 4).

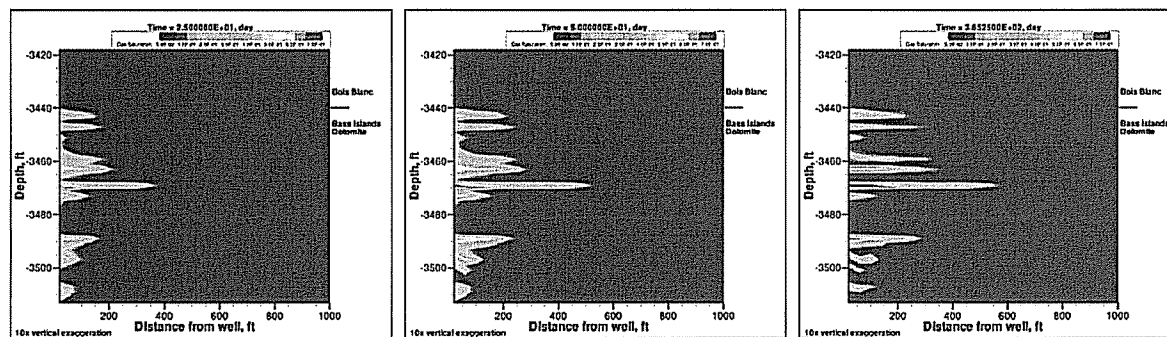


**Figure 4. STOMP CO<sub>2</sub> simulated CO<sub>2</sub> gas saturation at 25, 50, and 365 days for an injection scenario 200 metric tons CO<sub>2</sub> for 50 days.**

Monitoring technologies for CO<sub>2</sub> sequestration were reviewed and a subset of options was selected based on the proposed injection system specifications and geologic setting (Table 1). Consequently, a monitoring program was designated for the site consisting of temporal wireline RST monitoring in a monitoring well, cross-well seismic imaging of CO<sub>2</sub> field, microseismic monitoring of the CO<sub>2</sub> injection, brine chemistry analysis, downhole pressure gauging, soil gas monitoring of PFT tracers in the injectate, injection system monitoring, and health and safety monitoring. This monitoring suite provides a very comprehensive array of techniques aimed at assessing the injection test.

**Accomplishments to Date:**

All work at this site has been completed leading up to the point of beginning injection operations:

- Site preparation activities were completed in the Summer of 2006.
- A preliminary geologic assessment was completed by Western Michigan/Michigan Core Research Laboratory describing the regional geologic setting, target sequestration rock formations, and other issues in the Fall of 2006
- A new test/injection well of about 5000 ft depth was drilled and an existing nearby EOR well was recompleted as a monitoring well about 500 ft laterally from the injection well. This all occurred in the November, December 2006 timeframe.
- Approximately 180 ft of full rock core were collected from the Bois Blanc-Bass Islands interval in four core runs (this represents the first full rock core obtained from this formation in the Michigan Basin).
- A Class V UIC permit was completed through Region 5 EPA, however, a late appeal in September 2007 by an individual owning land near the injection site caused the permit to be placed on hold pending review by the EPA Environmental Appeals Board (EAB). We are currently awaiting resolution by the EAB. The preliminary assessment is that the appeal, which focuses on property rights, is outside the scope of EPA's UIC process.

**Summarize Target Sink Storage Opportunities and Benefits to the Region:**

- The target sink is the Bass Islands interval at a depth of about 3400-3500 ft.
- Core analysis from the test well confirms permeability and porosity in the upper Bass Island Dolomite is suitable for injection. Average porosity was 21% with an average permeability of 22 mD. Consequently, this interval is being targeted for injection; although, the entire Bass-Island Dolomite-Bois Blanc interval from 3190-3515 ft is considered the storage interval.
- Added value in performing the test at an active oil and gas field in a real-world setting.
- Added value in utilizing the only existing CO<sub>2</sub> EOR pipeline in the eastern U.S. Much of the infrastructure for CO<sub>2</sub> capture, transport, and injection already exists at the Michigan Basin site. A gas processing plant exists near the site and will provide a supply of high-purity CO<sub>2</sub>.
- Added value in sequestering anthropogenic CO<sub>2</sub> as a byproduct from natural gas processing, resulting in actual net sequestration of CO<sub>2</sub>.
- Promotes CO<sub>2</sub> sequestration at Antrim gas fields, currently the 10<sup>th</sup> most prolific gas play in the continental U.S.
- Added value in utilizing existing 3D seismic data through site.
- Added value in access to EMU; technical capabilities for 4D seismic monitoring.

**Cost\*:**

**Total Project Cost: \$23,745,399**

**DOE Share: \$17,458,272 (73.52%)**

**Non-Doe Share: \$6,287,127 (26.48%)**

(\*) Costs are for overall MRCSP Phase II project

**Field Project Key Dates:**

**Baseline Completed: Fall 2006**

**Drilling Operations Begin: Late Fall 2006**

**Injection Operations Begin: ~Mid 2007**

**MMV Events: TBD**

**Table 1. Measurement Technologies Employed at Field Test Site**

Measurement technique	Measurement parameters	Application
Introduced and natural tracers	Travel time	Tracing movement of CO <sub>2</sub> in the storage formation
	Partitioning of CO <sub>2</sub> into brine or oil Identification sources of CO <sub>2</sub>	Quantifying solubility trapping Tracing leakage
Water composition	CO <sub>2</sub> , HCO <sub>3</sub> <sup>-</sup> , CO <sub>3</sub> <sup>2-</sup> Major ions Trace elements	Quantifying solubility and mineral trapping Quantifying CO <sub>2</sub> -water-rock interactions
	Salinity	Detecting leakage into shallow groundwater aquifers
Subsurface pressure	Formation pressure	Control of formation pressure below fracture gradient
	Annulus pressure Groundwater aquifer pressure	Wellbore and injection tubing condition Leakage out of the storage formation
Well logs	Brine salinity Sonic velocity CO <sub>2</sub> saturation	Tracking CO <sub>2</sub> movement in and above storage formation
		Tracking migration of brine into shallow aquifers Calibrating seismic velocities for 3D seismic surveys
Vertical seismic profiling and crosswell seismic imaging	P and S wave velocity Reflection horizons Seismic amplitude attenuation	Detecting detailed distribution of CO <sub>2</sub> in the storage formation
		Detection leakage through faults and fractures
Passive seismic monitoring	Location, magnitude and source characteristics of seismic events	Development of microfractures in formation or caprock CO <sub>2</sub> migration pathways
Soil gas sampling	Soil gas composition Isotopic analysis of CO <sub>2</sub>	Detect elevated levels of CO <sub>2</sub>
		Identify source of elevated soil gas CO <sub>2</sub> Evaluate ecosystem impacts

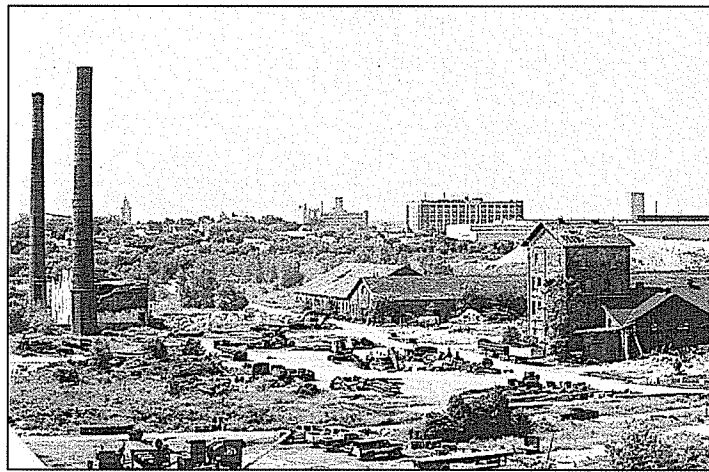
**Attachment 6  
NRC3-09-0026**

**Reference No. 2 from RAI 02.04.13-6**

**Simulation of Ground-Water Flow, Surface Water Flow, and a Deep Sewer  
Tunnel System in the Menomonee Valley, Milwaukee, Wisconsin  
(following 48 pages)**

**In cooperation with the U.S. Environmental Protection Agency, Region 5,  
and City of Milwaukee, Wisconsin**

## **Simulation of Ground-Water Flow, Surface-Water Flow, and a Deep Sewer Tunnel System in the Menomonee Valley, Milwaukee, Wisconsin**



Scientific Investigations Report 2004–5031

# **Simulation of Ground-Water Flow, Surface-Water Flow, and a Deep Sewer Tunnel System in the Menomonee Valley, Milwaukee, Wisconsin**

By C.P. Dunning, D.T. Feinstein, R.J. Hunt, and J.T. Krohelski

In cooperation with the U.S. Environmental Protection Agency, Region 5,  
and City of Milwaukee, Wisconsin

Scientific Investigations Report 2004–5031

**U.S. Department of the Interior  
U.S. Geological Survey**

**U.S. Department of the Interior**  
Gale A. Norton, Secretary

**U.S. Geological Survey**  
Charles G. Groat, Director

U.S. Geological Survey, Reston, Virginia: 2004

For sale by U.S. Geological Survey, Information Services  
Box 25286, Denver Federal Center  
Denver, CO 80225

For more information about the USGS and its products:  
Telephone: 1-888-ASK-USGS  
World Wide Web: <http://www.usgs.gov/>

Any use of trade, product, or firm names in this publication is for descriptive purposes only and does not imply endorsement by the U.S. Government.

# Contents

Abstract.....	1
Introduction .....	1
Purpose and Scope .....	5
Hydrogeologic Setting .....	5
Acknowledgments .....	7
Conceptual Models for Ground-Water Flow in the Menomonee Valley Brownfield.....	8
Methods .....	9
Stepwise Modeling.....	9
Analytic-Element Model .....	10
Finite-Difference Model.....	12
Model Calibration .....	13
Application of Stepwise Modeling .....	13
Model Domains .....	13
Development of the Analytic-Element Model .....	13
Construction .....	13
Calibration.....	14
Development of the Finite-Difference Model.....	15
Construction .....	15
Calibration and Sensitivity.....	17
Model Limitations .....	21
Uncertainties in the Hydrogeologic System.....	21
Uncertainties in MODFLOW Target Values .....	21
Uncertainties of Discretization and Scale.....	22
Limitations Arising from Extraction of Boundary Conditions.....	22
Simulation of Ground-Water Flow.....	23
Ground-Water Contributing Areas.....	23
Sources and Sinks .....	23
Traveltimes .....	25
Implications for Contaminant Transport.....	29
Summary and Conclusions.....	31
References Cited .....	32
Appendix. Calibration targets August 14, 2001 (well name, location, screen interval, model layer, measured and simulated head, residual) .....	35

## Figures

1–2.	Maps showing:	
	1.	Location of Milwaukee County, the Menomonee Valley Brownfield study area, the Menomonee Valley Brownfield, and downtown Milwaukee, Milwaukee County, Wis. ....2
	2.	Location of downtown Milwaukee, surface-water features, the Inline Storage System (ISS), U.S. Geological Survey streamflow-gaging stations, Falk Dam, 27th Street, and zones of estimated average recharge across the Menomonee Valley Brownfield study area, Milwaukee County, Wis. ....3
	3.	Stratigraphic section for the Menomonee Valley Brownfield study area, Milwaukee County, Wis. ....4
	4.	Block diagram of a part of the Menomonee Valley Brownfield study area, including a part of the Inline Storage System, Milwaukee County, Wis. ....5
	5.	Figure showing end-members for a conceptual model of the Menomonee Valley Brownfield study area, Milwaukee County, Wis. ....8
	6.	Map showing model domains in the Menomonee Valley Brownfield study area, Milwaukee County, Wis. ....11
7–8.	Figures showing:	
	7.	Schematic hydrostratigraphic section across the Menomonee Valley Brownfield study area, Milwaukee County, Wis. ....12
	8.	MODFLOW section and layering, Menomonee Valley Brownfield study area, Milwaukee County, Wis. ....16
	9.	Map showing locations of channel deposits, nested wells, and minipiezometers in the Menomonee Valley Brownfield study area, Milwaukee County, Wis. ....17
10a.		Calibration plot of measured hydraulic heads plotted against MODFLOW-simulated heads in the unlithified sediments (layers 1 through 4), Menomonee Valley Brownfield study area, Milwaukee County, Wis. ....19
10b.		Calibration plot of measured hydraulic heads plotted against MODFLOW-simulated heads in the dolomite (layers 5 through 8), Menomonee Valley Brownfield study area, Milwaukee County, Wis. ....20
11–12.	Figures showing:	
	11.	Water-table surface in the Menomonee Valley Brownfield study area, Milwaukee County, Wis., simulated with MODFLOW, and calibrated to August 14, 2001 hydraulic heads. ....23
	12.	Backward particle tracking from the Inline Storage System in the Menomonee Valley Brownfield study area, Milwaukee County, Wis., simulated with GFLOW .....24
	13.	Map showing capture zones simulated with MODFLOW and MODPATH for the Inline Storage System (ISS) in the Menomonee Valley Brownfield study area, Milwaukee County, Wis. ....25
14a–16.	Graphs showing:	
	14a.	Sectional view (row 38) of ground-water-flow directions simulated with MODFLOW and MODPATH in the Menomonee Valley Brownfield study area, Milwaukee County, Wis. ....26
	14b.	Sectional view (row 43) of ground-water-flow directions simulated with MODFLOW and MODPATH in the Menomonee Valley Brownfield study area, Milwaukee County, Wis. ....27

14c. Sectional view (row 48) of ground-water-flow directions simulated with MODFLOW and MODPATH in the Menomonee Valley Brownfield study area, Milwaukee County, Wis.....	28
15. Three-dimensional view generated by ModelViewer of ground-water flow-patterns in the Menomonee Valley Brownfield study area, Milwaukee County, Wis.....	29
16. Traveltime to the Inline Storage System (ISS) in the Menomonee Valley Brownfield study area, Milwaukee County, Wis., simulated with MODFLOW and MODPATH. ....	30

## Tables

1. Sources of data for the construction and calibration of GFLOW and MODFLOW models, Menomonee Valley Brownfield study area, Milwaukee County, Wis. ....	9
2. Hydraulic conductivities and effective porosities for calibrated GFLOW and MODFLOW models, Menomonee Valley Brownfield study area, Milwaukee County, Wis. ....	14
3a. MODFLOW calibration statistics for wells in the unlithified sediments of the Menomonee Valley Brownfield study area, Milwaukee County, Wis.....	18
3b. MODFLOW calibration statistics for wells in the dolomite of the Menomonee Valley Brownfield study area, Milwaukee County, Wis. ....	18
4. MODFLOW vertical-gradient calibration for the Menomonee Valley Brownfield study area, Milwaukee County, Wis. ....	18
5. MODFLOW calibration to measured dry-weather infiltration to phases of the Inline Storage System (ISS) in the Menomonee Valley Brownfield study area, Milwaukee County, Wis. ....	18
6. Ranked sensitivities of the MODFLOW parameters in the Menomonee Valley Brownfield study area, Milwaukee County, Wis. ....	19
7. Direction of vertical gradients between river (estuary) and ground water below riverbed, Menomonee Valley Brownfield study area, Milwaukee County, Wis. ....	21
8. Statistics for simulated traveltime of recharge to surface-water sinks and the Inline Storage System, Menomonee Valley Brownfield study area, Milwaukee County, Wis. ....	25

## Conversion Factors, Vertical Datum, and Abbreviations

Multiply	By	To obtain
Length		
inch (in.)	2.54	centimeter (cm)
foot (ft)	0.3048	meter (m)
mile (mi)	1.609	kilometer (km)
Area		
acre	43,560	square foot (ft <sup>2</sup> )
Discharge		
cubic foot per day (ft <sup>3</sup> /d)	28.32	liter per day (L/d)
cubic foot per second (ft <sup>3</sup> /s)	2,446,575.5	liter per day (L/d)
Hydraulic conductivity*		
foot per day (ft/d)	0.3048	meter per day (m/d)

Temperature in degrees Celsius (°C) may be converted to degrees Fahrenheit (°F) as follows:

$$^{\circ}\text{F}=(1.8\times^{\circ}\text{C})+32$$

Vertical coordinate information is referenced to the National Geodetic Vertical Datum of 1929 (NGVD 1929).

\*Hydraulic conductivity: The standard unit for hydraulic conductivity is cubic foot per day per square foot of aquifer cross-sectional area (ft<sup>3</sup>/d)/ft<sup>2</sup>. In this report, the mathematically reduced form, feet per day (ft/d), is used for convenience.

Transmissivity: The standard unit for transmissivity is cubic foot per day per square foot times foot of aquifer thickness [(ft<sup>3</sup>/d)/ft<sup>2</sup>]ft. In this report, the mathematically reduced form, foot squared per day (ft<sup>2</sup>/d), is used for convenience.

Water year: Water year is the 12 month period from October 1 through September 30. The water year is designated by the calendar year in which it ends.

### Other abbreviations used in this report

Kg/d kilograms per day  
in/yr inches per year

# Simulation of Ground-Water Flow, Surface-Water Flow, and a Deep Sewer Tunnel System in the Menomonee Valley, Milwaukee, Wisconsin

By C.P. Dunning, D.T. Feinstein, R.J. Hunt, and J.T. Krohelski

## Abstract

Numerical models were constructed for simulation of ground-water flow in the Menomonee Valley Brownfield, in Milwaukee, Wisconsin. An understanding of ground-water flow is necessary to develop an efficient program to sample ground water for contaminants. Models were constructed in a stepwise fashion, beginning with a regional, single-layer, analytic-element model (GFLOW code) that provided boundary conditions for a local, eight layer, finite-difference model (MODFLOW code) centered on the Menomonee Valley Brownfield. The primary source of ground water to the models is recharge over the model domains; primary sinks for ground water within the models are surface-water features and the Milwaukee Metropolitan Sewerage District Inline Storage System (ISS). Calibration targets were hydraulic heads, surface-water fluxes, vertical gradients, and ground-water infiltration to the ISS. Simulation of ground-water flow by use of the MODFLOW model indicates that about 73 percent of recharge within the MODFLOW domain circulates to the ISS and 27 percent discharges to gaining surface-water bodies. In addition, infiltration to the ISS comes from the following sources: 36 percent from recharge within the model domain, 45 percent from lateral flow into the domain, 15 percent from Lake Michigan, and 4 percent from other surface-water bodies. Particle tracking reveals that the median traveltime from the recharge point to surface-water features is 8 years; the median time to the ISS is 255 years. The traveltimes to the ISS are least over the northern part of the valley, where dolomite is near the land surface. The distribution of traveltimes in the MODFLOW simulation is greatly influenced by the effective porosity values assigned to the various lithologies.

## Introduction

The City of Milwaukee, Wis. is actively promoting the revitalization of the Menomonee Valley Brownfield, a 1,500-acre industrial center, south and west of downtown (figs. 1 and 2). Of these 1,500 acres, 300 to 400 are currently abandoned or considered by the City to be underutilized. In 1998 the City of Milwaukee successfully applied to the U.S Environmental Protection Agency (USEPA), Region 5 for a Brownfields Assessment Demonstration Pilot Grant. The objective of the grant was to evaluate innovative methods of addressing ground-water contamination (real and perceived) within the Menomonee Valley Brownfield.

The Menomonee River Valley (from here on referred to as "the valley") is the natural, low-lying outlet of the Menomonee River as it flows to Lake Michigan. Prior to large-scale human settlement in the early 1800s, the valley was a ground-water-discharge area covered with marshes and tamarack swamps, and bordered by relatively steep bluffs on the north and south (Rodolfo Salcedo, Department of City Development, City of Milwaukee, written commun., 1998; SIGMA Environmental Services, Inc., 2002). The Menomonee River meandered eastward through the marshes of the valley to the shore of Lake Michigan. The development of Milwaukee as a major port and industrial center resulted in extensive changes to the natural topography of the valley. From 1835 to 1890, the bluffs bordering the valley were cut and graded. The material from the bluffs, as well as household and industrial wastes, were used to fill the marshes. Starting about 1865, the river channel within the valley was straightened and dredged, and canals and slips were constructed for navigation and port facilities. Today, the path of the river is controlled and the depth of the channel maintained over the eastern half of the valley. By 1900, the valley had become a regional coal distribution center, and for years, heavy

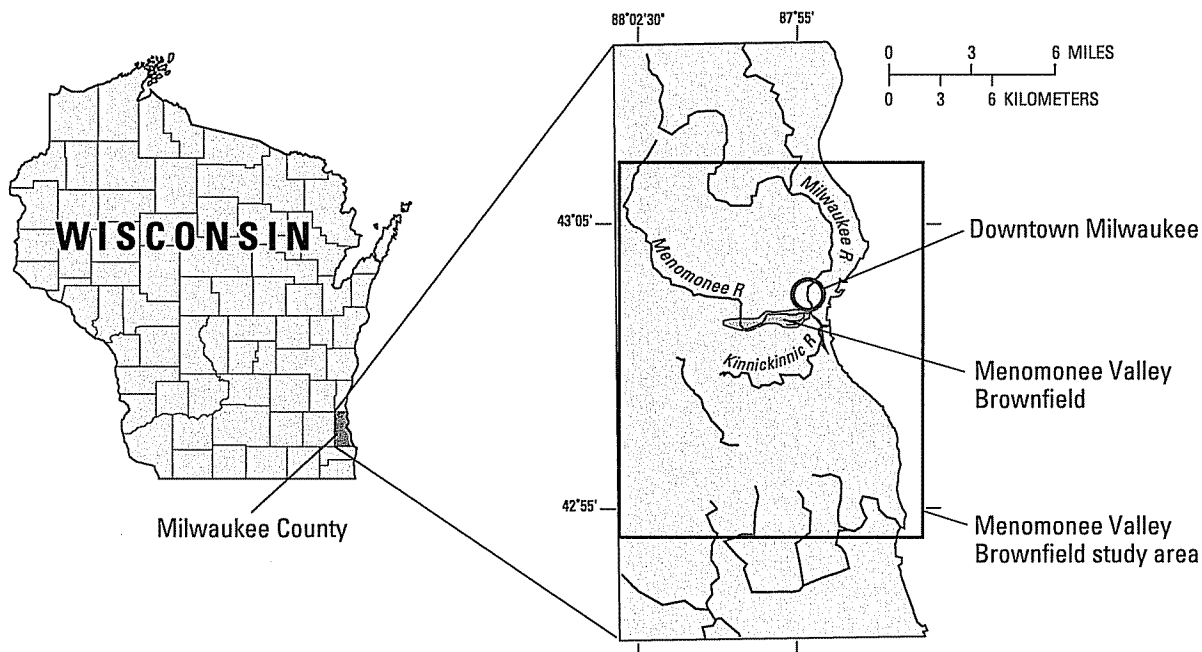


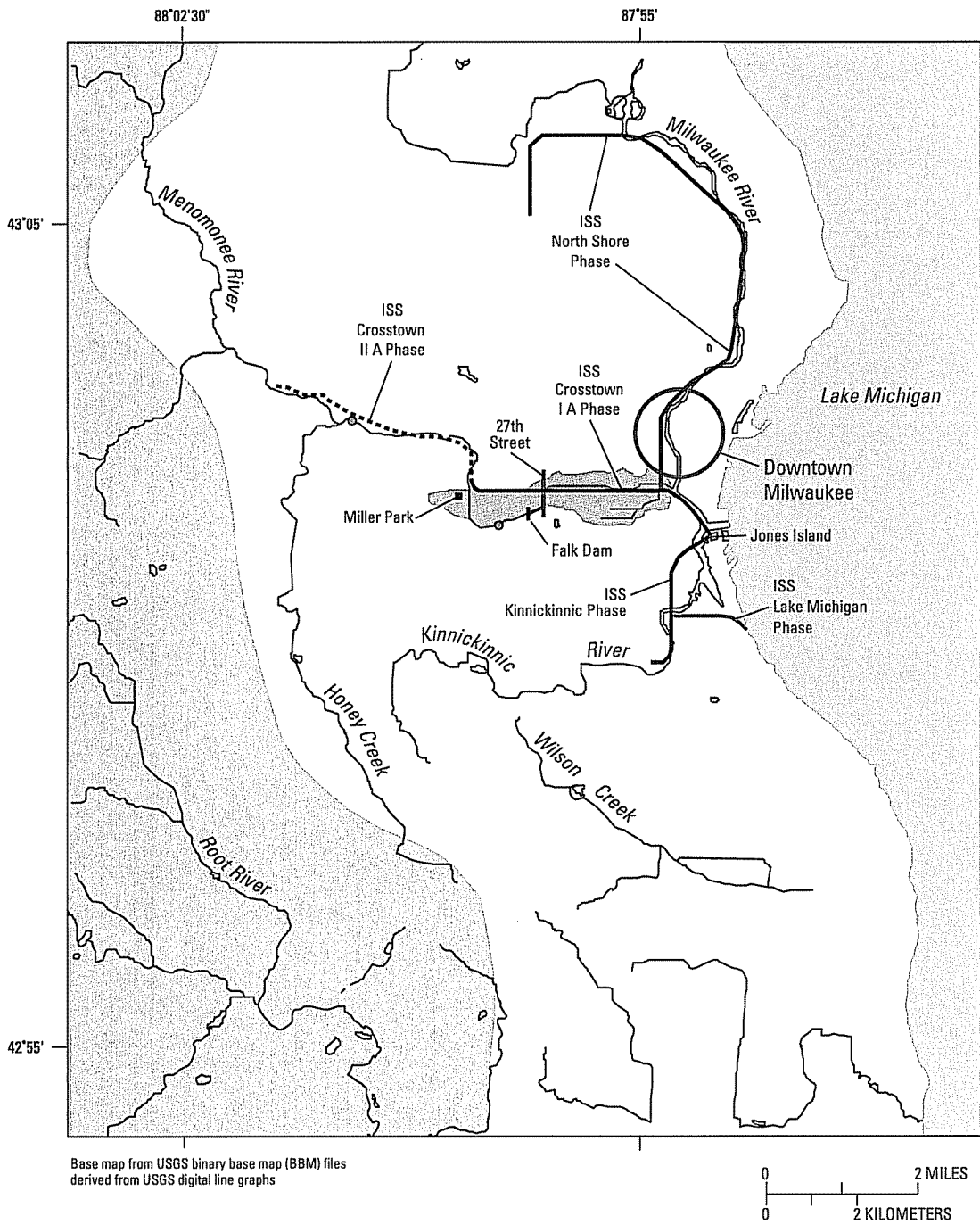
**Figure 1.** Location of Milwaukee County, the Menomonee Valley Brownfield study area, the Menomonee Valley Brownfield, and downtown Milwaukee, Milwaukee County, Wis.

industries operated in the area. These industries included foundries, power plants, coking and coal gasification plants, cement plants, junkyards, stockyards, tanneries, switching yards, engine repair shops, and chemical companies. Also common were various material storage piles, such as coal, clinker, sand, gravel, and salt. An extensive rail system, including a large rail yard, was built in the valley to support the movement of materials to and from the industrial sites. Industries in the valley became the major source of air and water pollution in Milwaukee. Valley industries once employed about 50,000 people, representing over 75 percent of the region's industrial employment base. Today, just over 7,000 people are employed at valley manufacturing firms. The relocation or demise of many of the valley's industries, and the establishment of newer industrial parks on Milwaukee's outskirts, have resulted in many vacant or underutilized properties within the valley (Rodolfo Salcedo, Department of City Development, City of Milwaukee, written commun., 1998; SIGMA Environmental Services, Inc., 2002).

Milwaukee, like a number of large metropolitan areas, has a combined-sewer system in which storm-sewer flow and sanitary-sewer flow are collected in the same pipe system. Historically in Milwaukee, if the capacity of the combined-sewer system was exceeded during a rain event, storm and sanitary overflow would be diverted to the Menomonee River or other surface-water body.

The occurrence of overflows became more numerous as Milwaukee and surrounding areas grew. To address this problem, the Milwaukee Metropolitan Sewerage District (MMSD) constructed the Inline Storage System (ISS), also known as the Deep Tunnel. The ISS was constructed in the Silurian dolomite (fig. 3) between 1986 and 1994, and its purpose is to collect combined-sewer overflow during rainstorms and store it for later treatment. The ISS comprises 19.4 mi of tunnels constructed in phases: the Crosstown IA and IIA, the North Shore, the Kinnickinnic, and the Lake Michigan Phases (fig. 2). These tunnels are 17 or 32 ft in diameter and run west through the valley of the Menomonee River, north along the valley of the Milwaukee River, and south through the valley of the Kinnickinnic River (figs. 2 and 4). The Crosstown IA phase of the ISS (32 ft in diameter) underlies the Menomonee Valley Brownfield, at a depth of 200 to 300 ft.

Industrial contaminants such as organic solvents, petroleum byproducts, tars, and metal waste are found in the soil in the valley. These contaminants can be dissolved by precipitation and move with the recharge to ground water (SIGMA Environmental Services, Inc., 2002). A primary objective of this study was to determine in what proportion the fate of recharge to the valley is divided between a deep sink (the ISS) and shallow sinks (surface-water features). The fate of potentially contaminated ground water in different parts of the valley is of interest



**EXPLANATION**

- |  |  |
|--|--|
| <p><b>Estimated recharge in inches per year</b></p> <ul style="list-style-type: none"> <li><span style="display: inline-block; width: 15px; height: 10px; border: 1px solid black; background-color: #e0e0e0; margin-right: 5px;"></span> 3.0</li> <li><span style="display: inline-block; width: 15px; height: 10px; border: 1px solid black; background-color: #ffffff; margin-right: 5px;"></span> 0.6</li> </ul> <p><span style="display: inline-block; width: 15px; height: 10px; border: 1px solid black; background-color: #cccccc; margin-right: 5px;"></span> <b>Menomonee Valley Brownfield</b></p> <p><span style="display: inline-block; width: 15px; border-bottom: 1px solid black; margin-right: 5px;"></span> <b>Hydrography</b></p> | <p><b>Inline Storage System (ISS)</b></p> <ul style="list-style-type: none"> <li><span style="display: inline-block; width: 15px; border-bottom: 2px solid black; margin-right: 5px;"></span> Crosstown I A Phase</li> <li><span style="display: inline-block; width: 15px; border-bottom: 2px dashed black; margin-right: 5px;"></span> Crosstown II A Phase</li> <li><span style="display: inline-block; width: 15px; border-bottom: 2px solid black; margin-right: 5px;"></span> North Shore Phase</li> <li><span style="display: inline-block; width: 15px; border-bottom: 2px solid black; margin-right: 5px;"></span> Kinnickinnic Phase</li> <li><span style="display: inline-block; width: 15px; border-bottom: 2px solid black; margin-right: 5px;"></span> Lake Michigan Phase</li> </ul> <p><span style="display: inline-block; width: 0; height: 0; border-left: 5px solid transparent; border-right: 5px solid transparent; border-bottom: 8px solid black; margin-right: 5px;"></span> <b>USGS streamflow-gaging station</b></p> |
|--|--|

**Figure 2.** Location of downtown Milwaukee, surface-water features, the Inline Storage System (ISS), U.S. Geological Survey streamflow-gaging stations, Falk Dam, 27th Street, and zones of estimated average recharge across the Menomonee Valley Brownfield study area, Milwaukee County, Wis.

Geologic time interval	Years before present	Stratigraphic unit	Lithology
<i>Quaternary Period</i>	0	(Holocene) sediments	Soil, estuarine and alluvial deposits
	10,000	(Pleistocene) Kewaunee, Oak Creek and New Berlin Formations	Three distinct till units
	20,000		Fine-, medium- and coarse-grained, proglacial-lake sediment Complex and variable ice margin unit
<i>Silurian and Devonian Periods</i>	380 million	Thiensville Dolomite Mayville Dolomite Racine Dolomite	Dolomite
	440 million	Maquoketa Shale Sinnipee Group Ansell Group Prairie du Chien Group	Shale and dolomite Dolomite with limestone and shale Orthoquartzite sandstone with minor limestone Dolomite with some sandstone and shale
<i>Ordovician Period</i>	550 million	Trempealeau Group Tunnel City Group Elk Mound Group	Sandstone with some dolomite and shale
<i>Cambrian Period</i>	680 million	Undifferentiated	Crystalline

**Figure 3.** Stratigraphic section for the Menomonee Valley Brownfield study area, Milwaukee County, Wis. (modified from Mudrey, 1982, and Need, 1983).

to regulators and developers because it influences decisions regarding the amount of monitoring and cleanup that is necessary before future development can go forward. An additional objective of this study was to estimate travel times from the points of recharge in the valley to the sinks. To accomplish these objectives, the U.S. Geological Survey (USGS), in cooperation with the City of Milwaukee and its consultants, and with support from USEPA

Region 5, used numerical modeling to simulate shallow ground-water flow in the Menomonee Valley Brownfield. The results and interpretations of this study, as well as the modeling approaches developed, may be useful as a case study for similar combined-sewer systems.

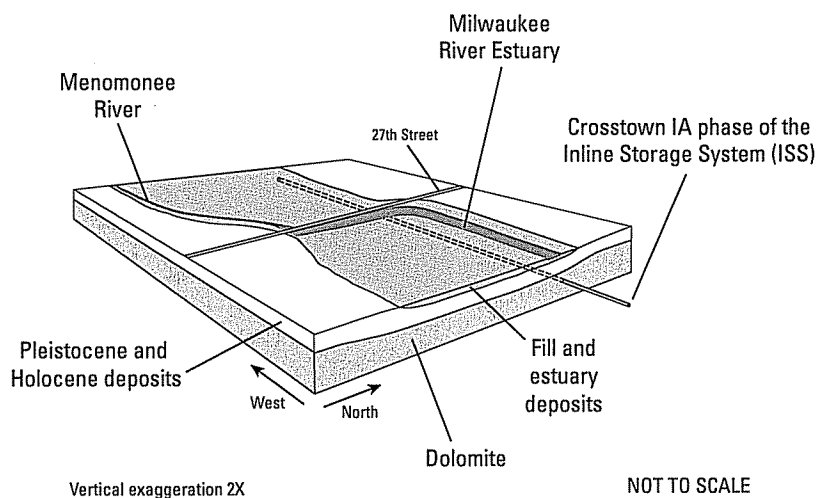


**Figure 4.** Block diagram of a part of the Menomonee Valley Brownfield study area, including a part of the Inline Storage System, Milwaukee County, Wis.

## Purpose and Scope

The purpose of this report is to discuss the hydrogeology of the Menomonee Valley Brownfield and shallow aquifers, and present simulations of ground-water flow. The report includes a summary of selected hydrologic data; conceptualization of the hydrogeologic setting of the Menomonee Valley Brownfield and shallow aquifers; details on the modeling approach, model construction and calibration, and model limitations; and delineation of ground-water recharge areas for shallow and deep sinks. The traveltimes and paths for recharge to move from the surface of the Menomonee Valley Brownfield to sinks are also discussed.

## Hydrogeologic Setting

An understanding of the hydrogeologic setting of the Menomonee Valley is integral to effective simulation of ground-water flow, surface-water flow, and the sewer tunnel system. Stratigraphy, recharge, the Inline Storage System, and surface- and ground-water flow systems are discussed in the following sections.

**Stratigraphy.** Crystalline bedrock, Precambrian in age, underlies southeastern Wisconsin and the Menomonee Valley (fig. 3). Sandstone and carbonate units of Cambrian and Ordovician age overlie the crystalline bedrock. These units consist of the Elk Mound Group, the Tunnel City Group, the Trempealeau Group, the Prairie du Chien Group, the Ancell Group, and the Sinnipee Group. Directly overlying the Sinnipee Group is the Maquoketa Shale, a layer with low hydraulic conductivity, that isolates strata

above (Silurian and younger) from strata below (Ordovician and older). Silurian units underlying the Menomonee Valley Brownfield are the Racine and Mayville Dolomites; Devonian units are represented by isolated occurrences of the Thiensville Dolomite. The shallow stratigraphy of the valley consists of unlithified Pleistocene and Holocene deposits overlying dolomite bedrock (figs. 3 and 4).

In this study, the Menomonee River Valley is identified topographically as land surface below 600 ft elevation and is the present-day expression of a Silurian bedrock valley that has been partially filled and narrowed by Pleistocene glacial deposits. These deposits are predominantly fine-grained regional till units with some coarser-grained proglacial-lake and ice-margin deposits. Detailed Quaternary stratigraphic information for the valley is presented in Need (1983). During the Holocene, estuarine and alluvial sediments were deposited over the glacial sediments in the marshy backwater and shallow estuaries of the valley. The estuarine deposits are typically organic-rich to peaty, silty clay and clayey silt. The alluvial deposits originated as channel and point-bar sediments and range in texture from sandy silt to gravel. These estuary and alluvial deposits have a combined thickness of up to 30 ft; they terminate abruptly against the bluffs north and south of the valley, and thin and pinch out gradually to the west as the land surface rises out of the valley (Southeast Wisconsin Regional Planning Commission, 1976; Need, 1983; and SIGMA Environmental Services, Inc., 1999). The bluffs along the valley have been reduced in many areas, and natural and manmade fill have been added to large areas

of the valley. Fill material consists of clay, silt, sand and gravel, and locally variable amounts of cinder, glass, wood, metal, rubble, brick, ash, and household-type trash. The combined thickness of the estuary/alluvial sediments and manmade fill materials can be as much as 60 ft (SIGMA Environmental Services, Inc., 1999).

**Recharge.** An upper bound to the rate of ground-water recharge for southeast Wisconsin is 8–10 in/yr, determined as the net discharge from surface- and ground-water sources in gaged streams (Gebert and others, 1989). Recharge commonly will vary spatially as a result of differences in watershed characteristics such as vegetation, urbanization, and evapotranspiration. Recent estimates of recharge rates in southeastern Wisconsin range from 0.0 to 4.0 in/yr over almost all of the Menomonee Valley Brownfield study area (Cherkauer, 2001). For this investigation, the estimated recharge values have been averaged and simplified to two zones, one of 3.0 in/yr and the other of 0.6 in/yr (fig. 2).

#### Hydrologic effects of the Inline Storage

**System.** The ISS fills with overflow from the combined-sewer system (storm-sewer flow and sanitary-sewer flow) during rainstorms and stores it for later treatment and discharge to Lake Michigan. Between storms the ISS is effectively empty and is a regional sink for the ground-water system. Dry-weather infiltration of ground water to phases of the ISS was evaluated by MMSD in the early 1990s using dye tracers and other techniques (Camp Dresser and McKee, 1998). In early 2002, consultants for MMSD visually inspected the ISS to better distinguish dry-weather flow from other outfalls (RUST/Harza, April 2002). This investigation found the total dry-weather ground-water infiltration rate to the ISS to equal 4.3 ft<sup>3</sup>/s (2.8 million gallons per day). As part of the same investigation, hydrographs for 46 wells were studied for the years following completion of the ISS (after 1993) to evaluate the degree to which the ground-water system was adjusting to changing subsurface stresses. Most monitoring wells in the dolomite near the ISS showed modest to significant increases in head; fewer showed declines in head. Two dolomite wells more distant from the ISS show a modest upward trend. It is possible that some heads were increasing because post-construction grouting has reduced water discharges to the ISS.

**Surface-Water-Flow System.** Surface-water features of the Menomonee Valley Brownfield study area include Honey Creek; the Milwaukee, Menomonee, Root, and Kinnickinnic Rivers; the Milwaukee River Estuary; and Lake Michigan (fig. 2). The Milwaukee River Estu-

ary is the name given to the Milwaukee, Menomonee, and Kinnickinnic Rivers once they reach the elevation of Lake Michigan. Downstream from this point, the stages of the rivers are controlled by the level of Lake Michigan. The Milwaukee and Kinnickinnic Rivers meet the estuary at the boundary of the valley itself, so gradients in stage are not appreciable within the valley. The Menomonee River, in contrast, has a gradient in stage from where it enters the brownfield near Miller Park to a point roughly at the site of the Falk Dam (fig. 2)—a river distance of about 1.5 mi. Above this point, the river stage is controlled by base flow, dry-weather outfalls to the river, and stormflow. Below this point, the stage of the water flowing through the valley is dominated by Lake Michigan water levels and occasional wind setup. Wind setup is the vertical rise of the stillwater level on the leeward side of a body of water due to wind blowing over the surface (Bates and Jackson, 1980). Data from 1860 to 1986 show the mean annual level for Lake Michigan is 580.11 ft above mean sea level. The maximum annual level was 582.57 and the minimum annual level was 576.95 (Quinn, 1988).

**Ground-Water-Flow System.** The three aquifer systems present in the Menomonee Valley Brownfield study area are:

- (1) (the un lithified aquifer consisting of the shallowest Pleistocene glacial and Holocene postglacial deposits;
- (2) the shallow Silurian dolomite aquifer; and
- (3) the Cambrian and Ordovician units, known collectively as the sandstone aquifer.

The un lithified aquifer is composed of sediments with three different origins: tills, outwash, and proglacial-lake deposits of Pleistocene age; alluvial and estuarine deposits of Holocene age; and fill material added to the valley over the last century. The Holocene materials and the fill are considered to be hydrologically similar and are treated as a single unit in the model. The glacial and postglacial deposits are variable in thickness—from 0 to 200 ft in the Menomonee Valley Brownfield study area. The fill averages 10 to 20 ft thick, though it can be as much as 50 ft thick locally. Saturated thickness of the un lithified aquifer can be as much as 180 ft.

Published values of horizontal hydraulic conductivity (Kh) for till in and around the valley range over more than four orders of magnitude, from 0.0004 to 9 ft/d. Published Kh values for glacial outwash in and around the valley range over about three orders of magnitude, from 0.0016

to 1.6 ft/d (though clean sands and gravels are up to 1,400 ft/d). Published Kh values for the estuary, alluvial, and fill sediments range from 4.5 to 197 ft/d (Carlson, 2000). The geometric mean of a set of slug tests on wells open to these sediments within the valley is 3.8 ft/d (SIGMA Environmental Services, Inc., 2002, table 6.15). Reported values of vertical hydraulic conductivity (Kv) values for the till and estuary materials extend over a very large range (Carlson, 2000, Appendix C). Carlson (2000) recommended that, for modeling purposes, till in the study area should be given a Kh equal to 0.4 ft/d and a Kv equal to 0.003 ft/d.

The Silurian dolomite aquifer underlies the entire Menomonee River Watershed. The relatively impermeable Maquoketa Shale underlies this aquifer and unlithified glacial and postglacial deposits overlie it (fig. 3). Although the dolomite is generally of low permeability, secondary porosity (fractures and dissolution), particularly near the top of the unit, helps to make it a productive aquifer. Porosity is about 5 percent (Carlson, 2000). Published values of Kh for the dolomite range over four orders of magnitude, from 0.0001 to 2.2 ft/d; published values of Kv for the dolomite range over three orders of magnitude, from 0.00006 to 0.07 ft/d (Carlson, 2000). On the basis of literature review and modeling of the dolomite units, Carlson (2002) estimated a Kh of 5 ft/day and a Kv of 0.01 ft/d for the weathered upper dolomite in the study area covered by this study. The unweathered lower dolomite has a Kh between 0.3 and 1.2 ft/d and a Kv between 0.0005 and 0.001 ft/d (Douglas Carlson, U.S. Geological Survey, written commun., 2000).

The sandstone aquifer is composed of geologic units above crystalline bedrock and below the Ordovician Maquoketa Shale (fig. 3), which is a confining unit (Feinstein and others, 2002). Significant lowering of the potentiometric surface in the deep sandstone aquifer (declines of as much as 400 ft) as a result of municipal pumping has resulted in appreciable gradients across the Maquoketa Shale confining unit. Potentiometric heads many miles inland are below the level of Lake Michigan (Southeast Wisconsin Regional Planning Commission, 1976).

Because it is separated from the shallow Silurian dolomite aquifer by the Maquoketa Shale confining unit, the sandstone aquifer is not included in simulations of ground-water flow in this investigation.

Predevelopment ground-water flow in the valley was generally from surrounding highlands to the Menomonee River or Milwaukee River Estuary and ultimately to Lake Michigan (Southeast Wisconsin Regional Planning Commission, 1976). The current potentiometric surface within the Silurian dolomite aquifer is below the level of Lake

Michigan in parts of the study area, particularly in an area centered on the Menomonee Valley Brownfield (Milwaukee Metropolitan Sewerage District, 1998; Plomb, 1989). This is primarily the effect of high-capacity wells that have pumped within the valley until recently. As a result of pumping, significant downward gradients have probably existed within the Menomonee Valley Brownfield for many years, from the estuarine, alluvial, and fill sediments to the underlying glacial sediments and Silurian dolomite (Southeast Wisconsin Regional Planning Commission, 1976; Camp Dresser and McKee, 1998). Although pumpage from the dolomite is currently much reduced from historical rates, the construction of the ISS has introduced an additional stress to the system. MMSD reports show that heads in monitoring wells in the dolomite near the ISS are appreciably lower than even the lowered potentiometric surface that resulted from a century of pumping (Camp Dresser and McKee, 1998). Strong downward gradients have been observed in piezometer nests installed in 1999 and 2000 by consultants to the City of Milwaukee (SIGMA Environmental Services, Inc., 2002). Recharge falling on the valley is subject to these vertical gradients, as well as to horizontal gradients driving water toward the river and estuary.

## Acknowledgments

The authors acknowledge the contributions of the following organizations and people: Jane Neumann of U.S. Environmental Protection Agency (USEPA) Region 5, provided guidance for project objectives and implementation. Jeffery Gohlke and staff of the Department of City Development for the City of Milwaukee provided project input. Mafizul Islam, Kristin Kurzka and Jodi VanderVelden of SIGMA Environmental Services, Inc., furnished much of the data and information that supported the modeling effort, as well as coordinated and carried out the collection of additional field data. Peter McAvoy of Milwaukee's 16th Street Community Health Center provided general support and feedback on project activities. Kevin Shafer, Susan Anthony, and Timothy Bate of the Milwaukee Metropolitan Sewerage District provided copies of engineering and scientific studies and assisted in the exchange of information between their staff and consultants, and the USGS. Menomonee Valley Partners provided general support and feedback on project activities. Colleague reviews were done by Douglas Yeskis, USGS, and Douglas Carlson, Louisiana Geological Survey. Graphic and publication assistance were provided by Michelle Greenwood, Jennifer Bruce, and Susan Jones, USGS.

## Conceptual Models for Ground-Water Flow in the Menomonee Valley Brownfield

A conceptual model of the hydrologic system is a precursor to numerical model construction. In defining a conceptual model, many of the general characteristics of the Menomonee Valley Brownfield must be considered. In the conceptual model, the dolomite and unconsolidated sediments above the Maquoketa Shale are assumed to compose a single aquifer, although there are recognized variations in hydrologic properties of the individual units. Over the last century, the hydrology of the Menomonee Valley Brownfield has become much more complicated with the physical alterations to the estuary (channelization and filling), high-capacity wells producing from the Silurian dolomite, and the recent completion of the ISS. Downward vertical gradients have been present in the valley for many years.

In addition, measured heads in minipiezometers installed at eight locations in river sediments (SIGMA Environmental Services, Inc., 2002) indicated that downward gradients were common across bottom sediments of the Menomonee River and Milwaukee River Estuary. Dry-weather infiltration of ground water into the ISS has been quantified, but whether its origin is local or distant is not certain. Given this background, the range of possible conceptual models for the Menomonee Valley Brownfield can be described by two end-members.

*Conceptual model A.* All recharge to the Menomonee Valley Brownfield flows ultimately to the Menomonee River, the Milwaukee River Estuary, or Lake Michigan (fig. 5a). In spite of measured downward vertical gradients, the dolomite presents a sufficient conductivity contrast to restrict flow from the valley through the dolomite into the ISS. Dry-weather inflow to ISS comes from distant sources.

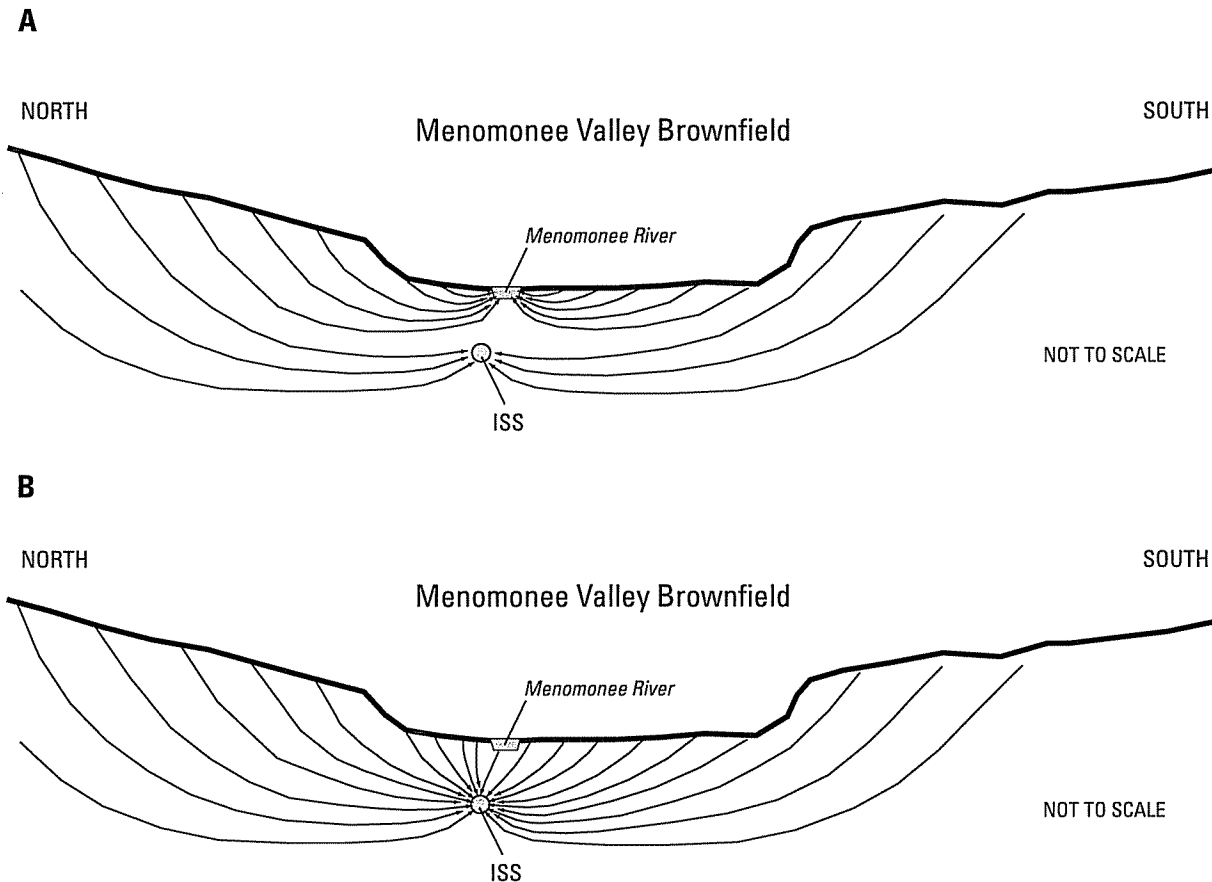


**Figure 5.** End-members for a conceptual model of the Menomonee Valley Brownfield study area, Milwaukee County, Wis.: (A) All recharge to the valley flows ultimately to Menomonee River, the Milwaukee River Estuary or Lake Michigan and dry-weather inflow to In-line Storage System (ISS) comes from distant recharge. (B) All recharge to the valley flows vertically to ISS.

**Table 1.** Sources of data for the construction and calibration of GFLOW and MODFLOW models, Menomonee Valley Brownfield study area, Milwaukee County, Wis.

Data	Source
Geologic logs with stratigraphic contacts	Need (1983); D.T. Feinstein (USGS, oral commun., 2002)
Stage data for surface-water features	USGS topographic maps
Slug tests in unconsolidated valley sediments	SIGMA Environmental Services, Inc. (2002)
Compendium of hydraulic conductivities from slug/aquifer tests and models	Carlson (2000)
Inline Storage System (ISS) flux measurements	Rust/Harza (2002)
Recharge estimates based on empirical equation tied to base-flow separation in selected basins	Cherkauer (2001)
Water-level measurements in wells in unlithified deposits, including well nests measured during 2001	SIGMA Environmental Services, Inc. (2002)
Water-level measurements in wells in dolomite, measured during 1994	Camp Dresser and McKee (1998), Milwaukee Metropolitan Sewerage District (1998)
Minipiezometer data	SIGMA Environmental Services, Inc. (2002)

*Conceptual model B.* All recharge to the Menomonee Valley Brownfield flows ultimately to the ISS (fig. 5b). Vertical gradients are large enough and the conductivity contrast is small enough that the ISS is the sink that captures all the recharge to the Menomonee Valley Brownfield. All surface-water features, including Lake Michigan, contribute flow to the ISS.

The conceptual model that was the starting point for the modeling effort falls in between the described end-members. The ISS probably has an influence on ground-water flow but probably does not capture all the recharge. A primary objective of the study was to determine in what proportion recharge to the valley is divided between these two sinks—the ISS and surface water features.

For simplicity, it was assumed for this study that overall the system is at steady state, so both upward and downward trends in hydrographs of local wells are ignored. A rough calculation of storage contributions based on water-level changes, rock volumes, and expected storage parameters shows that the flux going into and out of storage is very small relative to reported dry-weather ISS infiltration. For conservative values of specific storage, dolomite volume, and rate of head change, the storage released is only 1 percent of dry-weather infiltration.

## Methods

Numerical modeling was used to simulate ground-water flow in the Menomonee Valley Brownfield. Two

different mathematical approaches, analytic element (AE) and finite difference (FD), were used in a stepwise fashion to improve the efficiency of the modeling effort. Data for model construction and calibration came from numerous sources (table 1).

## Stepwise Modeling

As modeling tools have become more sophisticated, concerns have been raised with regard to the cost of model complexity, and informational benefits of increased model complexity (Bredehoeft and Hall, 1995; Hunt and Zheng, 1999). One suggested method to help ensure that the level of complexity is appropriate is to follow a stepwise modeling concept (Haitjema, 1995; Sun and others, 1998), whereby initial ground-water-flow models are relatively simple; that is, coarsely defined, and used in an exploratory fashion to help design data collection, test model assumptions, and provide boundary conditions for smaller-scale models.

In this study, the application of stepwise modeling involves the construction of a regional ground-water-flow model that is linked to a local inset model within its domain (Hunt and others, 1998). In this investigation of the Menomonee Valley Brownfield, the regional hydrology is simulated using a one-layer AE code based on Dupuit-Forchheimer assumptions (Haitjema, 1995), and the local model is simulated using a three-dimensional FD model with multiple layers. Flux boundary conditions for the FD model were initially extracted from the AE model. Both

models employ the same conceptual framework and incorporate the same sinks, but the local model adds a complex vertical stratigraphy, pronounced vertical anisotropy, and stresses originating at different elevations corresponding to shallow and deep sinks. As the modeling effort progressed, insight gained from the FD model was applied to the AE model, and a new extraction of boundary conditions was used for a revised FD model. This process continued in stepwise fashion until the FD model included the necessary hydrogeologic detail in the valley and was calibrated.

Both AE and FD models simulate the contributing areas that supply recharge to each sink. The FD model is used to provide quantitative estimates relating to the fate of recharge on the valley and the traveltime to sinks. Thus, in this approach, the AE model is called on only to provide boundary conditions. Application of the stepwise approach to modeling ground-water flow in the Menomonee Valley is thoroughly discussed in Feinstein and others (2003).

### Analytic-Element Model

The AE model was constructed to simulate the shallow aquifer (above the Maquoketa Shale confining unit) and its interaction with surface-water features. The software used in constructing the model for this study was GFLOW2000 (Haitjema, 2000). AE modeling methods have been extensively documented (Strack, 1989; Haitjema, 1995) and have been successfully used in hydrologic settings throughout Wisconsin (Hunt and Krohelski, 1996; Hunt and others, 1998; Krohelski and others, 2000; Hunt, Graczyk, and Rose, 2000; Hunt, Lin, and others, 2000).

The GFLOW2000 (GFLOW) model is a single-layer, steady-state model in which the aquifer is assumed to be infinite. The model uses the Dupuit-Forchheimer approximation by which a three-dimensional-flow problem is reduced to a two-dimensional, horizontal-flow problem. For this approximation to be appropriately applied, the length of a flowline must be large compared to the aquifer thickness. Within the Menomonee Valley Brownfield, the 460-ft thick shallow aquifer is about 3,000 ft wide north to south (across the valley) and about 18,000 ft long west to east (along the valley). Therefore, this aquifer is very thin relative to its horizontal extent, suggesting that ground-water flow in the valley is a horizontal-flow problem and can be appropriately evaluated by use of a Dupuit-Forchheimer approximation. This GFLOW model contains a conjunctive solution (Mitchell-Bruker and Haitjema, 1996)

that considers the interaction of surface-water and ground-water flow. Because of the proximity of the rivers and estuary, the conjunctive solution is an important consideration for evaluating ground-water flow in the Menomonee Valley Brownfield.

Important hydrologic features (rivers, streams, and lakes) are represented in the GFLOW model domain as analytic elements or strings of analytic elements (line-sinks). Each element provides an analytic solution to the ground-water-flow equation, and the superposition of many individual solutions provides a solution for the ground-water-flow system. The model domain consists of both a far field and a near field (fig. 6). The far field is beyond the area of interest but is included in the model to define hydrologic boundary conditions for the near field. Far-field elements are constant-head boundaries, and near-field elements are head-dependent boundaries. Far-field elements are usually coarsely defined and consist only of water-level information that is estimated from USGS topographic data. The near-field is the area of primary interest and contains important local hydrologic inhomogeneities; that is, areas where recharge and (or) aquifer parameter values differ from regional values. A hydrologic inhomogeneity is represented in the GFLOW model by a closed set of elements, within which the nonregional parameter values are present. Near-field analytic elements are made to more closely match the geometry of surface-water features and therefore require more line-sink vertices and solutions. Solutions for near-field elements also require information on the width and resistance of the represented feature. Regional values for aquifer parameters and recharge rate are applied across the entire GFLOW model domain. Aquifer parameters for the single-layer AE model are based on a generalized hydrostratigraphic section of the shallow aquifer (fig. 7).

The GFLOW model domain is not discretized into a grid; therefore, an exact solution for the flow equation can be calculated at any point in the domain. As a result, interpolation of heads or velocities is not necessary. Flow can also be examined at various scales without changing model input parameters or boundary conditions. This allows one GFLOW model to function at both a regional and a site scale without modification. GFLOW simulations are evaluated with respect to available composite head information and gaged streamflows. Finally, GFLOW is well suited as a regional model of the Menomonee Valley Brownfield because it allows the extraction of boundary conditions from a simulation directly into MODFLOW.

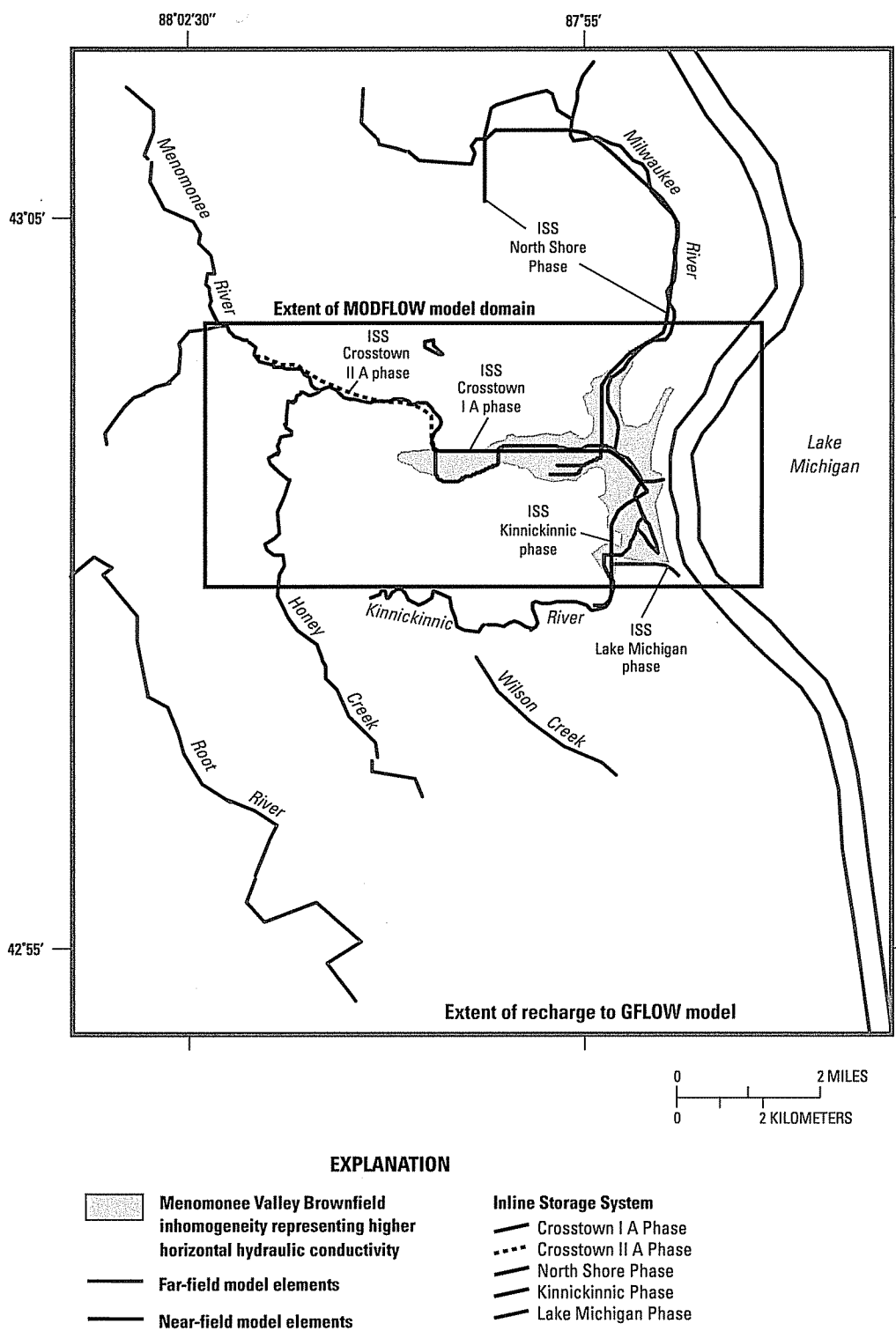
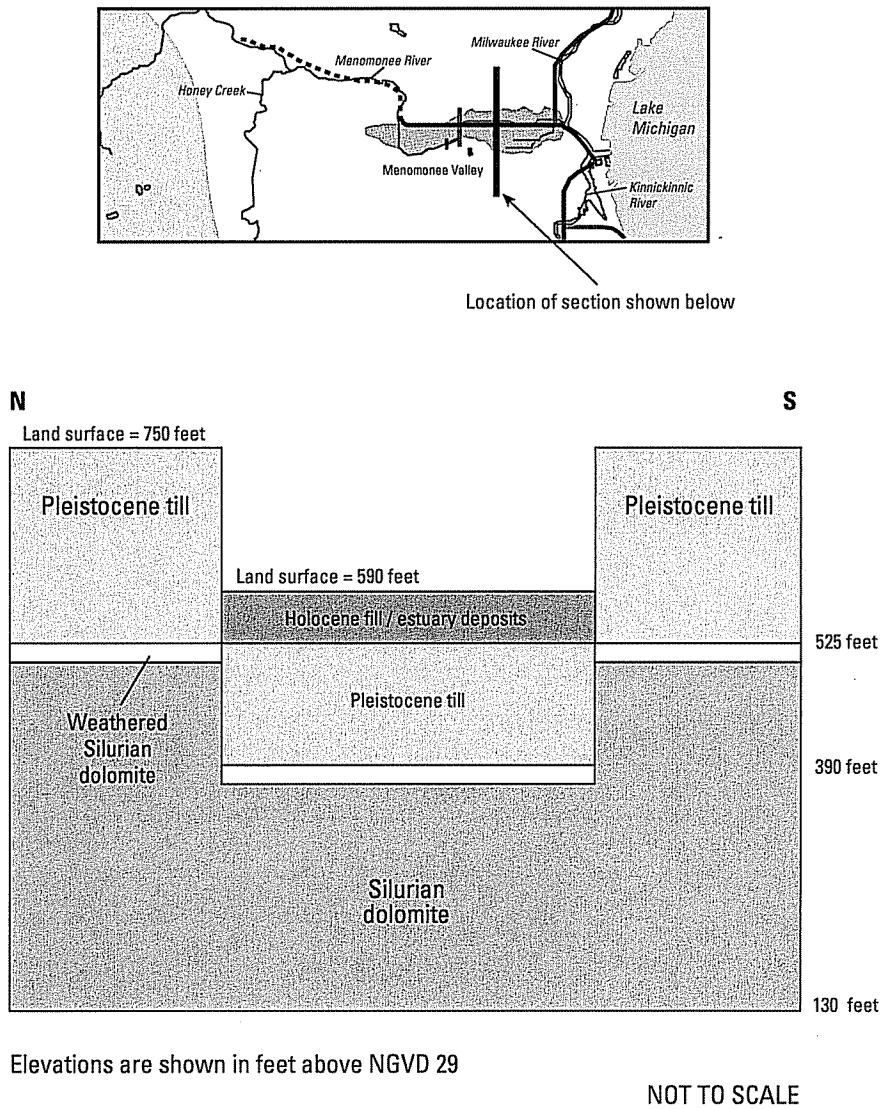


Figure 6. Model domains in the Menomonee Valley Brownfield study area, Milwaukee County, Wis.



**Figure 7.** Schematic hydrostratigraphic section across the Menomonee Valley Brownfield study area, Milwaukee County, Wis.

### Finite-Difference Model

The FD model was constructed to simulate the shallow aquifer (above the Maquoketa Shale confining unit) and its interaction with surface-water features and the ISS. The FD model, developed with the use of the computer program MODFLOW 88 (McDonald and Harbaugh, 1988), is a multilayer model in which the aquifer is bounded by constant-flux boundaries extracted from the GFLOW model simulation. The multiple layers allow for vertical discretization representing hydrogeologic variation, as well as simulation of vertical gradients and flow.

Two particle-tracking programs were used to determine the flow paths of recharge as it moves from the water table to sinks, such as streams or the ISS. Both MODPATH (Pollock, 1994) and PATH3D (S.S. Papadopoulos & Associates, 1991) are designed to work with MODFLOW model output and were used in this investigation. Output from MODFLOW simulations is used in MODPATH and PATH3D to compute paths for imaginary particles of water moving through the simulated ground-water system. In addition to computing particle paths, MODPATH and PATH3D keep track of the traveltime for particles moving through the system, making possible a wide range of analyses, such as delineating capture and recharge areas

or drawing flow nets (Pollock, 1994). A USGS computer program called Model Viewer (Hsieh and Winston, 2002) was used to render three-dimensional views of simulated pathlines.

## Model Calibration

Three types of targets were used in model calibration: (1) hydraulic heads measured in wells completed in various stratigraphic intervals, (2) measured dry-weather infiltration (flux) into several phases of the ISS, and (3) measured vertical gradients in well nests within and outside the valley. The availability of infiltration targets from ISS measurements improves the ability of the model to distribute flow between the shallow surface-water system and the ISS. Moreover, because it is a flux target, dry-weather infiltration to the ISS helps overcome the problem of nonunique solutions associated with correlated parameters. In particular, joint consideration of head and flux data allows estimation of hydraulic conductivity values to be, at least in part, isolated from evaluation of recharge. Matching the third target set, vertical gradients, is particularly important in this setting because of the large vertical head loss beneath the valley. All the hydraulic heads measured in the unlithified sediments used as targets in the MODFLOW model calibration were measured on a single day during a dry period— August 14, 2001 (appendix). For these targets, the variability in heads that may be expected from seasonal recharge events, surface-water fluctuations, and stormflow in the ISS has been eliminated. Hydraulic head data reported during 1994 were compiled for 33 wells completed in the Silurian dolomite (appendix). Because these data were collected on different dates during 1994, any one measurement may have been affected by recharge events or stormflow in the ISS.

The MODFLOW calibration was a two-step process. In the first step, initial values for  $K_h$  and  $K_z$  were chosen on the basis of published values. In the second step,  $K_h$  values were adjusted through a sensitivity analysis restricted to head calibration targets only, whereas  $K_z$  values were adjusted through a calibration process using head targets, ISS dry-weather infiltration targets, and vertical gradient targets. The GFLOW model cannot be calibrated in this way because the solution represents composite heads over the thickness of the aquifer rather than the water-table surface, the ISS inflow is fixed rather than model output, and GFLOW does not simulate vertical gradients. For this reason GFLOW is evaluated by comparison of results to available composite head and stream-

flow information, which is a less complex evaluation than is used for the MODFLOW model.

## Application of Stepwise Modeling

### Model Domains

Boundary conditions in a GFLOW model are applied at surface-water features. Because the solution to a GFLOW model assumes an infinite aquifer, the model domain should extend beyond ground-water and surface-water divides. The hydrologic boundaries used in this evaluation of the Menomonee Valley Brownfield are Lake Michigan; the Menomonee, Milwaukee, Kinnickinnic, and Root Rivers and their tributaries; and Honey Creek (fig. 6). The model domain (as defined by the GFLOW limits of recharge) covers about 195 mi<sup>2</sup>, including western areas of Lake Michigan.

The local domain covers about 26 mi<sup>2</sup>, which is appreciably smaller than the model domain. The local domain is defined by the extent of the MODFLOW model (fig. 6). The MODFLOW model consists of 87 rows and 185 columns; each cell is 250 ft on a side. The Menomonee Valley Brownfield, the primary area of interest, covers about 2.3 mi<sup>2</sup>. The MODFLOW grid is surrounded by specified-flux boundaries that were extracted from the GFLOW solution. Locations of surface-water bodies and the ISS are also shown in figure 6.

### Development of the Analytic-Element Model

#### Construction

Average stages for hydrologic boundaries in the GFLOW model (rivers, canals, and lakes) were estimated from USGS 7.5-minute topographic maps. Near-field line-sinks incorporate riverbed resistance, which is locally determined as the thickness of the riverbed sediments divided by the vertical hydraulic conductivity of those sediments. Hydraulic conductivity of the aquifer consisted of a regional  $K_h$  outside the Menomonee Valley Brownfield and an inhomogeneity corresponding to the area with land-surface elevations of 600 ft or lower (fig. 6). The regional  $K_h$ , and that of the inhomogeneity, are determined by the saturated-thickness-weighted average of the horizontal hydraulic conductivities assigned to the various vertically layered units. The unit conductivities are listed in table 2, and the unit thicknesses correspond to the elevations in fig-

ure 7. The recharge zones in the model are shown in figure 2. The ISS is represented by a series of discharge-specified line-sinks that remove water at the dry-weather discharge rate reported for different phases of the ISS. Lake Michigan and the other far-field water bodies are constant-head boundaries in the far field of the GFLOW model. The near-field water bodies were specified in the model as head-dependent-flux boundaries with assigned elevations, resistances, and widths.

## Calibration

The GFLOW model was calibrated by manually adjusting line-sink resistances throughout the near field, and hydraulic conductivity in the inhomogeneity; regional recharge rates and the dry-weather infiltration to segments of the ISS were fixed on the basis of previous work (Cherkauer, 2001; Rust/Harza, 2002). However, in the course of calibration, model simulations indicated that estuary line-sinks were contributing an unrealistic amount of water to the ISS and that Lake Michigan was contributing negligible amounts. Field evidence shows the opposite to be true (Cherkauer and Carlson, 1997). Gradients over a part of the shoreline of Lake Michigan adjacent to Milwaukee reversed from upward to downward after ISS construction, whereas ISS exchange with the Milwaukee and Kinnickinnic Rivers is affected to only a small degree (Douglas Carlson, U.S. Geological Survey, written commun., 2000). To bring the model closer to observed conditions, fluxes out of the estuary were limited where the ISS lies directly underneath. Within the Menomonee Valley Brownfield, this zone corresponds to the area east of 27<sup>th</sup> Street in

figures 2 and 4. Fluxes were limited by specifying a loss rate for the affected bodies. The selected flux rate for these reaches corresponds to a downward gradient of 1 ft/ft between the near-surface water table and the water level in the ISS and a vertical hydraulic conductivity of 0.001 ft/d for the intervening material. This vertical conductivity value represents an average of the till and dolomite vertical hydraulic conductivities used in cross-section models recently calibrated to local conditions (Carlson, 2000). The total specified flux from surface-water bodies overlying the ISS is 0.11 ft<sup>3</sup>/s, of which 0.10 ft<sup>3</sup>/s comes from surface water within the local domain. These rates are small compared to the 4.34 ft<sup>3</sup>/s gained by the entire ISS, of which 2.61 ft<sup>3</sup>/s discharges to the ISS within the local domain. To simulate the observed limited availability of water from the rivers and canals, these modifications increased the relative contribution of Lake Michigan to the ISS and increased the area over which recharge contributes to the ISS.

Because the unlithified and Silurian aquifers are simulated as one layer in the GFLOW model, composite heads are simulated between the water-table elevation (average altitude of about 590 ft) and the ground-water head in the dolomite (average altitude of about 295 ft). The gradient in the composite head field controls the movement of water from the far field to the near field of the model and from sources of water (such as recharge and Lake Michigan) to sinks of water (such as the ISS and some surface-water bodies). The data available against which to match the simulated composite heads are limited to one location in the Menomonee Valley Brownfield adjacent to the estuary. A well completed in dolomite at the elevation of the ISS, but 492 ft to the south, showed a head equal to 518 ft in

**Table 2.** Hydraulic conductivities and effective porosities for calibrated GFLOW and MODFLOW models, Menomonee Valley Brownfield study area, Milwaukee County, Wis.

Unit	Horizontal hydraulic conductivity, <sup>1</sup> feet per day	Vertical effective hydraulic conductivity, <sup>2</sup> feet per day	Porosity <sup>3</sup>
Fill/Estuary	4.0	0.0010	0.2
Channel <sup>4</sup>	10.0	.1000	.2
Till	.4	.0010	.1
Weathered dolomite	5.0	.0050	.05
Dolomite	.6 <sup>5</sup>	.0004	.01

<sup>1</sup>Horizontal hydraulic conductivities used in both GFLOW and MODFLOW models.

<sup>2</sup>Vertical hydraulic conductivities calibrated to MODFLOW solution.

<sup>3</sup>Effective porosities used to calculate traveltimes with MODFLOW and PATH3D.

<sup>4</sup>Channel deposits only represented in MODFLOW model.

<sup>5</sup>Dolomite horizontal hydraulic conductivity is zoned in MODFLOW model.

August 2001. A well open to till less than 984 ft from the dolomite well but about 213 ft above the ISS, showed a head equal to 564 ft for that date. The head produced by GFLOW should be some composite of these two values close to the average of 544 ft. The simulated head at the location is 541 ft.

A second way to evaluate the GFLOW model, particularly the suitability of the recharge zones, is through flux data. The base flow to the Menomonee River along the section between the two USGS streamflow-gaging stations shown in figure 2 can be estimated for pre-ISS conditions by use of flow-duration curves constructed from concurrent data collected in the early 1980s. The calculation yields a value of base flow for this section equal to 1.0 ft<sup>3</sup>/s. This estimate agrees well with the base flow of 0.78 ft<sup>3</sup>/s simulated by the GFLOW model for pre-ISS conditions.

## Development of the Finite-Difference Model

### Construction

In many respects, the MODFLOW model duplicates the input to the GFLOW model. Both models are steady-state representations of the flow system. The total volumetric rate of recharge entering the MODFLOW model domain is the same as the total volumetric rate of recharge that enters the corresponding area in the GFLOW model. The outline of the Menomonee Valley Brownfield Kh zone is the same for both models, and the Kh values assigned each of the units are also the same (table 2). The average thickness of units in the MODFLOW model corresponds to the thicknesses used to calculate the composite hydraulic conductivities in GFLOW. Lake Michigan is treated as a constant-head boundary in both models. The two models differ, however, with respect to how they simulate vertical flow, how near-river sediments are characterized, how recharge is zoned, and how boundary conditions are set.

Although GFLOW supports some three-dimensional flow features (for example, it allows flow under the estuary to the ISS), it does not explicitly account for differences in resistance to vertical flow within the shallow deposits and the dolomite units. The MODFLOW model incorporates the full flow system by dividing the hydrostratigraphic units between eight layers, and by varying the thickness of the layers on the basis of data from geologic logs on file at the Wisconsin Geologic and Natural History Survey (Daniel Feinstein, USGS, oral commun., 2002). The configuration of the units along an east-west section that intersect

the valley is shown in figure 8. The vertical hydraulic conductivities assigned to the fill/estuary, till, weathered dolomite, and dolomite units after calibration are included in table 2.

The MODFLOW input contains a zone of high Kv and Kh in layers 1 and 2 corresponding to coarse channel deposits that are likely to be associated with the free-flowing reaches of the rivers (upstream from the Milwaukee River Estuary) in the model (fig. 9). The introduction of this zone was necessary to reproduce the measured vertical gradient in the only well nest in the free-flowing reach of the Menomonee River. The channel deposits are not represented in the GFLOW model.

All phases of the ISS represented in the MODFLOW domain are in layer 7. The ISS is represented as a series of drains (a head-dependent-flux boundary that removes water from the model) to facilitate comparison of simulated infiltration to reported values. In other words, ISS dry-weather infiltration is used as a flux calibration target. The conductance of the drains represents the resistance to flow through the grouted circumference of the ISS. Conductances are based on an assumed grout hydraulic conductivity equal to 0.0004 ft/d (the same value assumed for the vertical hydraulic conductivity of the dolomite) and a grout thickness of 1.0 ft.

MMSD measured the dry-weather infiltration to each phase of the ISS (Rust/Harza, 2002). For purposes of model calibration, this information has been translated into target flux estimates for the western part of the Crosstown IIA phase (0.47 ft<sup>3</sup>/s), for the Crosstown IA phase (1.16 ft<sup>3</sup>/s), and for the parts of the Northshore, Kinnickinnic, and Lake Michigan phases included in the MODFLOW model (0.54, 0.31, and 0.16 ft<sup>3</sup>/s, respectively).

Specified fluxes are assigned to all perimeter nodes of the MODFLOW grid, except for the last column of the grid because it intersects constant-head nodes associated with Lake Michigan. The fluxes for a given MODFLOW boundary node are equal to the comprehensive flux extracted from GFLOW for the width of the row or column location and are distributed between the eight MODFLOW model layers according to their relative transmissivity. The remaining boundary conditions in the MODFLOW model are head-dependent conditions assigned to surface-water nodes and the ISS drains. The resistance of the riverbed material is set to 1 ft/(ft/day). This resistance corresponds to a riverbed of sand that is 5 ft thick, with hydraulic conductivity equal to 5 ft/d.

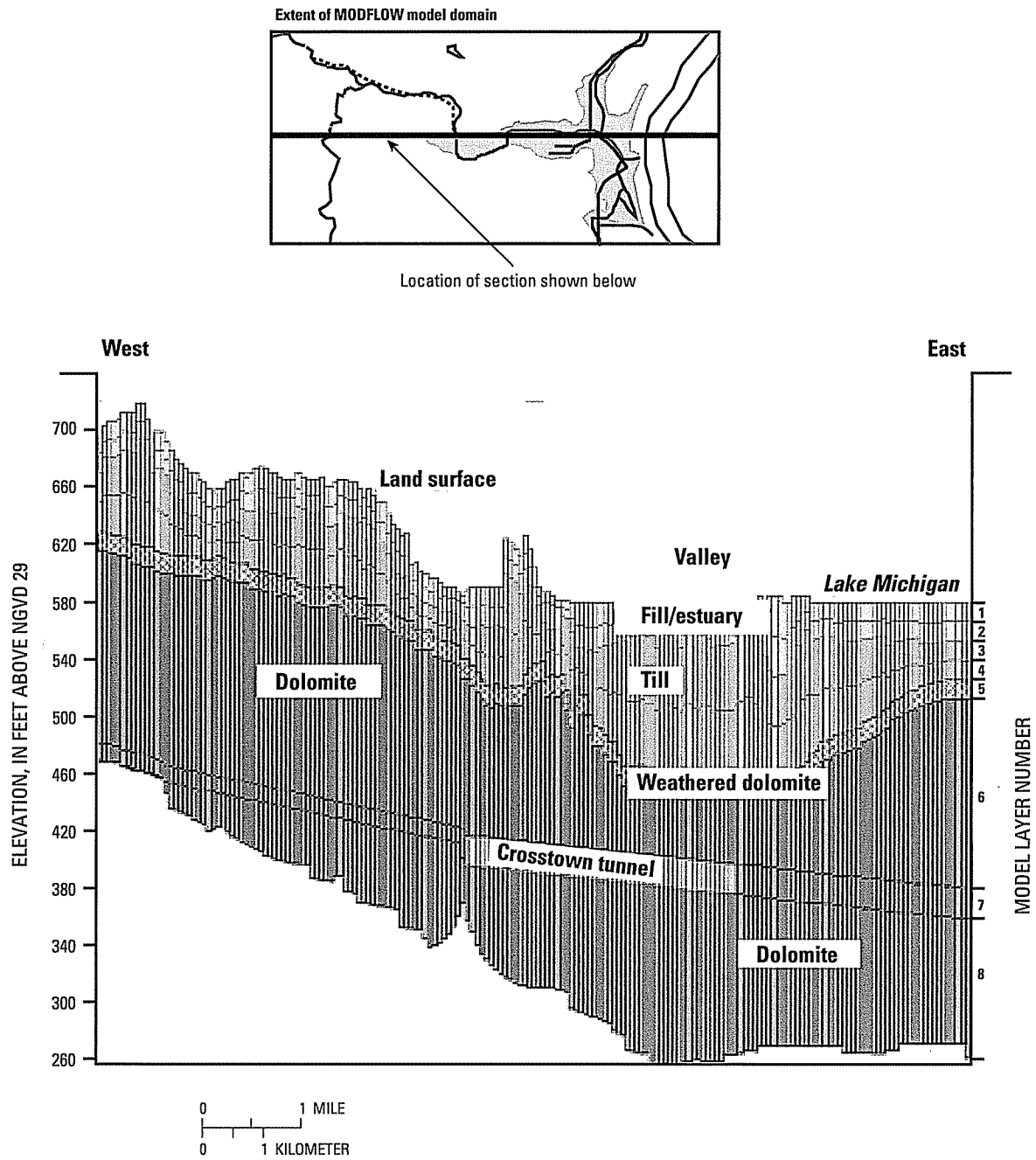


**Figure 8.** MODFLOW section and layering, Menomonee Valley Brownfield study area, Milwaukee County, Wis. (Section extends entire west to east distance of MODFLOW model domain shown in figure 6.)

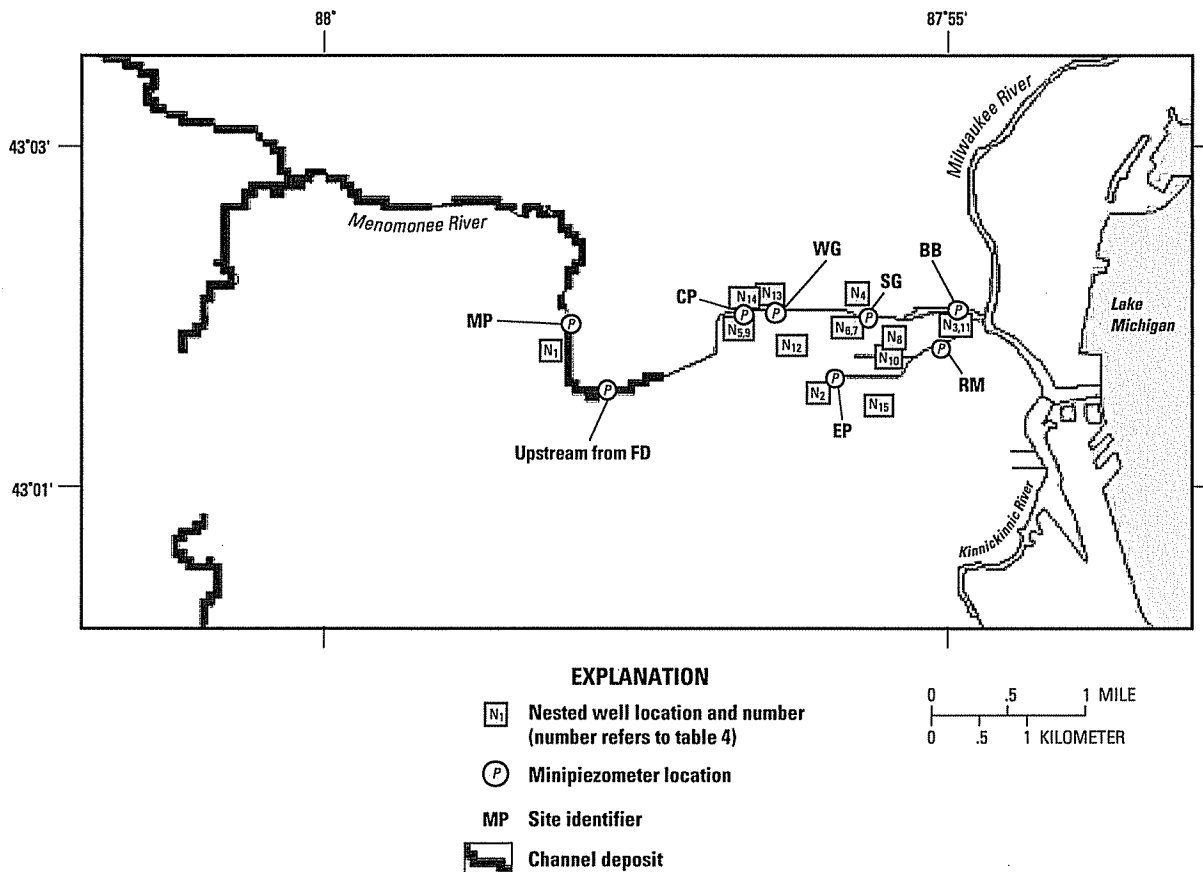


**Figure 9.** Locations of channel deposits, nested wells, and minipiezometers in the Menomonee Valley Brownfield study area, Milwaukee County, Wis.

## Calibration and Sensitivity

Calibration of the MODFLOW model depends on the match between measured and simulated heads, between the measured and simulated vertical gradient at well nests, and between the measured and simulated dry-weather infiltration for all or part of the five phases of the ISS.

Measurements of water levels on August 14, 2001, provided head targets at 101 wells open to un lithified sediments, of which 79 represented water-table conditions and the others corresponded to depths averaging about 33 ft below the water table. Water levels are also available from 1994 for 33 wells drilled in the dolomite, most of which are close to the ISS (appendix).

The data set from wells drilled in the un lithified sediments includes measurements at 12 nested well locations (fig. 9). The measured vertical gradient was downward at all but the westernmost nest location. The average downward gradient was equal to 0.09 ft/ft between the water table and the fill/estuary horizon at the mid-eleva-

tion in model layer 2; it was equal to 0.28 ft/ft between the water table and the till horizon at the mid-elevation in model layer 3. The increasing vertical gradient with depth reflects some combination of drainage to the ISS and the distribution of vertical hydraulic conductivities. Calibration results for the simulation that best matched the three sets of targets are shown in figures 10a, and 10b and tables 3a, 3b, 4, and 5. The agreement between the observed and simulated heads is not as close for the wells in bedrock as it is for the wells in un lithified sediments (tables 3a and 3b, and figures 10a and 10b). For the wells in un lithified sediments, the agreement is close not only with respect to the trend of the water-table surface but also with respect to the measured vertical gradients between the estuary and underlying till deposits (table 4).

The quality of the fit to wells drilled in bedrock is affected by at least three factors. First, bedrock head measurements are not synchronous with other targets used in model calibration.

Second, although many of the wells drilled in bedrock

**Table 3a.** MODFLOW calibration statistics for wells in the unlithified sediments of the Menomonee Valley Brownfield study area, Milwaukee County, Wis.

[Residual = observed – simulated; ft, feet]

Total number of wells	101
wells in layer 1	79
wells in layer 2	8
wells in layer 3	12
wells in layer 4	1
wells in layer 5	1
Residual mean	2.25 ft
Absolute residual mean	3.63 ft
Residual standard deviation	5.63 ft
Most negative residual	-7.84 ft
Most positive residual	29.03 ft
Number of negative residuals	43
Number of positive residuals	58
Number of residuals within +/- 2 ft	53

**Table 4.** MODFLOW vertical-gradient calibration for the Menomonee Valley Brownfield study area, Milwaukee County, Wis.

[Negative values indicate upward gradient]

Well nest <sup>1</sup>	Measured gradient	Simulated gradient
1. Water table-Estuary	-0.043	-0.028
2. Water table-Till	.03	.18
3. Water table-Estuary	.06	.23
4. Water table-Till	.07	.35
5. Water table-Estuary	.12	.15
6. Water table-Estuary	.22	.27
7. Water table-Till	.27	.24
8. Water table-Till	.27	.16
9. Water table-Till	.28	.19
10. Water table-Till	.28	.23
11. Water table-Till	.30	.24
12. Water table-Till	.30	.12
13. Water table-Till	.36	.32
14. Water table-Till	.41	.31
15. Water table-Till	.58	.51
<b>Averages:</b>		
Overall	.23	.23
Water table-Estuary	.09	.16
Water table-Till	.28	.26

<sup>1</sup> Well nest is located by number in figure 9.

**Table 3b.** MODFLOW calibration statistics for wells in the dolomite of the Menomonee Valley Brownfield study area, Milwaukee County, Wis.

[Residual = observed – simulated; ft, feet]

Total number of wells	33
wells in layer 5	6
wells in layer 6	11
wells in layer 7	15
wells in layer 8	1
Residual mean	23.2 ft
Absolute residual mean	44.9 ft
Residual standard deviation	58.0 ft
Most negative residual	-69.0 ft
Most positive residual	188.1 ft
Number of negative residuals	15
Number of positive residuals	18
Number of residuals within +/- 2 ft	15

**Table 5.** MODFLOW calibration to measured dry-weather infiltration to phases of the Inline Storage System (ISS) in the Menomonee Valley Brownfield study area, Milwaukee County, Wis.

[ft<sup>3</sup>/s, cubic feet per second]

Inline Storage System phase	Measured infiltration <sup>1</sup> ft <sup>3</sup> /s	Simulated infiltration ft <sup>3</sup> /s
Crosstown IIA	0.46	0.60
Crosstown IA	1.16	.97
Northshore	.54	.53
Kinnickinnic	.31	.37
Lake Michigan	.16	.26
<b>Total within local MODFLOW model</b>	<b>2.63</b>	<b>2.73</b>

<sup>1</sup> Rust/Harza, 2002, Internal inspection of the Inline Storage System; report prepared for the Milwaukee Metropolitan Sewerage District.

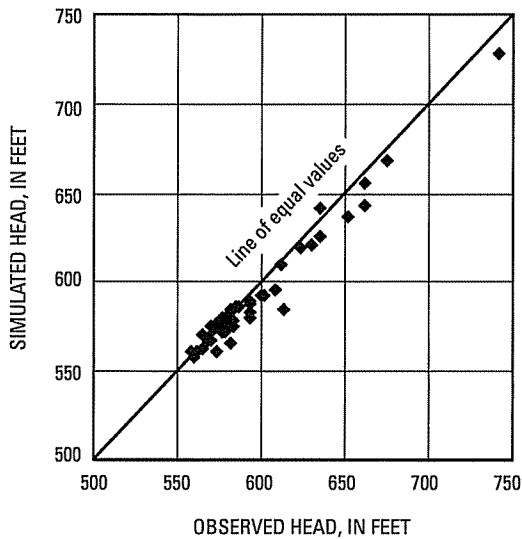


**Figure 10a.** Calibration plot of measured hydraulic heads plotted against MODFLOW-simulated heads in the unlithified sediments (layers 1 through 4), Menomonee Valley Brownfield study area, Milwaukee County, Wis.

are completed within a few feet of the deep tunnel, the model simulates water levels at an appreciably greater distance from the tunnel because model cells are 250 ft wide. Third, the ISS is not grouted everywhere, so gradients into the tunnel are variable from place to place. Given the difficulty in matching local conditions around the tunnel, the model was more closely calibrated to the estimated dry-weather infiltration into the five phases of the ISS (table 5) than to the adjacent ground-water levels. Because the tunnel infiltration is an integrated measure of the response of the ground-water system to the stress imposed by segments of the ISS, it is less affected by variations in local conditions.

The match between measured and simulated targets is reasonably close across the range of targets, and the overall calibration is considered acceptable. The calibrated horizontal hydraulic conductivities and recharge rate in the MODFLOW model are unchanged from those in the GFLOW simulation that provided the specified-flux conditions to the MODFLOW perimeter boundary. The head calibration is very sensitive to recharge and the distribution of vertical hydraulic conductivity (tables 1 and 6). Measured gradients between surface water and ground water provide a check on the model calibration. Streamflow-gaging stations paired with minipiezometers inserted just below the riverbed yield the direction and magnitude of the hydraulic gradient connecting surface water to ground water at the locations shown in figure 9. The estuary and

**Table 6.** Ranked sensitivities of the MODFLOW parameters in the Menomonee Valley Brownfield study area, Milwaukee County, Wis.

[Head calibration is most sensitive to first-listed parameter (Recharge) and least sensitive to the last-listed parameter (Kh of the estuary deposits); Kh, horizontal hydraulic conductivity; Kg, hydraulic conductivity of grout; Kv, vertical hydraulic conductivity; ISS, Inline Storage System]

Recharge	
Kh	Weathered dolomite
Kg	Crosstown IA phase of the ISS
Kh	Inline Storage System dolomite
Kg	Northshore, Lake Michigan, and Kinnickinnic phases of the ISS
Kv	Till
Kh	Till
Kh	Mayville Dolomite
Kh	Racine Dolomite
Kv	Racine Dolomite
Kg	Crosstown IIA phase of the ISS
Kv	Mayville Dolomite
Kv	Estuary deposits
Kv	ISS dolomite
Kv	Weathered dolomite
Kh	Estuary deposits

estuary canal locations were sampled seven times between June 2001 and September 2001. The two upstream locations were sampled in spring and summer 2000. The direction of the gradient over the measurement periods is shown in table 7. Upward gradients imply discharge of ground water to surface water. Downward gradients imply discharge of surface water to ground water. The model simulation matched the observed upward flow in the upstream locations and the generally downward flow in the estuary locations.

No attempt was made during the calibration process to match the magnitude of the observed hydraulic gradients. Seiche in the estuary (oscillation of water level initiated chiefly by local changes in atmospheric pressure, aided by winds and tidal currents [Bates and Jackson, 1980]) causes the river and canal levels to change significantly over a short time, with a corresponding effect on the measured gradient at a given streamflow-gaging station. In addition, the variability in the deposits constituting the riverbed (sand in some places, industrial fill in others) means that matching even average observed gradients would require changing the hydraulic conductivity of the riverbed over several orders of magnitude from one moni-

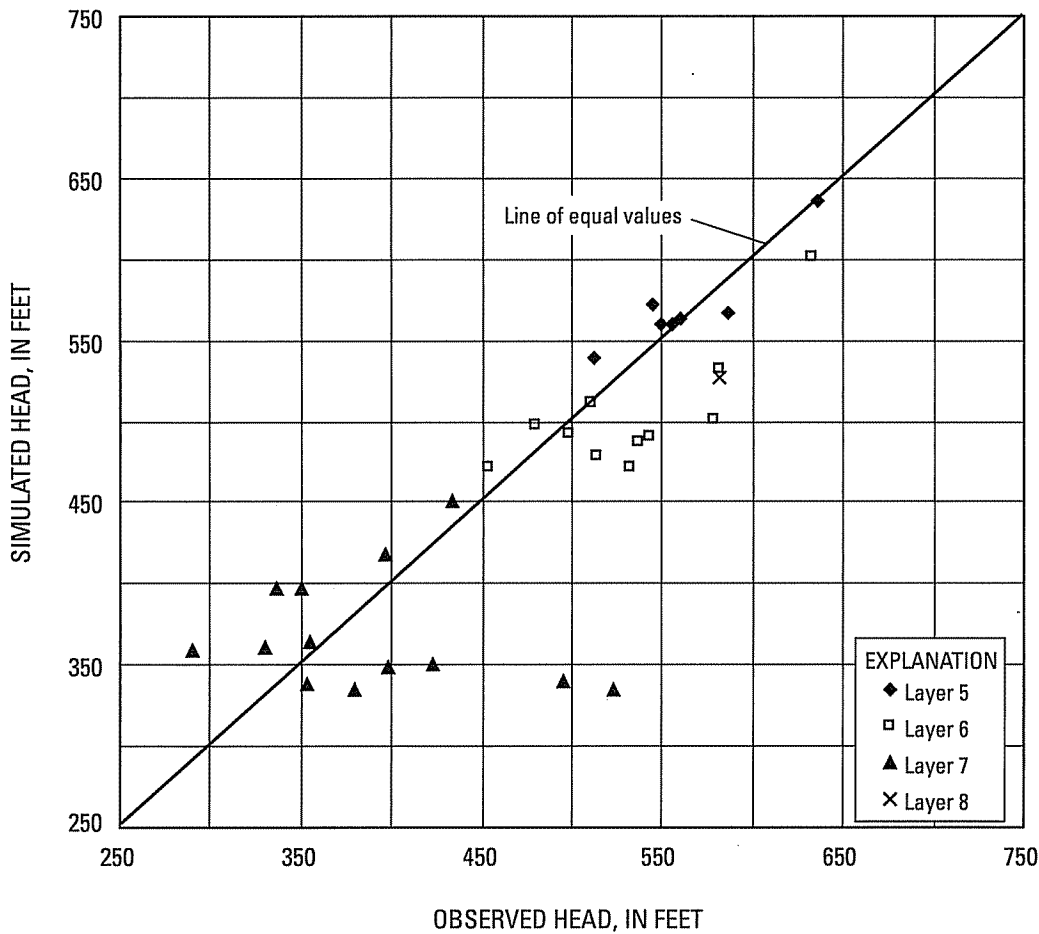


**Figure 10b.** Calibration plot of measured hydraulic heads plotted against MODFLOW-simulated heads in the dolomite (layers 5 through 8), Menomonee Valley Brownfield study area, Milwaukee County, Wis.

tored location to another without knowing what values to assign between these locations.

This gap in our knowledge of the system, however, does not affect the reliability of the model. A sensitivity analysis on riverbed hydraulic conductivity (in which it was varied everywhere from its base value of 5 ft/d—corresponding to a sand—to values as low as 0.005 ft/d—corresponding to a silt) demonstrated that the model calibration and model results are almost completely insensitive to the value selected. The match to water levels, to vertical gradients, and to tunnel inflow is largely unaffected. Model findings (for example, the simulated areas of contribution for the deep tunnel and the surface water) are nearly identical over the entire range of riverbed values. The reason for this insensitivity is that decreases in riverbed hydraulic conductivity are linked to corresponding increases in the simulated hydraulic gradient, so the model simulates the same direction and approximately the same magnitude of

flow between the ground water and surface water throughout the model over the tested range. This insensitivity to riverbed hydraulic conductivity has been noted in other studies (an example is given in Hunt, 2000).

The value assigned riverbed hydraulic conductivity in the model has little influence on the simulated flow lines connecting Menomonee Valley Brownfield recharge to discharge locations. However, if this model were to be applied at a finer scale to better understand the exchange of ground water with surface water over time at a specific location, it would be necessary to collect sufficient data to reproduce the cyclic changes in estuary stage and to map the local variations in riverbed hydraulic conductivity.

**Table 7.** Direction of vertical gradients between river (estuary) and ground water below riverbed, Menomonee Valley Brownfield study area, Milwaukee County, Wis.

[Minipiezometer locations are shown on figure 9; Falk Dam site is about one-half mile upstream from the dam; gradient was observed only one day at the Falk Dam site; at all other sites, gradient was observed on seven dates between June 2001 and September 2001]

Site	Observed direction	Simulated direction
Miller Park (MP)	Up	Up
Falk Dam (FD)	Up	Up
Central Repair (CP)	Down	Down
Wisconsin Gas (WG)	Down	Down
SIGMA (SG)	Variable	Down
Bridges and buildings (BB)	Down	Down
Emmpak (EP)	Down	Down
RACM (formerly Crabby Al's) (RM)	Variable	Down

## Model Limitations

Simulation of hydrology in this complex urban environment unavoidably involves a number of uncertainties over and above the values assigned to model parameters.

### Uncertainties in the Hydrogeologic System

**Assumed impermeability of Maquoketa Shale.** An appreciable downward gradient exists across the Maquoketa Shale as a result of ongoing pumping from the underlying sandstone aquifer. In addition, the construction of some deep wells (abandoned and active) may provide a conduit across the Maquoketa Shale confining unit. As a result it is possible that the model underestimates the total recharge to the water table by the amount that moves downward from the shallow to deep aquifer systems. However, the downward leakage is known to be very small below the study area (Feinstein and others, 2004), while the downward flow across multiple aquifer wells is assumed to be a minor component of total recharge.

### Uncertainties in MODFLOW Target Values

**Bias in shallow (unlithified) hydraulic head data.** The primary calibration data set for the model consists of heads measured on a single day (August 14, 2001) in wells open to the shallow (unlithified) sediments. A

synoptic data set such as this is preferable to data collected over many dates under potentially very different hydrologic conditions; however, it is not known how representative these synoptic measurements are of long-term average heads. It is known that these heads generally fall between heads measured in the same wells for the only other two available measurement dates—one in the spring (June 2000) when the water table was relatively high and one in the winter (December 1999) when the water table was relatively low. Thus, the August data represent intermediate conditions across the three available measurement periods.

**Bias in deep (dolomite) hydraulic head data.** The calibration data set for deep wells drilled in bedrock is much less reliable than the data set for the shallow wells. These heads correspond to different dates of measurement in 1994 (rather than to a single measurement date in 2001 as in wells drilled in unlithified sediments). Water-level conditions from that time are likely different than those in 2001 because the hydrologic system is not in steady state. In addition, many of the deep wells drilled in bedrock are very close to the ISS (as little as 10 ft distant), so the water levels represent conditions just outside the tunnel rather than at the middle of the 250-ft by 250-ft model cell that encompasses the tunnel. For these reasons, the set of calibration targets in the dolomite bedrock serves at best as only a qualitative check on the ability of the model to approximate deep hydraulic conditions.

**Uncertainty in vertical gradient targets.** The presence of strong vertical gradients requires calibration to heads in different layers of the model. However, vertical discretization of the model and necessary interpolation of target heads at the center of screened intervals to the center elevation of model layers introduces additional uncertainty.

**MMSD estimate of ISS dry-weather infiltration.** Uncertainty will always be associated with estimates of dry-weather infiltration, although the most recent evaluation (Rust/Harza, 2002) was designed specifically to quantify dry-weather infiltration and is believed to be an improvement over earlier estimates. Dry-weather infiltration has likely changed over time and for this reason corresponds to changing head. In this connection, it is noteworthy that the recent infiltration estimates made in early 2002 are close in time to the calibration-target water levels collected in the unlithified sediments in late 2001 but are significantly separated in time from the set of calibration targets collected in 1994 for wells completed in the dolomite.

## Uncertainties of Discretization and Scale

**MODFLOW cell size in the valley.** The 16,095 model cells are uniformly 250 by 250 ft. This level of discretization does not allow incorporation of the myriad manmade features of the industrial Menomonee Valley that will influence local gradients and flow.

## Limitations Arising from Extraction of Boundary Conditions

### Linking of GFLOW and MODFLOW models.

These models are parallel in that the average transmissivity of the MODFLOW model is the same as the spatially constant transmissivity assigned to the GFLOW model. Similarly, the average recharge to the MODFLOW model is identical to the spatially constant recharge to the GFLOW model. These parallels notwithstanding, the boundary conditions provided by GFLOW are subject to some error. The greatest source of error is that the distance from the major stress induced by the ISS to the local model boundary is less than the desired minimum of 3 times the characteristic leakage length, lambda ( $\lambda$ ). Lambda is calculated by means of the following equation:

$$\lambda = (KHc)^{1/2} \quad (1)$$

where

$\lambda$  is the characteristic leakage length (L),

K is horizontal hydraulic conductivity of the aquifer ( $LT^{-1}$ ),

H is the thickness of the aquifer (L), and

c is resistance, the ratio of confining unit thickness (d) to its vertical hydraulic conductivity (K),

$$c = d/K_c \quad (T)$$

In calculating  $\lambda$ , average aquifer transmissivity was assumed to be 500 ft<sup>2</sup>/d, and vertical resistance through the glacial material and dolomite was equated to that used in the MODFLOW model (average 400 ft thickness divided by  $K_v=0.004$  ft/d, yielding 100,000 days). The resulting  $\lambda$  value is 7,100 ft. To minimize runtime, the MODFLOW grid was made fairly small. The 2-mi distance that separates the ISS in the valley from the north and south edges of the local model area is only 1.5 times the calculated  $\lambda$ . It follows that the stress from the ISS near the bottom of the section produces some vertical flow components at the boundary that are not reflected in the fluxes extracted from

the GFLOW model. The vertical-flow effect decreases exponentially with distance from the ISS. Application of the exponential factor [ $1-e^{-x/\lambda}$ ], where  $x/\lambda$  is set equal to 1.5, indicates that about 78 percent of the vertical-flow component has disappeared at the MODFLOW boundary. (Haitjema and others, 2001, equation 4). Sensitivity analyses show that changes in the vertical distribution of the constant flux at the MODFLOW model boundary have virtually no effect on the simulated flow system within the Menomonee Valley Brownfield.

Because the MODFLOW model derives the lateral flow into its grid from GFLOW, that it receives the same quantity of water as recharge as does the GFLOW model, and that the strength of the ISS sink is identical in both representations, it is expected that the overall capture zone simulated by the two models should be similar. In fact, as demonstrated in the following section of the report, capture zones for the ISS simulated by GFLOW and MODFLOW are very close in shape and extent.

MODFLOW results are reported in more detail than GFLOW results because MODFLOW provides more accurate estimates for traveltimes from source to sink, which are useful for consideration of natural attenuation of contaminants. Experience in this study also showed that although GFLOW was adequate to simulate capture zones for flow systems dominated by two-dimensional flow, a full three-dimensional analysis was needed to more rigorously predict the effect of the ISS on the base flow to overlying streams.

**Vertical distribution of flux to the MODFLOW model.** From the standpoint of mass balance, the GFLOW model should supply the proper amount of water across each part of the extracted MODFLOW model boundaries (for the given model inputs) to allow recharge and the surface water to supply the ISS. What is at issue is the vertical distribution of flux at each lateral boundary and the assumption that the constant flux from the GFLOW solution divides proportionally to the transmissivity of the MODFLOW layers. To evaluate the effect of distributing the flux in this way, several sensitivity runs were done in which the flux was distributed differently. In the first run, all the flux simulated by GFLOW was assigned only to the MODFLOW dolomite layers; in the second run, all the flux was assigned to the top weathered dolomite layer; and in the third run, all the flux was assigned to the glacial material across layers 1 through 4. In each case, the simulated ISS infiltration and head calibration statistics agreed closely with the original run. The ISS infiltration for the sensitivity runs ranges from 2.60 to 2.75 ft<sup>3</sup>/s, with the base value equal to 2.73 ft<sup>3</sup>/s. The absolute residual

mean of the head calibration targets for the sensitivity runs ranges from 3.35 to 3.51 ft, with the base value equal to 3.48 ft. These small differences indicate that the distribution of the boundary flux has little effect on model results.

## Simulation of Ground-Water Flow

The calibrated MODFLOW model was used to simulate shallow ground-water flow in the Menomonee Valley Brownfield study area, to address questions about sources and sinks for ground water, and to estimate traveltimes from the points of recharge in the valley to sinks. The simulated water table within the MODFLOW local domain ranges in altitude from about 570 to 800 ft (fig. 11). Water-table altitudes are around 570 ft in the Menomonee Valley Brownfield and rise quickly to the north, west, and south. The highest water-table altitudes are in the southwest corner of the MODFLOW domain.

## Ground-Water Contributing Areas

At the regional scale, the GFLOW model simulated capture areas for particles flowing from the water table outside the Menomonee Valley Brownfield to the ISS. The simulated traveltime for these particles is as much

as 600 years (fig. 12). In defining these capture areas, the assumed composite effective porosity for the till and dolomite is 0.05. Particle-tracking routines MODPATH (Pollock, 1994) and PATH3D (S.S. Papadopoulos & Associates, 1991) were applied to the MODFLOW results to determine what part of recharge to the local domain flows downward to the ISS and what part circulates back upward to surface-water bodies. The capture pattern for the local domain is shown in figure 13.

## Sources and Sinks

Within the local MODFLOW domain, the comparison of the total simulated infiltration to the ISS (2.74 ft<sup>3</sup>/s) and total available recharge (1.36 ft<sup>3</sup>/s for the assumed recharge rate equal to 0.6 in/yr) demonstrates that the ISS is the major sink for ground water and that it captures much water that would otherwise discharge as base flow to streams. In addition to local recharge, sources for infiltration to the ISS include lateral flow into the model (originating largely as recharge outside the MODFLOW domain), flow from Lake Michigan, and losses from rivers and canals. The MODFLOW model provides the following sources of infiltration to the ISS as percentages: 36 percent from recharge within the model domain, 45 percent from lateral flow into the domain, 15 percent from Lake Michi-

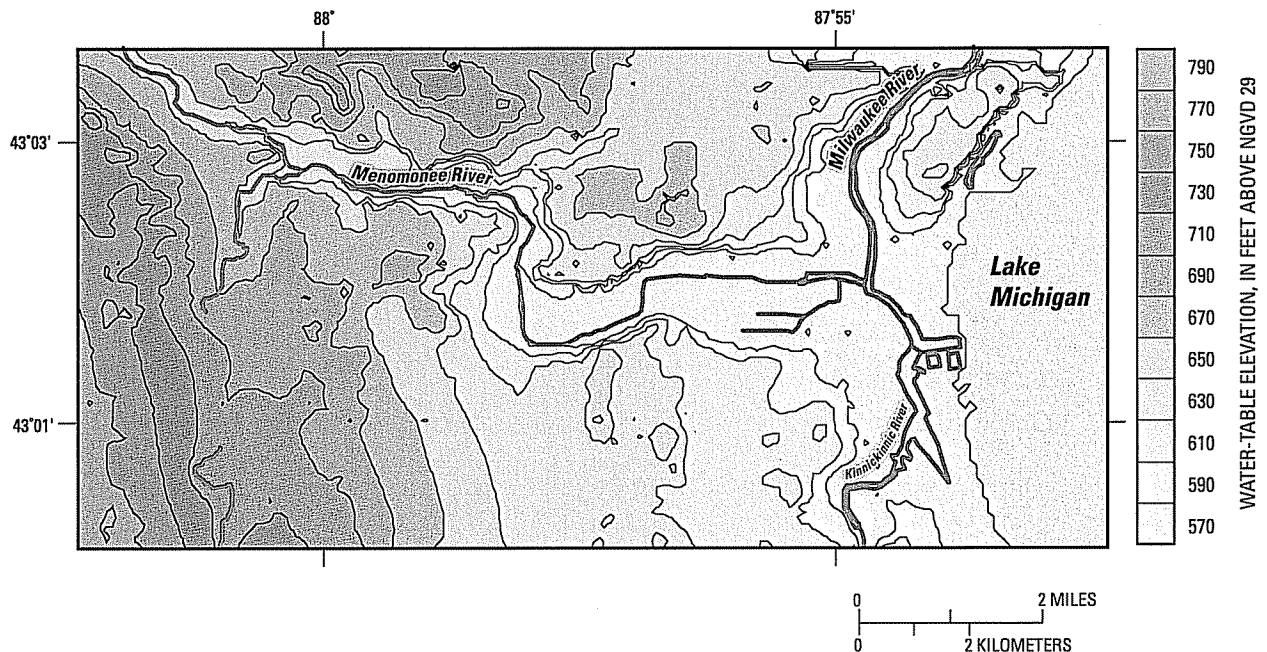


**Figure 11.** Water-table surface in the Menomonee Valley Brownfield study area, Milwaukee County, Wis., simulated with MODFLOW, and calibrated to August 14, 2001 hydraulic heads.

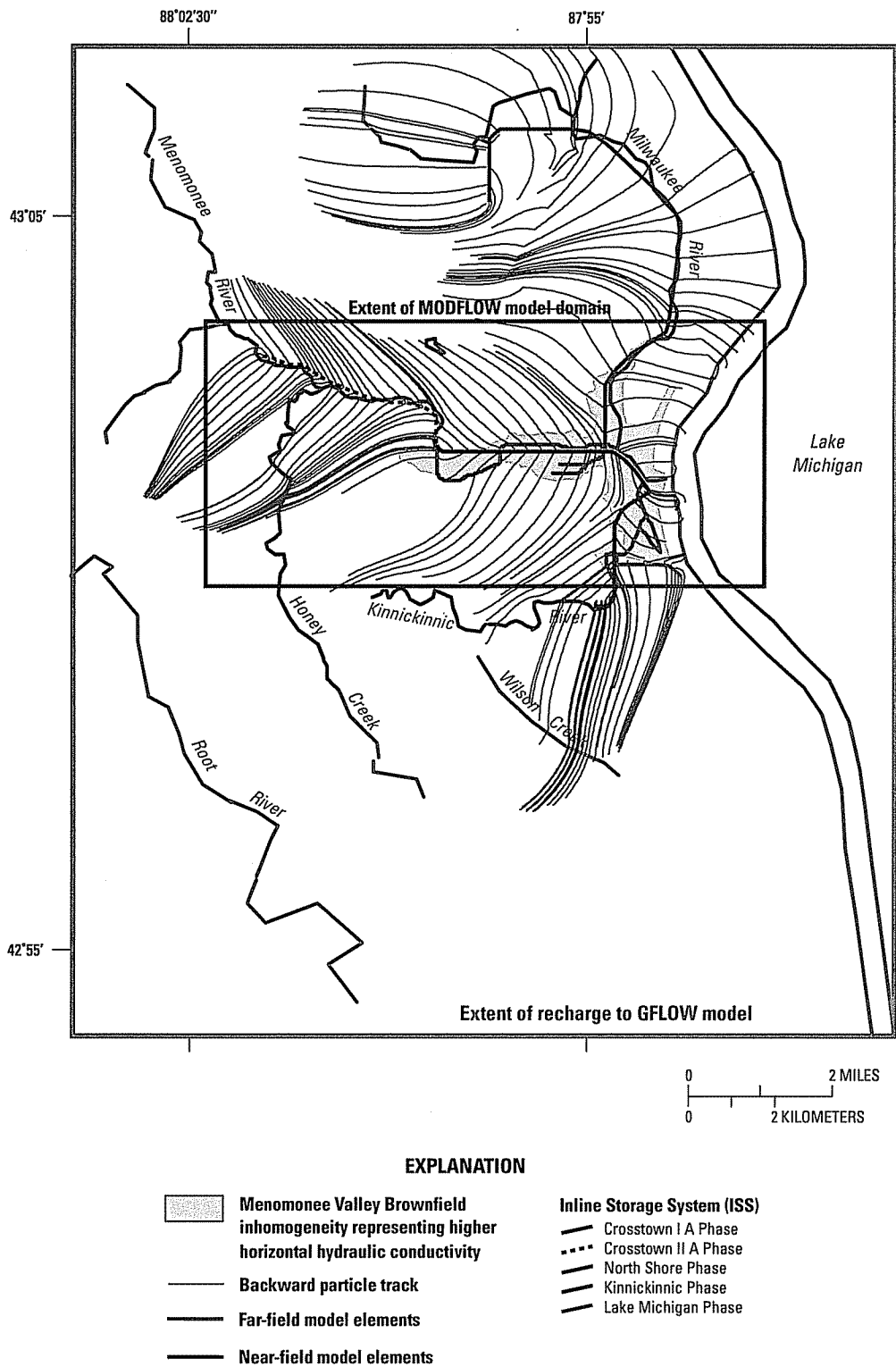


**Figure 12.** Backward particle tracking from the Inline Storage System in the Menomonee Valley Brownfield study area, Milwaukee County, Wis., simulated with GFLOW.

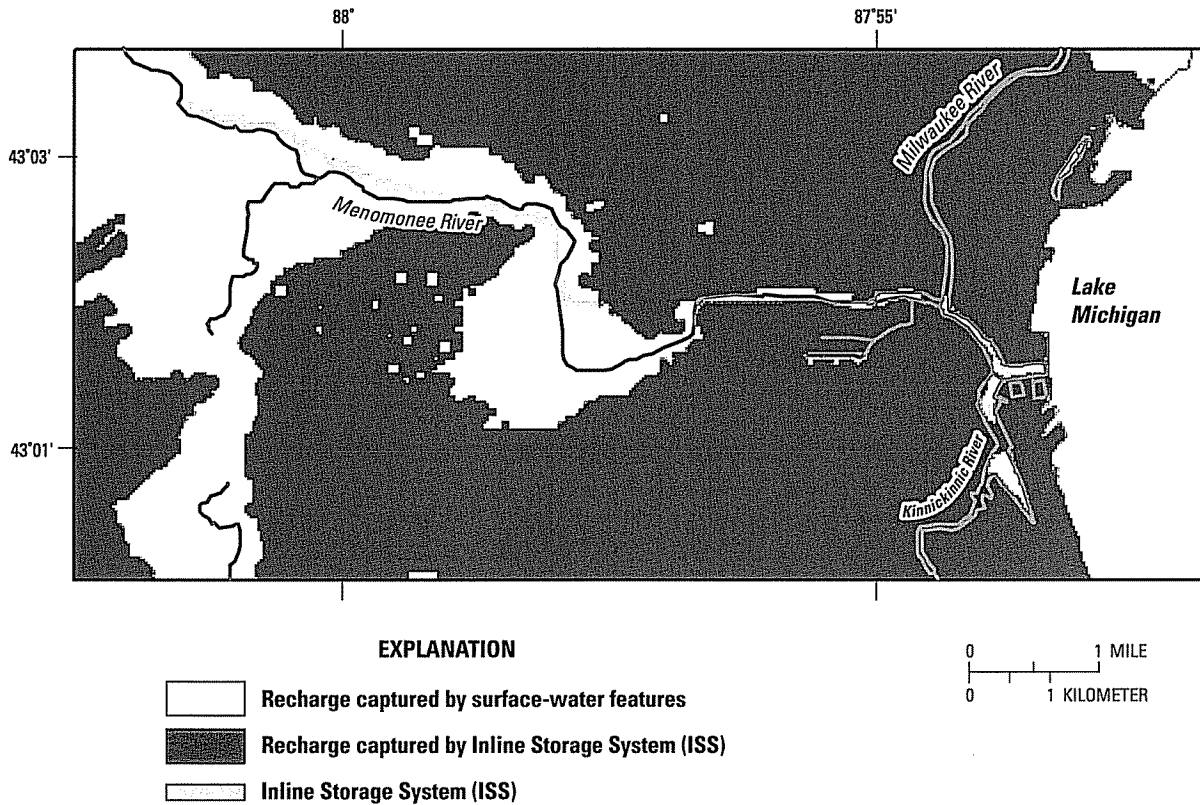


**Figure 13.** Capture zones simulated with MODFLOW and MODPATH for the Inline Storage System (ISS) in the Menomonee Valley Brownfield study area, Milwaukee County, Wis.

gan, and 4 percent from other surface-water bodies. About 73 percent of recharge within the MODFLOW domain (excluding the area occupied by surface-water nodes) discharges to the ISS, and 27 percent discharges to gaining surface-water bodies. This suggests that the conceptual model that best fits the Menomonee Valley Brownfield is one intermediate to the end-members discussed earlier (fig. 5). The simulated flux from losing surface-water bodies overlying the ISS is 0.11 ft<sup>3</sup>/s, which compares well with the corresponding GFLOW rate specified at 0.10 ft<sup>3</sup>/s and therefore increases confidence in the stepwise approach. Three east-west sections are presented that illustrate the flowpaths of recharge to the MODFLOW model domain (fig. 14a, b, and c). A three-dimensional representation that illustrates simulated flow paths from selected areas of the Menomonee Valley Brownfield is shown in figure 15.

**Traveltimes**

The patterns of discharge to surface sinks and the ISS simulated by the MODFLOW model are distinguished by the traveltimes involved. For the assumed values of effec-

tive porosity assigned different units (table 2), it is possible to calculate the range of traveltimes for recharge to the valley to circulate back to the surface and for recharge to the valley to discharge to the ISS (table 8).

The median traveltime to surface water is 8 years; the median time to the ISS is 255 years. The distribution of traveltimes to the ISS based on the assumed effective porosities (table 2) is shown in figure 16. The traveltime

**Table 8.** Statistics for simulated traveltime of recharge to surface-water sinks and the Inline Storage System, Menomonee Valley Brownfield study area, Milwaukee County, Wis.

[Traveltime and range in years]

	Surface-water sinks	Inline Storage System
Average traveltime	30	230
Median traveltime	8	255
Range (90 percent of traveltimes fall within range)	1–99	34–355

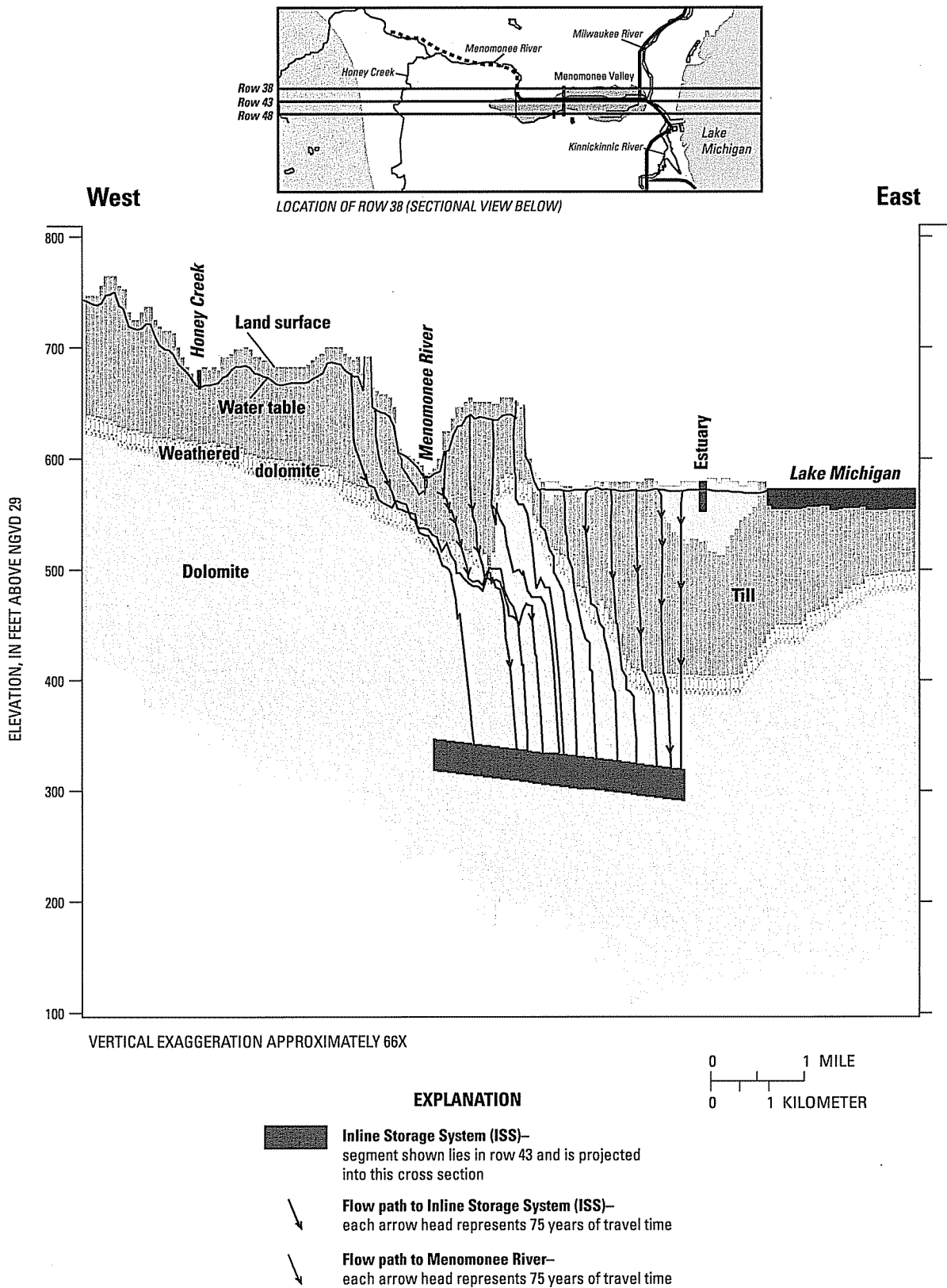


**Figure 14a.** Sectional view (row 38) of ground-water-flow directions simulated with MODFLOW and MODPATH in the Menomonee Valley Brownfield study area, Milwaukee County, Wis.

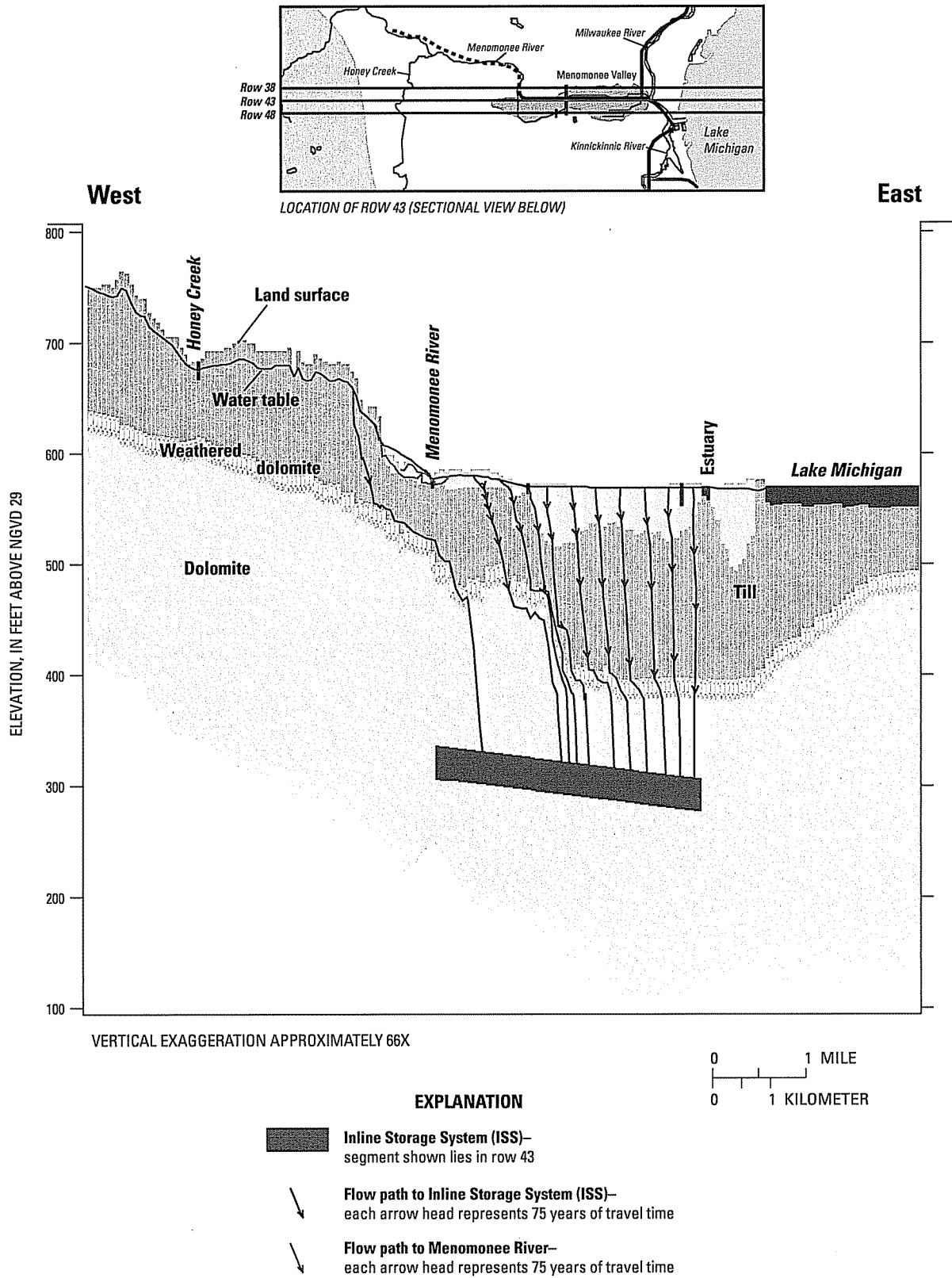
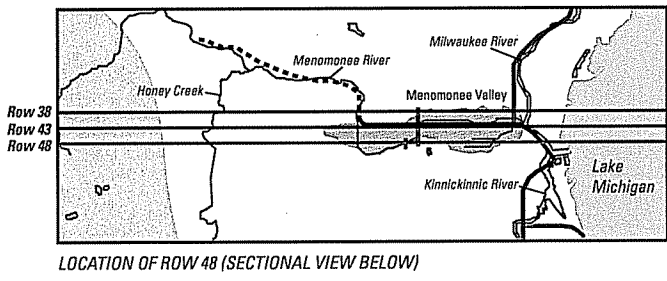
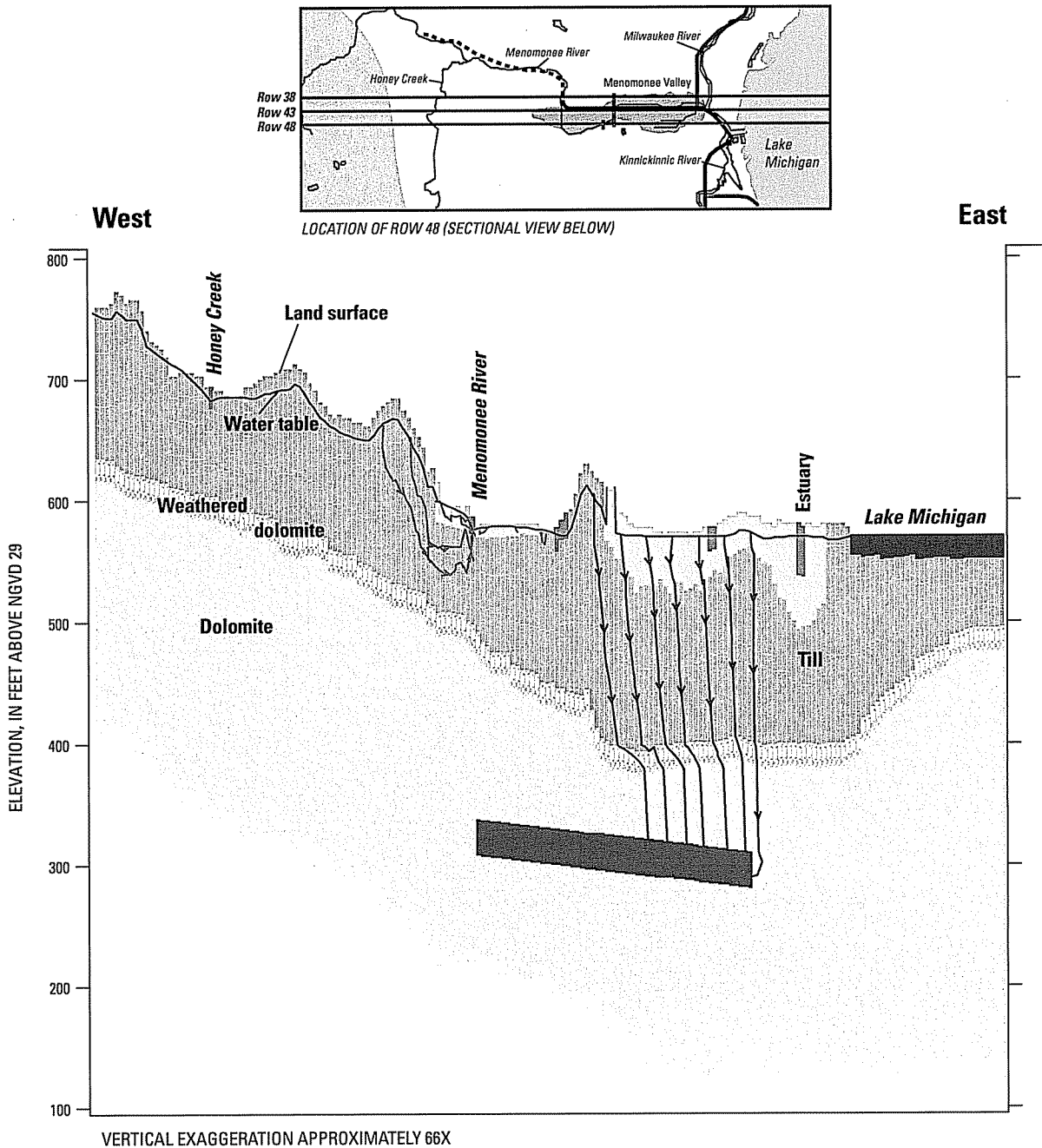


**Figure 14b.** Sectional view (row 43) of ground-water-flow directions simulated with MODFLOW and MODPATH in the Menomonee Valley Brownfield study area, Milwaukee County, Wis.



**EXPLANATION**

-  **In-line Storage System (ISS)**—segment shown lies in row 43 and is projected into this cross section
-  **Flow path to In-line Storage System (ISS)**—each arrow head represents 75 years of travel time
-  **Flow path to Menomonee River**—each arrow head represents 75 years of travel time

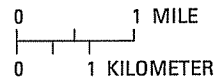


**Figure 14c.** Sectional view (row 48) of ground-water-flow directions simulated with MODFLOW and MODPATH in the Menomonee Valley Brownfield study area, Milwaukee County, Wis.

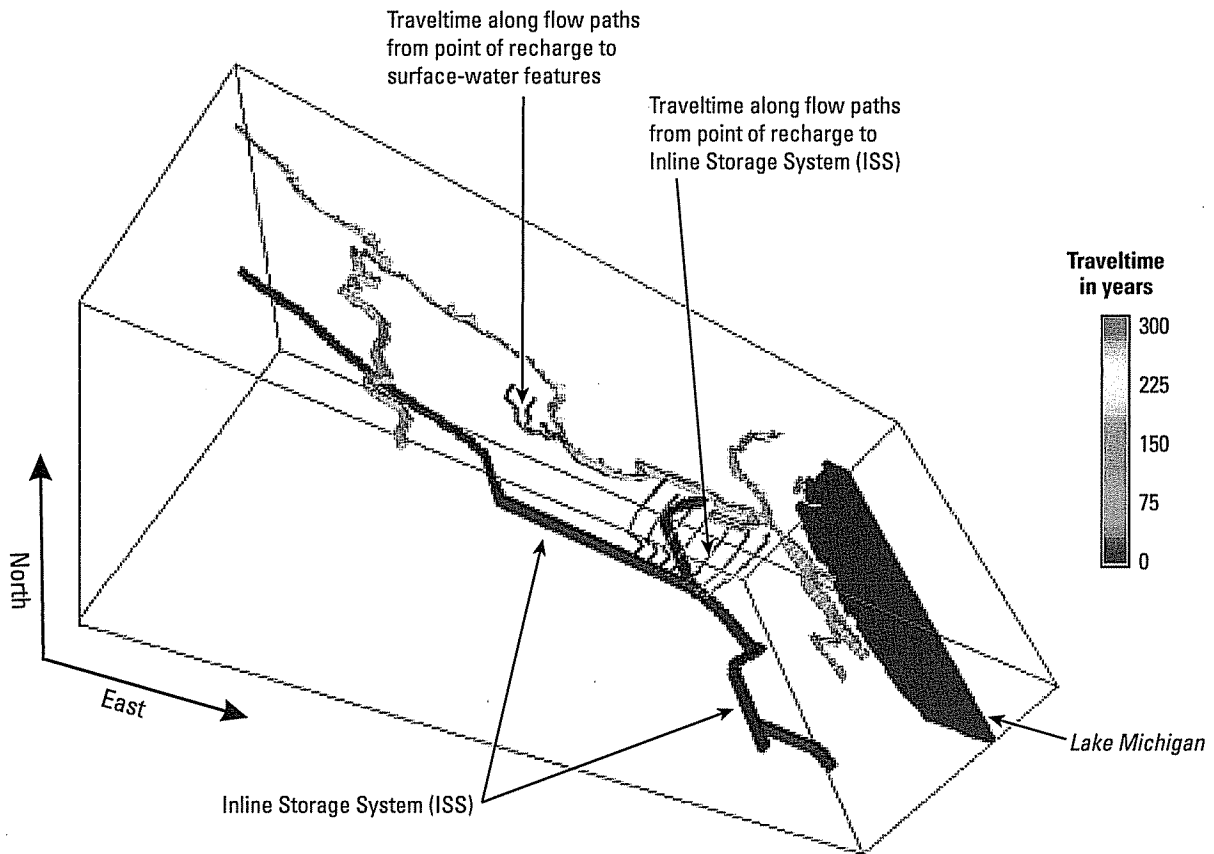


**Figure 15.** Three-dimensional view generated by ModelViewer of ground-water flow-patterns in the Menomonee Valley Brownfield study area, Milwaukee County, Wis.

from a given location is largely dictated by the length of flowpath in the unlithified deposits (where higher porosities result in slower velocities) as opposed to the fractured dolomite. The traveltimes to the ISS are least over the northern part of the valley where the dolomite is near the land surface.

### Implications for Contaminant Transport

A primary reason to model ground-water flow in the Menomonee Valley is to address questions that arise from the designation of the valley as a brownfield site. The soil in the valley contains industrial contaminants such as organic solvents, petroleum byproducts, tars, and metal waste. Recharge to the valley can dissolve these contaminants from the soil and transfer them to the ground water (SIGMA Environmental Services, Inc., 2002). The fate of potentially contaminated ground water in different parts of the valley is of interest to regulators and developers because it influences decisions about the amount of

monitoring and cleanup that is necessary before future redevelopment can go forward. As a first step in an evaluation process, an advective transport analysis could be done in which the potential threat posed by ground-water contamination is determined by the traveltime from a point of recharge in the Menomonee Valley Brownfield to any destination. The advective traveltime (time it takes for the bulk movement of the ground water from the point of recharge to a destination) will be less than the actual time of movement for many contaminants, because these contaminants are subject to retarding mechanisms such as sorption. Destinations include discharge to the water table, to surface-water bodies, and to manmade structures such as the ISS. As the dissolved constituents move from recharge areas to discharge areas, their characteristics and concentration can be changed by mechanisms such as chemical transformation, volatilization, precipitation, sorption, dispersion, and dilution. This process is known as natural attenuation. The rate of natural attenuation of

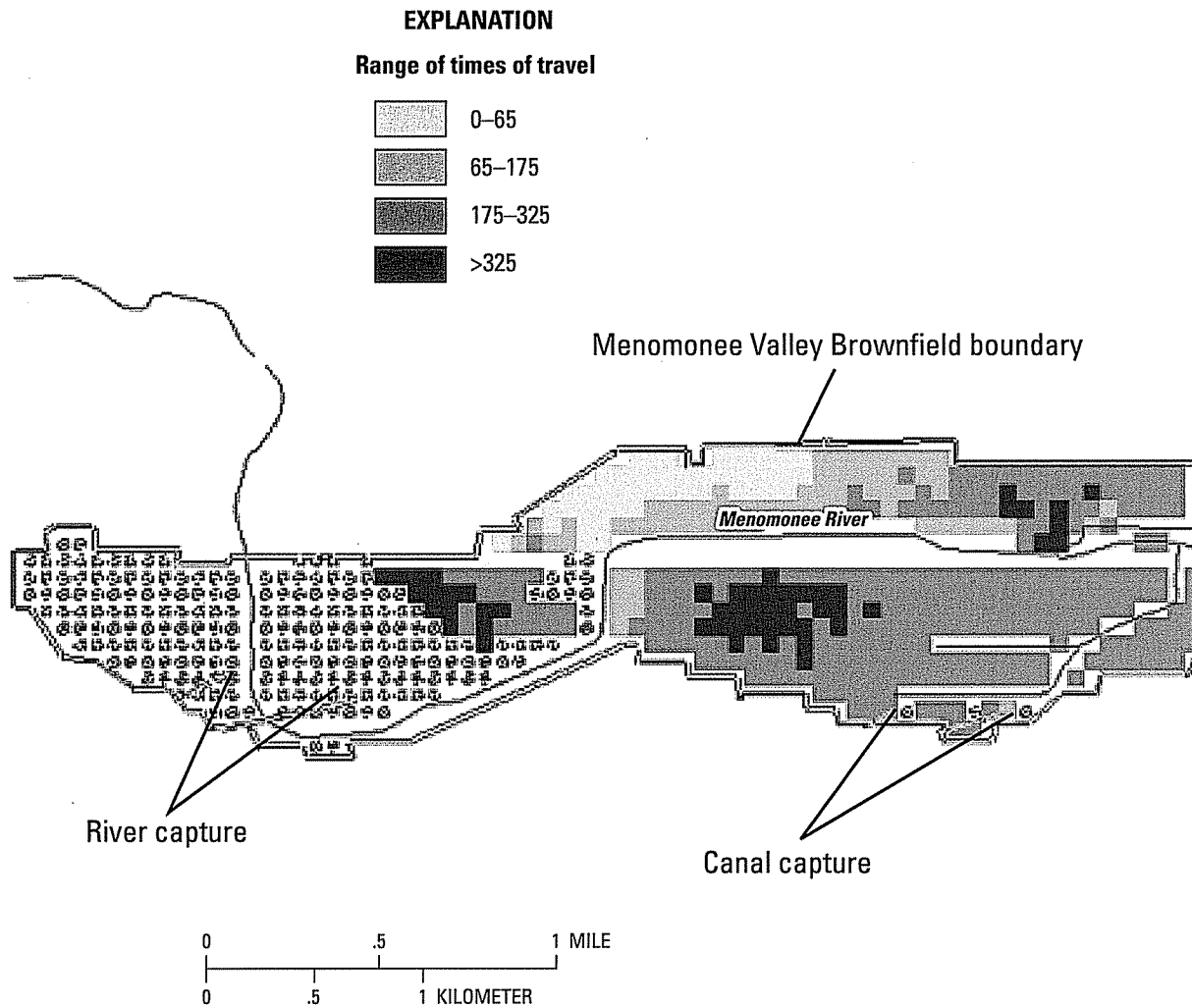


**Figure 16.** Traveltime to the In-line Storage System (ISS) in the Menomonee Valley Brownfield study area, Milwaukee County, Wis., simulated with MODFLOW and MODPATH.

any particular contaminant will depend on its physical and chemical properties and those of the matrix.

The results of the MODFLOW model provide the destination of ground-water flowpaths and approximate advective traveltime. A three-dimensional view of simulated ground-water-flow in the Menomonee Valley Brownfield is shown in figure 15. In the eastern part of the Menomonee Valley Brownfield, ground water is simulated as moving downward to the ISS. The ground water that infiltrates into the ISS is routed to Jones Island at the extreme eastern end of the valley (fig. 2), where all the water is treated at a wastewater plant before being discharged to Lake Michigan. In the western areas, recharge follows local flowpaths that circulate back to the water table and surface-water bodies (fig.15). Model results indi-

cate that most of this flow goes into the Menomonee River or the Menomonee River Estuary.

This method of evaluating contaminant transport processes by simulating advective transport alone is subject to many limitations. In particular, the traveltime results are very sensitive to the assumed values of effective porosity. The results presented in table 8 vary linearly with the assumed porosity. Consequently, if the porosities for each unit were reduced by 50 percent (resulting, for example, in a porosity value for till of 0.05 instead of 0.10), then the simulated traveltimes would be reduced by 50 percent for ground water discharging to the surface and to the ISS.

The analysis also depends on the stability of the simulated flow system. The relatively long travel paths to the ISS depend on the long-term presence of the ISS. If

the ISS were to be closed (and filled so as not to be a sink) sometime in the future, the flow system would change, and water previously destined for the ISS may reverse course and discharge to surface-water features or to Lake Michigan.

## Summary and Conclusions

The City of Milwaukee, Wis., is actively promoting the revitalization of the Menomonee Valley Brownfield, a 1,500-acre industrial center, about a quarter of which is abandoned or underutilized. An understanding of ground-water flow within the brownfield is requisite for evaluation of ground-water contamination. The U.S. Geological Survey (USGS), in cooperation with the City of Milwaukee and its consultants, and with support from USEPA Region 5, used numerical modeling to simulate shallow ground-water flow in the Menomonee Valley Brownfield. Modeling objectives were to simulate the fate of ground-water recharge to the valley, and estimate the traveltime from points of recharge to the ground-water sinks.

Shallow ground-water flow in the valley is driven by sources, primarily recharge to the valley and lateral flow from outside the valley, and sinks, primarily surface-water features and the Milwaukee Metropolitan Sewerage District In-line Storage System (ISS). The ISS is a deep tunnel in the Silurian dolomite bedrock, 17 or 32 ft in diameter, which fills with combined storm-sewer flow and sanitary-sewer overflow during rainstorms. This water is stored for later treatment and discharge to Lake Michigan. Between storms, the ISS is effectively empty and is a regional sink for the ground-water system.

Numerical models were used to simulate ground-water flow and to determine the fate of recharge falling on the Menomonee Valley. A stepwise modeling approach was used in this study, whereby a relatively simple, regional ground-water-flow model was used in an exploratory fashion to help design data collection, test model assumptions, and provide boundary conditions for a local multi-layer model. The regional model was constructed by use of the analytic-element modeling code GFLOW. The GFLOW model domain (as defined by limits of recharge and the far-field analytic elements) covers about 195 mi<sup>2</sup> (square miles), including western areas of Lake Michigan. The local model is 8-layers and was constructed by use of the finite-difference modeling code MODFLOW. The MODFLOW model domain covers about 26 mi<sup>2</sup> and is centered on the Menomonee Valley Brownfield, which covers about 2.3 mi<sup>2</sup>. The MODFLOW grid is surrounded

by specified-flux boundaries that were extracted from the regional GFLOW solution.

The GFLOW model was calibrated by adjusting line-sink resistances and hydraulic conductivity values; regional recharge rates and the dry-weather infiltration to segments of the ISS were set based on previous work. Only one location was available to match GFLOW-simulated composite hydraulic heads. The GFLOW-simulated head at this location was 541 ft compared to a composite average of 544 ft. The GFLOW calibration was also evaluated in comparison to surface-water flow. Base flow to the Menomonee River along the section between the two U.S. Geological Survey (USGS) streamflow-gaging stations was estimated for pre-ISS conditions by means of flow-duration curves constructed from data collected in the early 1980s. Calculated base flow for this section is 1.0 ft<sup>3</sup>/s (cubic feet per second). This estimate agrees well with 0.78 ft<sup>3</sup>/s, the base flow simulated by the GFLOW model for pre-ISS conditions.

The MODFLOW model was calibrated to measured heads (101 wells in unlithified sediments, 33 wells in dolomite), measured vertical gradients at 12 well nests, and measured dry-weather infiltration for five phases of the ISS. Head calibration in the unlithified sediments used water levels measured on August 14, 2001. Head calibration in the dolomite used water levels measured during 1994. Final calibrated values for horizontal hydraulic conductivity and rate of recharge for the MODFLOW model are unchanged from the GFLOW simulation that provided the flux boundary conditions. MODFLOW head calibration was very sensitive to rate of recharge and the distribution of vertical hydraulic conductivity; however, the solution proved almost totally insensitive to the resistance assigned to nodes representing rivers and canals. The simulated flux from losing surface-water bodies directly above the ISS is 0.11 ft<sup>3</sup>/s, which compares well with the corresponding GFLOW rate specified at 0.10 ft<sup>3</sup>/sec and, therefore, increases confidence in the stepwise approach.

About 73 percent of ground-water recharge within the MODFLOW domain discharges to the ISS, and 27 percent discharges to gaining surface-water bodies. MODFLOW simulates the following sources of infiltration to the ISS as percentages: 36 percent from recharge within the model domain, 45 percent from lateral flow into the domain, 15 percent from Lake Michigan, and 4 percent from other surface-water bodies. The median traveltime for recharge falling on the valley to reach surface-water bodies is 8 years; the median traveltime to the ISS is 255 years. The traveltime from a given location is largely dictated by the length of a flowpath in the unlithified deposits (where

higher porosities imply slower velocities) as opposed to the fractured dolomite. The traveltimes to the ISS are shortest over the northern and western parts of the valley where the dolomite is near the land surface.

## References Cited

- Bradbury, K.R., Swanson, S.K., Krohelski, J.T., and Fritz, A.K., 2000, Hydrogeology of Dane County, Wisconsin: Wisconsin Geological and Natural History Survey, University of Wisconsin-Extension, Open-File Report 1999-04, 66 p., 2 pls.
- Bates, R.L., and Jackson, J.A., 1980, Glossary of Geology, second edition: Falls Church Virginia, American Geological Institute, 749 p.
- Bredehoeft, J.D., and Hall, P., 1995, Ground-water models: *Ground Water*, v. 33, no. 4, p. 530-531.
- Carlson, D.A., 2000, Dependence of conductivities and anisotropies of geologic properties within the near-surface aquifer in Milwaukee, Wisconsin: University of Wisconsin-Milwaukee, Ph.D. dissertation.
- Camp Dresser and McKee, 1998, ISS/bedrock interaction hydraulic evaluation: Prepared for Milwaukee Metropolitan Sewerage District, 51 p.
- Cherkauer, D.S., 2001, Distribution of ground-water recharge in southeastern Wisconsin: Final Report to Source Water Protection Program, Wisconsin Department of Natural Resources.
- Cherkauer, D.S. and Carlson, D.A., 1997, Interaction of Lake Michigan with a layered aquifer stressed by drainage: *Ground Water*, v. 35, no. 6, p. 981-989.
- Feinstein, D.T., Dunning, C.P., Hunt, R.J., and Krohelski, J.T., 2003, Stepwise use of GFLOW and MODFLOW to determine relative importance of shallow and deep receptors: *Ground Water*, v. 41, no. 2, p. 190-199.
- Feinstein, D.T., Hart, D.J., Eaton, T.T., Krohelski, J.T., and Bradbury, K.R., 2004, Simulation of regional groundwater flow in southeastern Wisconsin: Wisconsin Geological and Natural History Survey Open File Report 2004-01.
- Gebert, W.A., Graczyk, D.J., and Krug, W.R., 1989, Average annual runoff in the United States 1951-1980: U.S. Geological Survey Hydrologic Atlas HA-710, scale 1: 7, 5000,000.
- Haitjema, H.M., Kelson, V.A., and de Lange, W., 2001, Selecting MODFLOW cell sizes for accurate flow fields: *Ground Water*, v. 39, no. 6, p. 931-938.
- Haitjema, H.M., 2000, GFLOW2000—Groundwater flow modeling system, Haitjema Software.
- Haitjema, H.M., 1995, Analytic element modeling of groundwater flow: San Diego, Calif., Academic Press, 394 p.
- Hsieh, P.A., and Winston, R.B., 2002, User's guide to Model Viewer, a program for three-dimensional visualization of ground-water model results: U.S. Geological Survey Open File Report 02-106.
- Hunt, R.J., 2002, Evaluating the importance of future data collection sites using parameter estimation and analytic element ground-water flow models in *Computational Methods in Water Resources—Proceedings of the 14th International Conference on Computational Methods in Water Resources*, June 23-28, 2002: Delft, The Netherlands, p. 755-762.
- Hunt, R.J., Anderson, M.P., and Kelson, V.A., 1998, Improving a complex finite-difference round water flow model through the use of an analytic element screening model: *Ground Water*, v. 36, no. 6, p. 1011-1017.
- Hunt, R.J., Graczyk, D.J., and Rose, W.J., 2000, Water flows in the Necedah Wildlife Refuge: U.S. Geological Survey Fact Sheet FS-068-00, 4 p.
- Hunt, R.J. and Krohelski, J.T., 1996, The application of an analytic element model to investigate groundwater-lake interactions at Pretty Lake, Wisconsin: *Journal of Lake and Reservoir Management*, v. 12, no. 4, p. 487-495.
- Hunt, R.J., Lin, Y., Krohelski, J.T., and Juckem, P.F., 2000, Simulation of the shallow hydrologic system in the vicinity of Middle Genesee Lake, Wisconsin, using analytic elements and parameter estimation: U.S. Geological Survey Water-Resources Investigations Report 00-4136, 16 p.
- Hunt, R.J., and Zheng, C., 1999, Debating complexity in modeling: *EOS Transactions, American Geophysical Union*, v. 80, no. 3, p. 29.
- Krohelski, J.T., Bradbury, K.R., Hunt, R.J., and Swanson, S.K., 2000, Numerical simulation of groundwater flow in Dane County, Wisconsin: Wisconsin Geological and Natural History Survey, University of Wisconsin-Extension, Bulletin 98, 31 p.
- McDonald, M.G., and Harbaugh A.W., 1988, A modular three-dimensional finite-difference ground-water flow model: *Techniques of Water-Resources Investigations of the U.S. Geological Survey*, book 6, chap. A1, [variously paged].
- Milwaukee Metropolitan Sewerage District, 1998, Assessment of Tunnel Water Migration: Report prepared by Camp Dresser and McKee.

- Mitchell-Bruker, S., and Haitjema, H.M., 1996, Modeling steady state conjunctive groundwater and surface water flow with analytic elements: *Water Resources Research*, v. 32, no. 9, p. 2725–2732.
- Mudrey, M.G., Jr., Brown, B.A., and Greenberg, J.K., 1982, Bedrock geologic map of Wisconsin: University of Wisconsin-Extension, Wisconsin Geological and Natural History Survey, scale 1:1,000,000
- Need, E.A., 1983, Quaternary stratigraphy of the Lower Milwaukee and Menomonee River Valleys, Milwaukee, Wisconsin, *in* Late Pleistocene history of southeastern Wisconsin, Mickelson, M. and Clayton, Lee, eds., Wisconsin Geologic and Natural History Survey, Geoscience Wisconsin, v. 7, p. 24–42.
- Plomb, 1989, A 3-D finite element model to predict drawdown caused by infiltration into a 32-foot diameter tunnel, *in* Solving groundwater problems with models: Association of Ground Water Scientists & Engineers proceedings, 4th conference, Indianapolis, Ind., February 1989.
- Pollock, D.W., 1994, User's Guide to MODPATH/MPATH-PLOT, version 3—A particle tracking post-processing package for MODFLOW, the U.S. Geological Survey finite-difference ground-water flow model: U.S. Geological Survey Open-File Report 94–464, [variously paged].
- Quinn, F.H., 1988, Likely effects of climatic change on water levels in the Great Lakes: Proceedings of the 1<sup>st</sup> North American conference on preparing for climate change: a cooperative approach, Washington, D.C., October 27–29, 1987, by the Climate Institute of Washington D.C., p. 481–487.
- Rust/Harza, April 2002, Internal inspection of the Inline Storage System: Milwaukee, Wis., Report prepared for the Milwaukee Metropolitan Sewerage District, [variously paged].
- SIGMA Environmental Services, Inc., 1999, Summary of existing data collection and review activities completed for Menomonee River Valley Brownfields Demonstration Pilot Project: Milwaukee, Wis., prepared for the City of Milwaukee Department of City Development, 10 p.
- SIGMA Environmental Services, Inc., 2002, Area-wide groundwater investigation report for the Menomonee River Valley Brownfields Demonstration Pilot Project: Milwaukee, Wis.
- Southeast Wisconsin Regional Planning Commission, 1976, A comprehensive plan for the Menomonee River Watershed—Volume One, inventory findings and forecasts: Waukesha, Wis., 481 p.
- S.S. Papadopoulos and Associates, 1991, PATH3D User's Manual: Rockville, Md., [variously paged].
- Strack, O.D.L., 1989, Groundwater mechanics: Englewood Cliffs, N.J., Prentice-Hall, 732 p.
- Sun, Ne-Zheng, Yang, S., and Yeh, W-G., 1998, A proposed stepwise regression model for model structure identification: *Water Resources Research*, v. 34, no. 10, p. 2561–2572.



# Appendix

---

Calibration targets, August 14, 2001

(well name, location, screen interval, model layer, measured and simulated head, residual)

MODEL X ORIGIN = 1,362,612 ft in UTM coordinates  
 MODEL Y ORIGIN = 15,620,203 ft in UTM coordinates

Well	Xmodel	Ymodel	Column	Row	Measure point	Layer	Observed head	Simulated head	Residual
Wells in un lithified sediments – August 14, 2001 is the date of all measurements									
<b>Distant Wells</b>									
#1436	39,364.00	21,542.00	158	1	613.31	1	613.31	584.28	29.03
#3790	19,850.00	873.00	80	84	634.17	1	634.17	642.01	-7.84
#4292	30,742.17	741.00	123	85	629.82	1	629.82	621.61	8.21
CLARK	24,475.00	13,471.00	98	34	662.14	1	662.14	656.02	6.12
FORESTRY	16,897.00	16,030.00	68	23	623.28	1	623.28	620.24	3.04
HTOWN	9,515.00	971.00	39	84	741.57	1	741.57	727.29	14.28
<b>Bluff Wells</b>									
BL_JK434	30,390.74	8,555.84	122	53	597.03	1	601.24	593.44	7.80
BL_JM081	19,968.26	8,287.00	80	54	608.85	1	612.30	610.21	2.09
BL_JM718	26,687.00	13,536.00	107	33	671.15	1	674.33	667.63	6.70
BL_JY481	16,124.00	11,321.00	65	42	630.72	1	651.71	636.63	15.08
BL_JY505	23,271.00	6,811.00	94	60	657.83	1	662.33	642.96	19.37
BL_JY551	19,218.26	9,850.00	77	48	596.04	1	608.67	595.13	13.54
BL_JY556	30,112.00	13,996.00	121	32	628.69	1	635.36	625.37	9.99
<b>Valley Wells</b>									
J1093	2,9275.00	11,438.00	118	42	572.64	1	577.12	579.17	-2.05
J1094	2,9565.20	11,442.64	119	42	573.35	1	579.12	579.17	-0.05
J1098	2,9971.00	11,404.00	120	42	572.49	1	575.85	579.17	-3.32
J1100	2,9361.00	11,371.00	118	42	574.45	1	581.12	579.17	1.95
JL774	31,146.09	10,634.97	125	45	576.19	1	582.50	579.14	3.36
JL775	31,114.00	10,368.00	125	46	576.95	1	581.38	579.23	2.15
JL776	30,971.00	11,103.00	124	43	577.41	1	581.55	579.17	2.38
JL958	29,533.94	11,371.00	119	42	574.43	1	581.05	579.17	1.88
JM108	28,521.00	12,060.00	115	39	575.84	1	578.84	579.40	-0.56
JM714	33,125.00	11,609.00	133	41	574.51	1	578.55	579.20	-0.65
JM715	33,066.00	11,511.00	133	41	574.93	1	578.73	579.20	-0.47
JM716	33,133.30	11,513.34	133	41	574.73	1	578.42	579.20	-0.78
JM719	28,501.00	12,126.00	115	39	575.76	1	578.98	579.40	-0.42
JM720	28,514.00	12,027.00	115	39	575.22	1	578.88	579.40	-0.52

MODEL X ORIGIN = 1,362,612 ft in UTM coordinates  
 MODEL Y ORIGIN = 15,620,203 ft in UTM coordinates

Well	Xmodel	Ymodel	Column	Row	Measure point	Layer	Observed head	Simulated head	Residual
<b>Valley Wells (continued)</b>									
JW045	29,518.00	11,470.00	119	42	573.85	1	580.52	579.17	1.35
JY482	25,521.00	9,886.00	103	48	575.02	3	578.91	572.87	6.04
JY521	22,497.00	11,929.00	90	40	591.53	3	593.32	589.01	4.31
JY522	32,442.51	9,441.64	130	50	588.51	1	593.03	583.64	9.39
JY523	32,487.00	12815.00	130	36	588.02	1	592.64	579.48	13.16
JY531	23,718.00	9,993.00	95	48	575.98	1	579.46	580.71	-1.25
JY541	33,122.64	11,479.17	133	42	574.43	1	578.37	579.20	-0.83
JY542	33,105.49	11,427.00	133	42	574.26	1	578.43	579.20	-0.77
JY543	29,830.00	11,404.00	120	42	573.42	1	576.43	579.17	-2.74
JY545	29,826.00	11,444.00	120	42	573.67	1	576.09	579.17	-3.08
JY546	29,849.00	11,437.00	120	42	573.25	1	575.26	579.17	-3.91
JY547	20,440.00	8,878.00	82	52	581.47	1	582.31	584.04	-1.73
JY548	20,440.00	9,009.00	82	51	580.95	1	582.32	585.43	-3.11
JY550	20,424.00	8,943.00	82	52	581.29	1	582.33	584.04	-1.71
JY555	19,677.00	10,491.00	79	46	583.04	1	585.11	586.97	-1.86
JY558	29,055.00	10,912.00	117	44	576.38	1	578.87	579.08	-0.21
JY560	29,115.00	10,912.00	117	44	573.29	1	578.90	579.08	-0.18
JY561	29,203.00	11,010.00	117	43	579.04	1	580.51	579.09	1.42
JY562	28,786.00	10,387.00	116	46	574.31	1	578.81	579.17	-0.36
JY563	28,760.00	10,387.00	116	46	574.52	1	578.89	579.17	-0.28
JY564	28,773.00	10,356.00	116	46	574.51	1	579.03	579.17	-0.14
JY569	29,361.00	10,256.00	118	46	576.11	1	578.84	579.20	-0.36
JY571	29,259.00	10,321.00	118	46	576.92	1	579.91	579.20	0.71
JY572	29,075.00	10,190.00	117	47	577.93	1	581.28	579.23	2.05
JY573	29,088.00	10,256.00	117	46	576.45	1	579.20	579.17	0.03
JY574	29,092.00	10,354.00	117	46	577.55	1	580.43	579.17	1.26
JY575	29,101.00	10,420.00	117	46	577.83	1	580.42	579.17	1.25
JY576	29,105.00	10,485.00	117	46	577.74	1	580.77	579.17	1.60
JY577	30,135.00	11,207.00	121	43	579.03	1	580.54	579.13	1.41
JY581	28,629.00	11,207.00	115	43	577.98	1	578.72	579.17	-0.45

MODEL X ORIGIN = 1,362,612 ft in UTM coordinates  
 MODEL Y ORIGIN = 15,620,203 ft in UTM coordinates

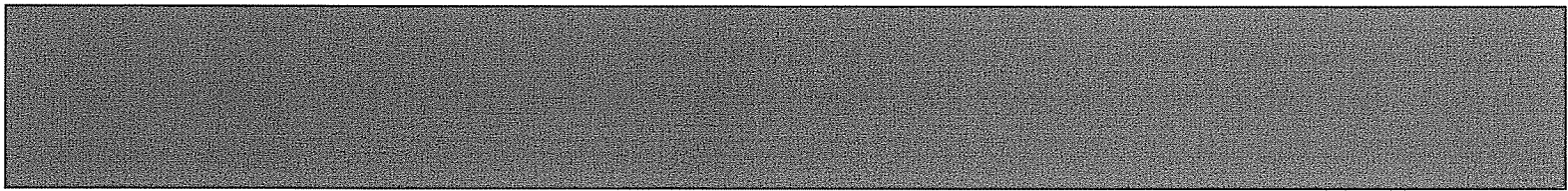
Well	Xmodel	Ymodel	Column	Row	Measure point	Layer	Observed head	Simulated head	Residual
<b>Valley Wells (continued)</b>									
JY582	27,057.00	11,273.00	109	42	573.42	1	579.49	579.54	-0.05
JY583	27,247.00	10,748.00	109	45	576.53	1	580.61	579.55	1.06
JY591	28,547.00	12,027.00	115	39	576.40	1	578.78	579.40	-0.62
JY592	28,580.00	11,929.00	115	40	575.21	1	578.86	579.50	-0.64
JY593	28,590.00	12,060.00	115	39	573.88	2	579.09	573.78	5.31
JY594	28,619.00	11,994.00	115	40	575.25	1	578.55	579.50	-0.95
JY595	29,046.00	11,404.00	117	42	574.33	1	581.39	579.21	2.18
JY596	29,046.00	11,371.00	117	42	577.23	1	581.16	579.21	1.95
JY597	28,990.00	11,437.00	116	42	577.00	1	581.24	579.23	2.01
JY598	29,036.00	11,437.00	117	42	577.39	1	581.26	579.21	2.05
JY599	29,115.00	11,470.00	117	42	577.10	1	578.48	579.21	-0.73
JY600	29,108.00	11,437.00	117	42	575.12	1	578.90	579.21	-0.31
JY614	31,300.26	11,226.68	126	43	573.58	1	581.03	579.11	1.92
JY617	29,940.00	12,386.00	120	38	573.02	1	576.36	578.26	-1.90
JY618	29,938.00	12,382.00	120	38	543.94	3	572.91	560.66	12.25
JY631	26,835.00	12,482.00	108	38	570.44	1	576.03	578.19	-2.16
JY647	25,521.69	11,771.60	103	40	538.76	3	568.95	569.41	-0.46
<b>Nested Wells (D=deep, S=shallow, W=water table)</b>									
N1D_JY507	25,495.00	11,456.00	102	42	532.36	3	565.77	570.45	-4.68
N1S_JY506	25,483.00	11,443.00	102	42	562.34	2	573.45	575.77	-2.32
N1W_JY508	25,483.00	11,466.00	102	42	571.51	1	576.63	579.72	-3.09
N2D_JY502	33,114.00	11,615.00	133	41	510.18	3	560.06	558.72	1.34
N2S_JY501	33,115.00	11,605.00	133	41	561.05	2	576.86	572.11	4.75
N2W_JM717	33,125.00	11,609.00	133	41	575.07	1	578.53	579.20	-0.67
N3D_JY649	26,055.00	12,020.00	105	39	539.96	3	568.91	567.91	1.00
N3W_JY648	26,055.00	12,020.00	105	39	579.03	1	583.37	579.08	4.29
N4D_JY513	29,403.00	11,437.00	118	42	511.05	3	564.51	563.01	1.50
N4S_JL119	29,376.00	11,471.00	118	42	569.99	2	577.11	574.26	2.85
N4W_JW180	29,271.96	11,419.72	118	42	574.11	1	581.03	579.17	1.86

MODEL X ORIGIN = 1,362,612 ft in UTM coordinates  
 MODEL Y ORIGIN = 15,620,203 ft in UTM coordinates

Well	Xmodel	Ymodel	Column	Row	Measure point	Layer	Observed head	Simulated head	Residual
<b>Nested Wells (D=deep, S=shallow, W=water table)</b>									
N5D_JY619	27,153.00	10,511.00	109	45	529.09	2	570.59	575.28	-4.69
N5W_JY557	7,182.00	10,702.00	109	45	577.43	1	581.04	579.55	1.49
N6D_JY613	30,325.43	8,712.30	122	53	560.50	3	562.00	560.60	1.40
N6W_MW-3	30,311.78	8,710.81	122	53	595.22	1	599.36	593.44	5.92
N7B_JY644	25,182.00	12,513.00	101	37	545.19	5	585.67	567.14	18.53
N7W_JY643	25,181.00	12,507.00	101	37	582.87	4	587.32	587.17	0.15
N8D_JY646	26,008.00	12,106.00	105	39	533.96	3	570.77	567.91	2.86
N8W_JY645	26,008.00	12,104.00	105	39	578.93	1	583.33	579.08	4.25
N9D_JY510	19,325.00	10,470.00	78	46	558.98	2	585.54	586.32	-0.78
N9W_JY511	19,325.00	10,470.00	78	46	578.84	1	585.01	585.97	-0.96
N11D_JY612	30,658.00	10,281.00	123	46	523.04	3	558.15	561.37	-3.22
N11W_JY611	30,658.00	10,286.00	123	46	572.28	1	578.98	579.27	-0.29
N12D_JY616	28,478.00	8,947.00	114	52	549.95	3	581.53	566.59	14.94
N12W_JY615	28,479.37	8,944.13	114	52	581.09	2	582.90	575.98	6.92
N13S_JL777	31,018.00	10,677.00	125	45	553.99	2	572.04	573.24	-1.20
N13W_JL773	30,849.97	10,693.00	124	45	578.20	1	582.23	579.17	3.06
<b>Wells in bedrock used to monitor Deep Tunnel – data gathered during 1994</b>									
CT-MW-01	37,678	8,278	151	54	587.27	7	290.24	359.25	-69.01
CT-MW-02	34,322	10,630	138	45	594.20	7	422.66	349.98	72.68
CT-MW-03	32,369	11,303	130	42	585.94	7	352.74	338.26	14.48
CT-MW-04	30,551	11,436	123	42	587.57	7	398.91	349.28	49.63
CT-MW-05	25,514	11,318	103	42	589.58	7	330.50	360.39	-29.89
CT-MW-06	20,660	11,141	83	43	640.21	7	350.74	397.48	-46.74
CT-MW-07	18,913	14,484	76	30	664.80	7	336.05	396.93	-60.88
CT-MW-08	14,286	15,713	58	25	633.96	7	396.31	416.96	-20.65
CT-MW-09	8,475	18,250	34	15	661.02	7	434.32	450.71	-16.39
CT-MW-10	23,787	11,260	96	42	597.68	7	355.06	364.42	-9.36

MODEL X ORIGIN = 1,362,612 ft in UTM coordinates  
 MODEL Y ORIGIN = 15,620,203 ft in UTM coordinates

Well	Xmodel	Ymodel	Column	Row	Measure point	Layer	Observed head	Simulated head	Residual
Wells in bedrock used to monitor Deep Tunnel (continued)									
CT-MW-11	34,322	10,630	138	45	594.02	6	453.70	471.34	-17.64
CT-MW-12	23,918	12,025	96	39	597.74	6	510.21	511.70	-1.49
CT-MW-13	20,655	12,082	83	39	640.52	6	581.36	531.92	49.44
NS-MW-01	33,301	12,292	134	38	590.21	6	532.72	470.89	61.83
NS-MW-02	33,296	15,889	134	24	592.34	6	536.30	486.74	49.56
NS-MW-03	35,857	19,589	144	9	630.09	6	479.73	496.65	-16.92
KK-MW-01	35,643	6,810	143	60	586.36	7	378.96	334.46	44.50
KK-MW-02	34,064	3,746	137	73	599.54	7	523.60	335.47	188.13
KK-MW-03	34,218	678	137	85	587.10	7	496.08	340.42	155.66
KK-MW-05	35,643	6,810	143	60	585.27	5	512.59	538.38	-25.79
LAM-MW-01	39,397	1,467	158	82	595.42	6	579.47	500.13	79.34
NS-MR-05S	34,587	17,093	139	19	592.15	6	543.89	490.39	53.50
NS-MR-05D	34,587	17,093	139	19	591.91	7	413.87	383.01	30.86
CT-MR-06S	28106	11717	113	41	587.76		499.01	491.67	7.34
CT-MR-06D	28049	11717	113	41	586.88	7	516.10	73.10	143.00
CT-MR-07S	13462	14073	54	31	696.99	5	635.82	635.23	0.59
CT-MR-07D	13438	14083	54	31	698.04	8	582.06	526.11	55.95
I30-25-CT	31667	12575	127	37	NA	6	514.06	479.08	34.98
I30-CT-DS-6	25553	12514	103	37	NA	5	554.85	558.90	-4.05
I30-17-CT	10190	17064	41	19	NA	6	632.67	601.56	31.11
C44-PZ-06	33044	2391	133	78	NA	5	560.58	563.05	-2.47
C10-07-KK	34048	420	137	86	NA	5	544.52	571.66	-27.14
I30-10-NS	36927	20933	148	4	NA	5	549.00	558.99	-9.99



Printed on recycled paper